

Review on Cell Mechanics: Experimental and Modeling Approaches

Marita L. Rodriguez

Department of Mechanical Engineering,
University of Washington,
Seattle, WA 98195
e-mail: maritar@uw.edu

Patrick J. McGarry

Department of Mechanical
and Biomedical Engineering,
National University of Ireland,
Galway, Ireland
e-mail: patrick.mcgarry@nuigalway.ie

Nathan J. Sniadecki

Adjunct in Bioengineering,
Department of Mechanical Engineering,
University of Washington,
Seattle, WA 98195
e-mail: nsniadec@uw.edu

The interplay between the mechanical properties of cells and the forces that they produce internally or that are externally applied to them play an important role in maintaining the normal function of cells. These forces also have a significant effect on the progression of mechanically related diseases. To study the mechanics of cells, a wide variety of tools have been adapted from the physical sciences. These tools have helped to elucidate the mechanical properties of cells, the nature of cellular forces, and mechanoresponses that cells have to external forces, i.e., mechanotransduction. Information gained from these studies has been utilized in computational models that address cell mechanics as a collection of biomechanical and biochemical processes. These models have been advantageous in explaining experimental observations by providing a framework of underlying cellular mechanisms. They have also enabled predictive, in silico studies, which would otherwise be difficult or impossible to perform with current experimental approaches. In this review, we discuss these novel, experimental approaches and accompanying computational models. We also outline future directions to advance the field of cell mechanics. In particular, we devote our attention to the use of microposts for experiments with cells and a bio-chemical-mechanical model for capturing their unique mechanobiological properties. [DOI: 10.1115/1.4025355]

1 Introduction

Cells are the basic building blocks of tissue. They are dynamic, living structures that have mechanical properties which can change in accordance with their functional state or in response to stimuli within their environment. In particular, cells can reinforce their cytoskeletons through polymerization of their structural, filamentous proteins and form stronger adhesions [1], but they can also fluidize their cytoskeletons to reduce their structural stiffness and remodel in response to a change in their mechanical environment [2]. Cells also generate physical forces to crawl, contract, and probe their physical environment [3]. Together, these responses help to maintain homeostasis for a cell for both its function as well as its mechanics.

If a cell misinterprets a mechanical cue or finds itself within an abnormal environment, its normal function can be disrupted and disease states can arise [4]. Many pathological diseases, such as asthma [5], osteoporosis [6], deafness [7], atherosclerosis [8], cancer [9], osteoarthritis [10], glaucoma [11], and muscular dystrophy [12] can be directly caused by or catalyzed by irregular cellular or tissue mechanics [4]. However, the specific mechanisms by which mechanical irregularities lead to disease states, as well as how or if they can be remedied, are still unclear.

While these diseases grow to impair the function of tissues in an organism, their initiation and development starts within individual cells. Therefore, it is important to decouple the role of mechanics at the single-cell level from the role at the tissue level in order to better understand these processes. Furthermore, when studying the mechanical response of an entire cell population, rare or transient phenomena can be obscured when one averages together the responses of individual cells [13]. Therefore, single-cell approaches, whether experimental or computational, can provide a fundamental basis on which to interpret the progression of diseases and disabilities.

To better understand a cell's mechanics, it is important to closely translate results from in vitro experiments into

mathematical relationships for in silico models. Experimental efforts focused on cell mechanics have yielded ample information regarding the mechanical properties of cells, as well as their response to different chemical and mechanical stimuli. Using the information gained from these experiments, various computational models have been developed to perform simulations that match closely with experimental observations. These efforts have helped to gain information on complex physiological properties or conditions, which would have been otherwise unable to study [14]

In this review, we provide an overview of the experimental and modeling efforts explored within the field of cell mechanics. We first provide a basic background on the biological aspects of cell mechanics and cellular forces. We then highlight key computational and experimental innovations, as well as describe the more widespread tools and models, used for cell mechanics. Due to our research backgrounds and expertise, we focus on studies using micropost arrays first developed by Tan et al. [15] in Sec. 4, and on a bio-chemical-mechanical model, first developed by Deshpande et al. [16], in Sec. 6. Finally, we close with a future outlook for emerging directions in cell mechanics.

2 Cell Mechanics and Cellular Forces

Animal cells, unlike those belonging to plants or fungi, lack an enclosing cell wall. Therefore, they require specialized structures to maintain their cellular integrity. These structures have received a large amount of interest in the field of cell mechanics because they have been found to define the physical properties and behaviors of a cell. However, a cell's membrane, nucleus, and cytoplasm also contribute to the mechanics of a cell (Fig. 1). In this section, we briefly highlight these other structures and then turn our attention to the principal components of the cytoskeleton.

The cellular membrane is composed of a thin lipid bilayer, which is approximately 5–10 nm in thickness [17] and has a bending stiffness of 10^{-19} – 10^{-20} N·m [18]. The main role of the cell membrane is to act as a barrier between the cell interior (cytosol) and the extracellular environment; however, the cell membrane also plays many other important roles. For example, it contains

Manuscript received December 21, 2012; final manuscript received September 3, 2013; published online October 15, 2013. Assoc. Editor: Francois Barthelat.

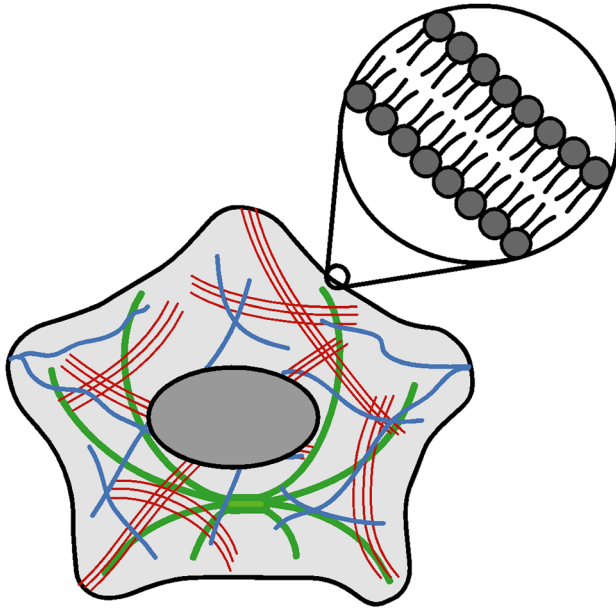


Fig. 1 Major structural components of a cell. The cytoskeleton is composed of actin (parallel filaments), intermediate filaments (wavy filaments), and microtubules (thick filaments). The mechanics of a cell is also defined by its membrane (cell border), nucleus (oval), and cytoplasm (region between membrane and nucleus).

protein structures that act as receptors for signaling molecules, transport channels for ions, or tethers between a cell's cytoskeleton and the extracellular environment [19]. The nucleus lies within the central region of the cell and is composed of two main regions: the nuclear interior, which contains DNA and proteins, and the nuclear envelope, which is a lipid bilayer akin to the cellular membrane. The main role of a cell's nucleus is to regulate gene expression, but it also has a degree of structural stiffness and plasticity that can play a role in cell mechanics and mechanotransduction [20–23]. The cytoplasm surrounds the nucleus and is a crowded microenvironment of proteins, protein complexes, and organelles. The crowded nature of the cytoplasm leads to its rheological properties [24–26] and also causes limited diffusion and a high degree of nonspecific interactions for proteins in the cytoplasm that hamper their chemical reactions rates [27].

The cytoskeleton lies within the cytoplasm and consists of a network of filamentous proteins. In addition to maintaining a cell's shape, it organizes a cell's organelles, serves as pathways for molecular motor proteins to shuttle cargo between regions of a cell, and acts as a dynamic structure that resists, transmits, and generates cellular forces [28,29]. Three groups of protein filaments define the cytoskeleton: microtubules, intermediate filaments, and actin filaments (Fig. 2).

Microtubules are stiff, hollow structures that radiate outward from a central organelle near the nucleus called the microtubule-organizing center (MTOC) [30]. Microtubules are composed of alternating helical layers of its monomers, α -tubulin and β -tubulin. They grow dynamically by polymerization at their ends furthest from the MTOC [31] and can resist cellular compressive forces [32]. Microtubules serve as transportation highways for motor proteins, kinesin and dynein, to shuttle cargo through a cell [33] or separate chromosomes during cell division [34]. The diameter of a microtubule is generally about 24 nm and their persistence length is on the order of millimeters, which leads to their straighter appearance in comparison to the other cytoskeletal filaments [35].

Intermediate filaments, on the other hand, provide strength, integrity, and organization for both the cell and its nucleus [35,36]. These filaments are composed of tetramer subunits, known as pro-

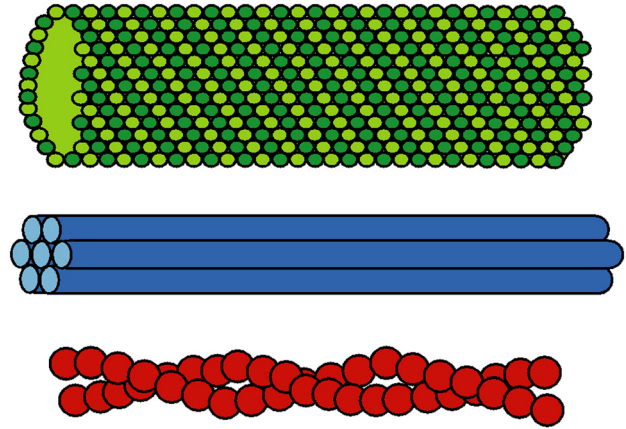


Fig. 2 Three major protein filaments make up the cell cytoskeleton: microtubules (top), intermediate filaments (center), and actin filaments (bottom).

tofilaments. Many protofilaments are bundled together to form the large filamental structure with a diameter of approximately 10 nm, and persistence length on the order of hundreds of nanometers [35]. Intermediate filaments, which can take on a number of different structural configurations, make up a compliant meshwork within the cell cytoplasm that acts as a “stress absorber” [36].

Actin filaments act as the primary structural component of the cytoskeleton, and with the aid of myosin proteins, are integral in creating and maintaining the forces required for cellular movement or contraction [28]. A single actin filament is made up of globular actin monomers known as G-actin. These monomers are used to form F-actin, which is a polarized, double-helical filament with a modulus of elasticity between 1 and 2 GPa, a diameter ranging from 5 to 9 nm, and a persistence length on the order of tens of micrometers [35]. F-actin undergoes polymerization and depolymerization through the association and dissociation of free G-actin at its filamental ends [35]. F-actin filaments can be linked together through Arp2/3 proteins that form branches in the network at 70 deg angles from the original filament, which help the cell membrane protrude outward during cellular migration or spreading [37,38]. Structures known as stress fibers consist of two or more F-actin filaments that are bundled together in parallel through α -actinin and nonmuscle myosin II (Fig. 3).

Myosin is a molecular motor that ratchets along actin, causing parallel F-actin filaments to slide past each other [39]. This sliding of actin leads to force generation in a cell that is akin to the shortening of sarcomeres in muscle cells. The structure of nonmuscle myosin consists of two heads, two necks, and a coiled tail region [19,35]. The heads of myosin can bind to actin, while its tails serve as locations for myosin-to-myosin binding that allow for the formation of bipolar filaments. Like myosin in muscle tissue, nonmuscle myosin is able to convert chemical energy from ATP hydrolysis into mechanical energy that moves its head into a cocked position. This ratcheting of myosin creates approximately 3–4 pN of force [40].

The shortening of many stress fibers in a cell can lead tension at points of contact outside the cell, e.g., cell–matrix adhesions and/or cell–cell junctions. Tension at the cell–matrix junction acts

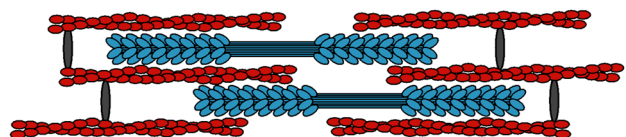


Fig. 3 Stress fibers are the force-generating structures in a cell. Shown are F-actin (helical filaments), myosin (branched filaments), and α -actinin (ovals).

predominately at focal adhesions, which are protein complexes that have both a structural and mechanosignaling role [41]. Focal adhesions are an aggregate of cytoplasmic proteins at the inner surface of a cell's membrane. Focal adhesion proteins, like vinculin or talin, connect F-actin to transmembrane receptors known as integrins, which subsequently connect to ligands in the extracellular matrix (ECM) [19]. The forces produced by myosin can be transmitted through focal adhesions to the integrin-ECM interface, where they act as traction forces. The spatial and temporal coordination of a cell's traction forces enable it to migrate to during wound healing. Traction forces also provide a prestress against the ECM that regulates cell adhesion and the signaling pathways associated with focal adhesions.

At cell-cell junctions, tension from actin and myosin in one cell can be transmitted to a neighboring cell [42]. A cell-cell junction is the general name given to a family of physical adhesive molecules that intracellularly connect two cells. These interactions facilitate not only cell-to-cell adhesion, but are also a conduit for chemical, mechanical, or electrical information between cells. There are three primary types of cell-cell junctions: tight junctions, gap junctions, and anchoring junctions. Tight junctions are composed of proteins—occludin, claudin, and other junction adhesion molecules—which serve to form a seal between neighboring cells, and act as a physical barrier to solute diffusion between those cells [19,35]. Gap junctions, on the other hand, are essentially pores composed of connexins, innexins, and pannexins, which allow for the transport of small molecules between adjacent cells [35]. Lastly, anchoring junctions serve a more structural role, by maintaining cell integrity through cytoskeletal connections to other cells, as well as the extracellular matrix. Adherens junctions, desmosomes, and hemidesmosomes can all be classified as anchoring junctions: adherens junctions connect the actin filaments of neighboring cells through cadherin proteins, desmosomes join cellular intermediate filaments through desmosomal cadherins, and hemidesmosomes link a cell's intermediate filaments to the extracellular matrix through integrins [35].

In addition to forces created and sensed internally, cells also experience external forces acting on them. They can either be directly applied to the cell or transmitted to the cell via cell-ECM or cell-cell interfaces. These forces can be sensed by the same mechanosensory structures that detect internal forces, i.e., focal adhesions or adherens junctions, but they can also be sensed by structures like the glycocalyx, primary cilium, and stretch ion channels (Fig. 4) [43]. The glycocalyx is a lattice of semiflexible macromolecules that are anchored in the cell membrane and extend into the extracellular environment [44]. Primary cilia, on the other hand, are long, slender protrusions of the cell membrane that contain microtubules. Both the glycocalyx and primary cilia deflect much like a cantilever beam when subject to fluid flow [45]. Lastly, stretch ion channels are protein complexes in the cell membrane that open their central pore in response to externally applied strains [46–48]. It is postulated that forces applied to the cell membrane lead to an increase in membrane tension, which then opens the channels and increases the conductance of extracellular ions that activate signaling pathways that affect cell function and gene regulation [45,49].

3 Experimental Methods for Measuring Cell Mechanics

The mechanical behavior of cells has been studied extensively by a wide array of experimental techniques. Generally, the choice of experimental technique is based upon the size or type of biological structure that is being investigated and what specific information is desired regarding that structure, i.e., microscale structures require microscale tools, whereas nanoscale structures require nanoscale tools. Advances in technology have allowed for the development of a number of different specialized approaches, but here we discuss some of the most common and seminal techniques.

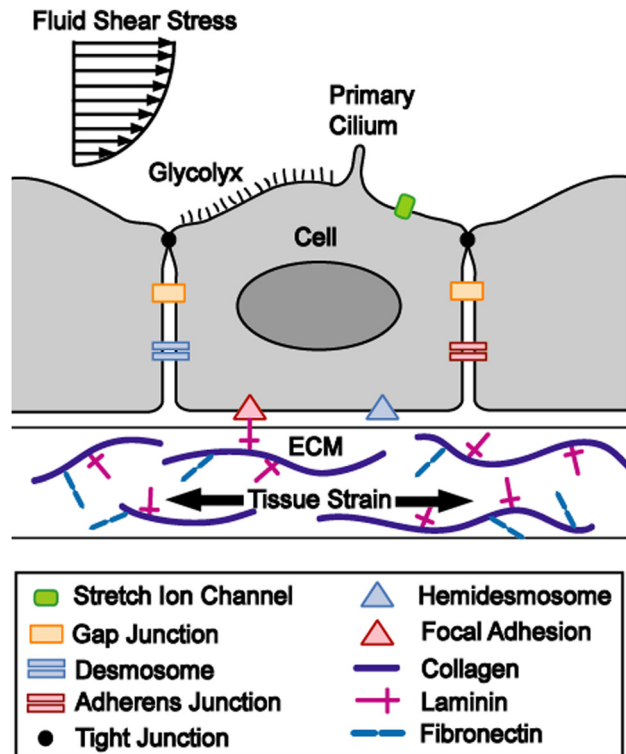


Fig. 4 Mechanotransduction pathways and force-sensing structures at cell-cell and cell-ECM junctions

In general, there are two different types of tools used for examining cell mechanics: force-application techniques (Fig. 5) and force-sensing techniques (Fig. 6). The former applies a force to the cell, and then records the cell's mechanical and/or biochemical response to this force, while the latter seeds cells onto deformable structures to measure their traction forces. However, tools within both techniques have spatial and force resolution limitations, which confines their applicability (Table 1).

3.1 Force Application Techniques. As mentioned above, force-application techniques measure a cell's response to an applied deformation or force. In addition to being used to investigate mechanotransduction, these techniques have been used to determine estimates of a cell's material properties. These measurements are invaluable as these properties are needed to define a cell within a computational framework.

3.1.1 Micropipette Aspiration. Micropipette aspiration techniques are often used to study whole-cell mechanics by examining how much cellular material is pulled into a glass pipette in response to negative pressure. Video microscopy is generally used to monitor the volume of cell material outside the pipette by tracking the radius of this material, as well as the length of cellular material within the glass pipette. If the cell is assumed to be a solid, homogenous continuum, its Young's Modulus (E) can be calculated from the applied vacuum pressure, the length of the cell inside the pipette, and the inner radius of the pipette [51]. Alternatively, if the cell is assumed to behave as a viscous solid, its viscosity can be determined from these values, the radius of the spherical portion of the cell outside the pipette, and the lengthening rate of the cellular material within the pipette [51].

Micropipette aspiration was first used to measure the elastic properties of sea urchin eggs in 1954 and is considered a "classical" technique in cell mechanics [52]. Since then, it has been employed to measure the elastic modulus and viscoelastic properties of various different cell types [53], e.g. leukocytes [54–58], red blood cells [59–61], chondrocytes [62–65], platelets

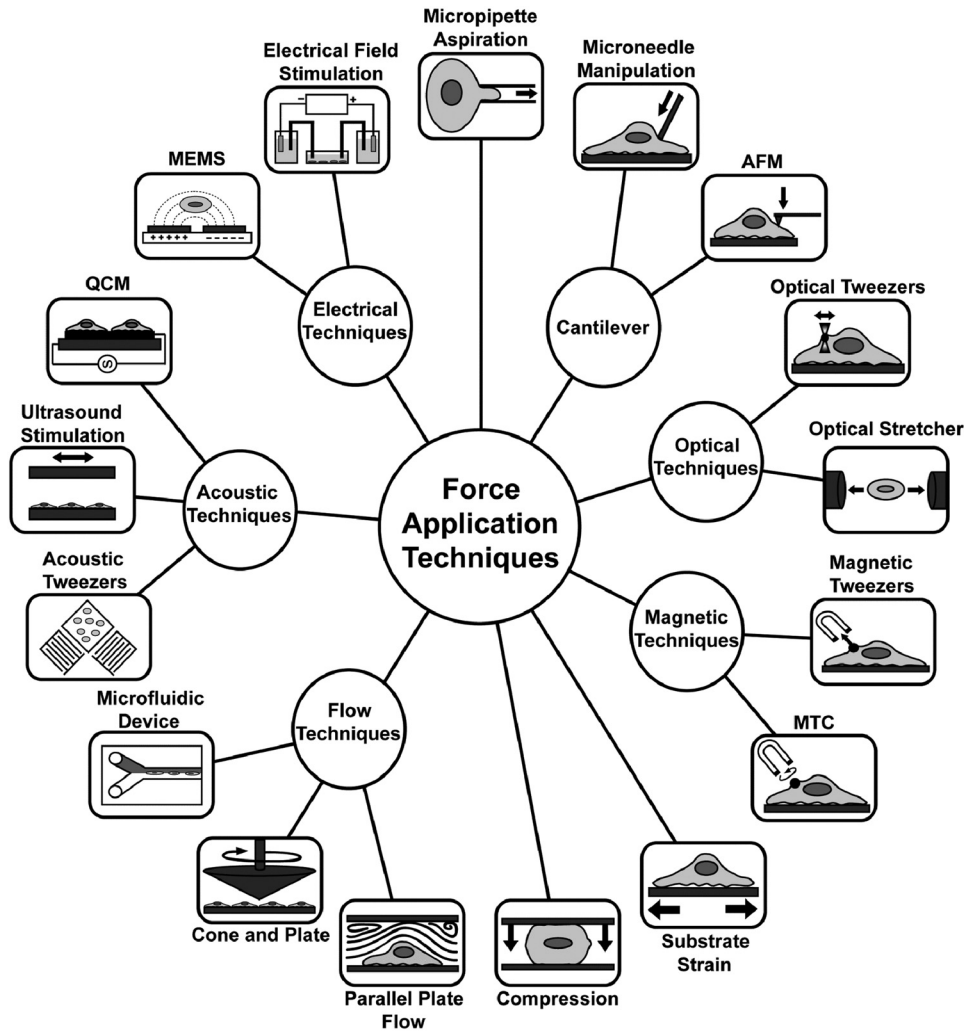


Fig. 5 Force-application techniques described in Sec. 3.1

[66–69], and endothelial cells [70,71]. Micropipette aspiration has also been used to study nuclear mechanics by gently extracting the nucleus from the cell and testing it with a pipette [22,72–75], as well as it has been used to study cell–cell junctions by a double-pipette configuration [76,77].

Some of the main advantages of micropipette aspiration include its relative simplicity and low cost with comparison to other methods, its ability to provide force resolution down to piconewtons, and the large range of cells that can be studied using this technique [51]. However, this technique is limited in spatial resolution to the micron scale, deforms (and possibly damages) the cell to a large degree during testing, and its accuracy is based on optical imaging limitations.

3.1.2 Cantilever Manipulation. Within this category of tools, the two most prominent techniques used within the field of cell mechanics are microneedles and the atomic force microscope (AFM).

Generally, in microneedle experiments, a thin and flexible glass microneedle is used to poke or tug on a cell or on one of its subcellular structures [78]. These needles are often made from a glass fiber whose end is heated until soft and pliable and then pulled into a fine tip. Since the glass microneedle acts like a cantilever spring, the force applied to the cell can be determined by the tip deflection of the needle, which can be measured electrically [79] or optically [80]. After calibrating the microneedle’s bending stiffness, the applied force can be calculated from Hooke’s Law. Moreover, by monitoring the microneedle force, as well as the

deformation it imparts to the cell, the cell’s elasticity can be determined from the slope of these experimental force-displacement curves.

When first developed in the early 1980s, microneedles (or cell pokers) were primarily used as a tool to investigate the response of cells to cytoskeletal indentation [80]. Later on, they were refined to determine the mechanical properties for different cell types (Table 2) [79,105–107]. Since then, microneedle manipulation techniques have been applied to study focal adhesion and adherens junction mechanotransduction [108,109], structural connectivity between the cytoskeleton and nucleus [110], opening of stretch ion channels [111], and neuron growth under tensile forces [112,113]. Improvements in the microneedle approach have come from dedicated electrical-mechanical systems to poke cells [81]. A recent study has demonstrated the importance of precise control of the probe height above a substrate for accurate measurement of cell stiffness [114]. Most recently, microfabricated cantilevers have been used to monitor cell forces with a higher degree of precision (see Sec. 3.2.3).

Overall, this technique is one of the simplest and most effective tools in the cell mechanics “toolbox.” It can provide useful information on a cell’s elastic properties and is straightforward to use for probing subcellular structures. However, the approach is somewhat data-limited because individual cells are tested serially and by hand, making it time-consuming for an experimentalist to reach a statistically significant set of data for their study. Development of automated, high-throughput devices for poking cells could provide a more data-rich approach [115].

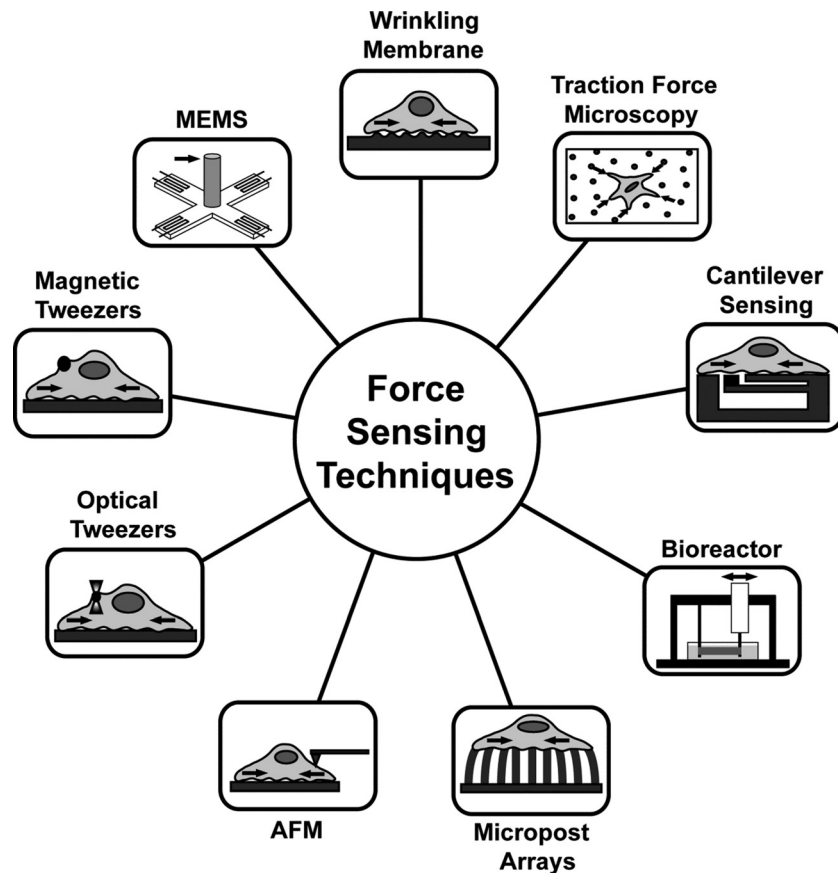


Fig. 6 Force-sensing techniques described in the Sec. 3.2

Table 1 Reported force and spatial sensitivity of select tools for cell mechanics

Tool	Force application	Force sensing	Spatial sens. (nm)
Micropipette aspiration	0.1–10 ³ nN	–	1–100 μm
Microneedle manipulation	1–10 ³ pN	–	1–10 ³ μm
AFM	10–10 ⁷ pN	10–10 ⁵ pN	1–10 ⁵ nm
Optical tweezers	0.01–10 ³ pN	1–100 pN	10–10 ³ nm
Optical stretcher	10–10 ³ pN	–	10–10 ⁶ nm
Magnetic tweezers	0.1–10 ⁴ pN	10–10 ³ pN	0.1–100 μm
MTC	1–100 pN	–	1–10 ³ μm
Strain	10–10 ⁶ nN	–	–
Compression	0.001–1 MPa	–	–
Dielectrophoresis	1–10 ³ Pa	–	0.1–10 μm
Wrinkling membrane	–	10–100 nN	–
Traction force microscopy	–	10–10 ⁶ pN	–
Micropost arrays	–	1–100 nN	1–10 ³ μm

References cited in the table are [50,53,150,223,274,342,372].

Atomic force microscopy is similar to microneedle manipulation in that it also uses a flexible cantilever with a fine tip at its free end, to probe cellular structures. The tip is used to probe a sample by measuring its displacement in the vertical direction as the tip is directed downward by a piezoelectric stage. The tip displacement is tracked by a laser and has excellent measurement precision. Additionally, using this technique, an approximation for the Young's Modulus of the indented cell can be determined based on the force applied by the AFM, the shape of the AFM tip, and the indentation depth [116].

Originally, AFM systems were developed to characterize the atomic and surface properties of materials for electronic devices [117]. Since then, AFMs have been adapted with environmental control chambers, and have been retrofitted for microscopy, to

investigate biological specimens such as cells. AFMs have been used to examine the mechanics of individual biomolecules [118–120], components of the cell nucleus [121,122], cytoskeletal structures [123,124], and whole cells [78,125–140]; as well as changes in these mechanics during differentiation [141] and disease progression [142–144]. They have also been used to investigate the mechanotransductive response of cells to applied forces [145,146] or ECM stiffness [131,147,148]. More recently, with some modification to their general setup, AFMs have also been used to resolve point forces exerted at the cell surface by attaching the tip of the AFM to the cell membrane, and then measuring the deflection of the cantilever arm due to contraction, migration, and other cellular events. In this configuration, AFMs have been used to measure forces at cell–ECM junctions [149–152], tugging

Table 2 Material constants used for cells

Cell type	Young's modulus (kPa)	Poisson's ratio	Technique	Reference(s)
Adipocyte				
Human joint	0.61		AFM	[82]
Cancer cells				
Bladder carcinoma	0.4–1.4		AFM	[129]
Chondrosarcomas	1–2.5	0.4	AFM/C	[83,275]
Melanoma	0.3–2		MTC	[84]
Human osteosarcoma	0.92–1.09	0.37	MN	[79]
Chondrocyte				
Bovine articular	0.69–8	0.26	MN/C	[106,287]
Bovine cartilage	2.55–2.7		C	[276,288]
Human cartilage	0.36–0.67	0.4	MP	[64,85]
Human femoral	1.1–1.3	0.36–0.38	AFM/MP	[62,82]
Porcine cartilage	0.6–1.2		AFM	[86]
Endothelial				
Bovine aortic	0.32		MP	[87]
Bovine aortic cytoplasm	0.5		C	[289]
Bovine aortic nucleus	5		C	[289]
Human aortic	1.5–5.6		AFM	[88]
Undisclosed Endothelial	0.5		MP	[51]
Epithelial				
A549 human alveolar	0.1–0.2		MTC	[89]
Human bladder	10–13		AFM	[129]
Monkey kidney cortex	0.16		MTC	[90]
Monkey kidney interior	0.04		PT	[90]
Fibroblast				
Avian heart	14.7		C	[285]
Murine L929	4		AFM	[91]
Murine 3T3	0.015–14		AFM/MN/PT/S/C/OT	[92–96,105,179,180]
Muscle cells				
Mouse myoblast C2C12	2		C	[286]
Mouse myogenic C2-7	0.66		S	[97]
Rat aortic smooth muscle	1.5–11		S	[98]
Rat myocyte (cardiac)	35–42		AFM	[99]
Osteoblast				
Human femoral	2.0–5.8		AFM	[82]
Human SaOS2	5.4–7.6		AFM	[100]
Murine MC3T3-E1	1–5		AFM	[136,94]
Murine neonatal long bone	14		AFM	[101]
Rat neonatal long bone	3.175–10	0.2–0.5	AFM	[145,146]
Stem cells				
Human bone marrow	0.56–33		AFM/MP	[82,102,103]
White blood cells				
Lymphocyte	0.2913		MN	[107]
Neutrophil	0.118		MN	[107]
Rat neutrophil	0.38–0.8		AFM	[104]

References cited in the table are [51,62,64,82,107,129,136,145,146,179,180,275,276,285–289].

Note: AFM = atomic force microscopy, C = compression, MN = microneedle, MP = micropipette aspiration, MTC = magnetic twisting cytometry, OT = optical tweezers, PT = particle tracking, and S = stretch.

forces at cell–cell interfaces [153,154], protrusive forces at the lamellipodia of a migrating cell [123,155–157], changes to cell forces upon chemical treatment [158], cell contractile forces [159], and the electrical activity of stimulated cells [160].

AFMs are sophisticated tools that can resolve piconewton forces and interrogate nanoscale structures of a cell. They can provide rich data at one discrete point of a cell at a time, but are limited in probing multiple points of a cell with high temporal resolution. Additionally, scanning with too high of a force can damage the cell; in addition, deformation to the cell membrane without any applied force can result in an overestimation of the force-indentation curve and subsequently the Young's modulus of the cell [161]. Furthermore, the shape of the AFM tip, as well as the location of tip attachment, affect the nature of the force-deformation curve and biases the results of the test; therefore results are not easily transferable between experiments employing different AFMs.

3.1.3 Optical Techniques. In general, optical techniques employ photon trapping to manipulate whole cells, or a portion of a cell. Of these techniques, the two most common are optical tweezers and optical stretching.

Optical tweezers or optical trapping, which was developed by Arthur Ashkin of Bell Telephone Laboratories [162,163], was originally used to trap individual atoms, viruses, and bacteria [164,165]. Optical tweezers use an infrared laser and a microscope to trap an object and control its movements through photons [150,166–169]. When photons pass through an object, there is a change in their direction based upon the object's refractive index. The change in direction causes a change in momentum, resulting in a force on the object. For light focused through a high powered microscope, photonic forces can trap an object at the center spot of the laser beam. For cell studies, if a spherical bead with radius $r \ll \lambda$ is used then the trapping force can be calculated from the intensity gradient of the laser, the refractive

index of the bead, and the refractive index of the surrounding cell culture medium [170].

The beads used in these studies are coated with ECM proteins like fibronectin, which allows for the cell's integrins to bind to these beads and form focal adhesion complexes. A trapping force that is closely equivalent to Hooke's Law can then be applied to the cell by adjusting the center position of the laser beam [171]. For this calculation, the stiffness of the optical trap can be found by exerting a known force on the trapped object, and then measuring its displacement from the trap center. This displacement is most often recorded using video-based position detection, but can also be determined via imaging or laser-based quadrant photodiode techniques [168].

In addition to being used as a tool for probing whole-cell mechanical properties of red blood cells [172–178], fibroblasts [179–181], tumor cells [177,181], chondrocytes/osteoblasts [182–184], epithelial cells [181], mesenchymal stem cells [185], optical tweezers have been used to determine the mechanical properties of subcellular structures such as DNA and proteins [186,187]. Optical tweezers have also been used to investigate the forces generated by molecular motors [40,188–195], those created by individual RNA polymerase molecules during transcription [196–200], and those developed during protein unfolding/folding [201–203] or binding/unbinding [204,205]. Lastly, optical tweezers have been used to simultaneously assess the mechanical and electrical properties of cells [206], and to stretch nonadherent cells [177,207].

Some of the advantages associated with using optical traps include the lack of physical contact between the cell and the force-producing mechanism, i.e., the laser, which can induce changes in the cell's mechanical properties, and can also be used to both apply and measure forces [171]. Moreover, by adding additional beads to the cell [173,174] and/or by creating multiple trapping beams [173,208–216], complex loading states, such as equibiaxial tension, can be applied to the cell. Additionally, bead systems allow for the perturbation of particular cell structures, via specific coatings to the bead surface. However, optical trapping is not without its limitations, especially within the context of biomechanical studies. Namely, the trap strength is sensitive to small optical perturbations and aberrations; therefore, for a lower index of refraction and better trap performance, the trapped particle must be in an aqueous solution (which limits the kinds of experiments that can be performed with optical traps) [150,170]. Additionally, due to limitations on the number of lasers that can be simultaneously used to trap different particles, only one or a small number of particles can be perturbed at a time. Lastly, it has been proposed that the optical trap may have detrimental effects on cells at higher laser power limits, due to the local heating from the high intensity of the laser, as well as photodamage [53,150,171,217]. Therefore, if used at a high intensity for long periods of time, it is possible that this heating could result in changes to the mechanical properties of the cell.

Alternatively, in an optical stretcher, laser light is coupled to one or more optical fibers with fiber couplers and delivered to the cell chamber [218]. Two-dimensional trapping can be achieved by using a single-beam fiber, while three-dimensional trapping requires two fibers [211]. If two fibers are used, the scattering forces from the laser beams results in axial optical trapping, while Gaussian gradient forces enable transverse trapping [219].

These systems can be used for the trapping and/or stretching of cells, and, thus far, have mostly been used to investigate the mechanical properties of cells [220], to distinguish between diseased and healthy cells [181], and to investigate the response of cells to stretching [221].

Some advantages associated with optical stretchers are their ability to manipulate cells within closed systems, the fact that they are able to operate over a longer working distance than optical tweezers, they can work with a large trapping volume, and they enable high throughput analysis [219]. However, this technique is only applicable to cells in suspension, and for stable

trapping in three-dimensions, the two fibers must be perfectly aligned [219].

3.1.4 Magnetic Techniques. The most prominent magnetic techniques used for studies in cell mechanics are magnetic tweezers and magnetic twisting cytometry. Magnetic tweezers apply discrete forces to a cell through attached ferromagnetic beads. They serve a similar purpose as optical tweezers by pulling on cells or subcellular structures; however, for magnetic tweezers, the beads movement is manipulated by a magnetic field gradient produced by an electromagnetic coil. The magnitude of the force applied to the bead is directly related to the intensity of the magnetic field [170].

Magnetic tweezers were initially developed to measure the mechanical properties of cells [122–226], but have since been employed for the manipulation of individual cellular components, such as DNA [227–229], lipid bilayers [230], and cell receptors [231]. Magnetic tweezers have also been used as a means to investigate the effect of applied force on individual ligand–receptor bonds [232], focal adhesion proteins [233–245], cell–cell junctions [246], and the effect of applying force to multiple different beads seeded within a cell [247].

One of the main advantages associated with the use of magnetic tweezers is bead attachment versatility. They can be bound with molecules that are ligand-specific, chemical-specific, or nonspecific to a cell's surface receptors, or one of its internal structures. Additionally, as opposed to optical methods, magnetic techniques induce little heat or photo-damage to biological specimens [248]. Furthermore, they can also be used within most materials and media types, as the majority of cell and media fluids have relatively small magnetic susceptibility. Lastly, magnetic tweezers have the ability to apply a constant force to the magnetic particle without a feedback loop, and can apply a large range of different forces (see Table 1) [161]. Limitations associated with the use of magnetic tweezers include the nonuniformity of stress profile applied by the bead to the sample, the variability in magnetic properties within a bead population, the inability of magnetic traps to eliminate bead torque, and resolution limitations due to video-based detection [170,248,249].

Alternatively, magnetic twisting cytometry utilizes ferromagnetic or superparamagnetic beads coated with ECM proteins or cell-adhesive peptides, to apply a torque to the surface or inside of a cell [250,251]. The torque is created at the bead–cell interface by applying a field in a direction perpendicular to the magnetic dipole of the bead [53]. The angular rotation of the bead can be determined via a magnetometer [252] or by optically tracking their motion as they roll across the surface of a cell [253].

Magnetic twisting cytometry was originally used to investigate the material properties of the cytoplasm [225,226], but has more recently been used to examine cell material properties, [253–255], mechanical strengthening at cell–ECM or cell–cell receptors [252,255–259], stress relaxation [260], the activation of mechanotransduction signaling pathways [261], the effect of localized stress on gene transcription [256,262], and cytoskeletal remodeling [263–265]. Magnetic twisting cytometry has many of the same advantages and disadvantages as magnetic tweezers, but with the added advantage of force application in a rotational frame.

3.1.5 Substrate Strain. In this technique, strain can be applied to cells cultured on top of an elastic membrane or gel coated with an ECM protein by stretching this underlying substrate with vacuum pressure or an indenter. This strain, which mimics the physiological strain imposed on cells within the body, can be used to apply strain in one direction (uniaxial), in two directions (biaxial), or equal strain in all directions (equibiaxial). Stretching techniques are most often used to investigate the effect of applied strain on a wide variety of different cellular properties, such as morphology, genetic regulation, metabolic activity, injury, and cell phenotype [53].

More specifically, applied mechanical strain has been used to investigate the phenomena of strain-induced cytoskeletal fluidization and resolidification [2,266,267] or reinforcement [2], actin reorganization [266,268,269], ECM protein recruitment and reorganization [270] action potential signaling [271], genetic activity [272], and cell motility [273]. Recently, this technique has been coupled with force-sensing methods to reveal information regarding the effect of globally applied mechanical strain on cell traction forces [2,266].

Advantages of this method include its relative ease of use and low cost, the ability to stretch multiple parallel substrates with the same strain profile, control over the stiffness of the substrate that the cells are cultured on (by modifying the substrate's elastic properties), the ability to change cell-substrate interactions (via the substrate's surface coating), and the ability to perform microscope observation during testing (for systems with stationary culture surfaces). Disadvantages of this technique include the anisotropy in the applied strain at the grip regions, and the inherent heterogeneity of the elastin substrates used in this technique.

3.1.6 Compression. This technique can be used to measure the mechanical responses of cells to unidirectional whole-cell compression. A typical experiment is performed by growing a population of cells on a flat plate, and then allowing a second plate to come into contact with these cells. The force applied to the cells is dependent on the mode of force application. If the second plate is simply allowed to rest on top of the cells, then the force applied to the cells is effectively the gravitational force produced by the second plate. However, most often, the second surface is mechanically driven towards the cells [274]. Alternatively, the cells can be seeded within a gel, and the cell can be compressed between two spacers [275,276], or the cells can be compressed laterally via the compression of their underlying substrate [277]. In the case of mechanically driven compression, the applied force must be calculated; moreover, if the cells are seeded within a gel, the mechanical properties of that gel must be taken into account for these calculations. In earlier studies, this was done by performing video microscopy and calculating changes to the cell's shape [275,276].

Initially, this method was used to investigate the mechanical properties of sea urchin eggs [278–283], as well as to study the effect of compression on bone cells [275,284]. More recently, it has been used to elicit the material properties of whole cells [285–288] and individual cell structures [289], as well as to investigate the effect of compression on cell structure [277].

Some positive aspects of this technique include the wide range of different stimulation profiles that are possible, as well as the ability to study either single cells or cell populations in two or three dimensions [274]. However, the Poisson-effect leads to anisotropy in the applied strain field, and there is strain heterogeneity at the specimen-plate interface as well as limited gas exchange in these closed-systems can lead to cell death [274].

3.1.7 Flow Techniques. There are a number of different primary cells resident within the human body that are either consistently or periodically subject to fluid flow. Shear flow systems mimic these flow conditions in order to yield more physiologically relevant experimental results. The three most popular kinds of shear flow devices are the cone-and-plate system, the parallel plate flow chamber, and microfluidic devices. Within these systems, cells can be subject to laminar, transitional, or turbulent flow profiles. The distinction between these profiles is determined based on the flow's dimensionless Reynolds number. A fluid with a Reynolds number of $Re < 2300$ is considered to be laminar, while flow with $Re > 4000$ is defined as turbulent flow, and anything in between $2300 < Re < 4000$ is deemed transitional flow.

In the cone-and-plate system, rotation of the fluid within the cell culture chamber is induced by spinning the cone perpendicular to the plate surface. The taper in the shape of the rotating cone

generates a shear stress that is homogeneous over the entire population of cells in the chamber [8,290–293]. Because of the large number of different combinations of cone taper and velocity, a vast number of different flow profiles can be achieved [274]. Alternatively, in a parallel plate flow chamber, a pressure differential between openings on either side of the chamber is used to drive fluid across a layer of cells. This pressure drop is generally achieved via gravitational fluid flow or through the use of a fluid pump.

There are also a wide range of microfluidic devices that have been developed to simultaneously study the effect of physical and chemical cues on cellular material properties. In general, these devices use fluid flow to direct cells and substances through complex, micromachined channels. Possible physical cues that can be delivered to a population of cells via a microfluidic device include various fluid flow profiles, changeable substrate topology and stiffness, and control over cell shape through microcontact printing. Possible chemical cues include the treatment or incubation of these cells with various different growth factors, drugs, and/or molecular agents. Microfluidic devices can also be designed to characterize the mechanical properties of either suspended or adherent cells through the incorporation of flow cytometry and microstructured elastomeric surfaces (such as post arrays), respectively.

A large number of different cellular phenomena have been found to be influenced by fluid shear stress. Namely, shear stress has been found to play a role in kinase activation [294], cytoskeletal organization [295–298], signal transduction [296,299,300], proliferation [301,302], apoptosis [303,304], gene expression [305,306], migration [307–311], cell-ECM interactions [312–314], and cell-cell junctions [315]. Furthermore, microfluidic devices have enabled investigations on the effect of hydrodynamic stretching on single cells [207,316], cell movement through fluid and/or solid environments of different geometries [317–321], the effect of multiple different applied forces on adherent cells [322,323], and the chemotactic movement of cells [324,325].

Some of the advantages of standard shear systems, such as parallel plate flow chambers and cone and plate systems, include the homogeneity of the applied shear stress, the relative simplicity of the equipment, and the ease of physical and optical access to the studied samples [274]. However, standard shear devices can be bulky, require large amounts of reagents, and do not allow for sophisticated control over the mechanical environment that the cells see. Alternatively, microfluidic devices have the ability to control the cell environment while simultaneously measuring cell mechanics, can be fabricated repeatedly, can be designed to handle adherent or nonadherent cells, can expose cells to pulsatile or chaotic flow, require small sample and reagent volumes, can be designed to approximate physiological conditions, and are capable of delivering or measuring multiple different kinds of mechanical, electrical, and/or chemical properties to cultured cells [326]. However, since these devices are generally designed to be closed systems, once they are fabricated, it is difficult if not impossible to manipulate them. Therefore, in order to make changes to a device, another one must be fabricated, and this fabrication process is generally relatively expensive and time consuming. Additionally, only certain materials (those that are nontoxic and provide for gas exchange) can be used to fabricate these devices in order to maintain cell viability. Furthermore, some of these devices operate on the assumption that there is not any heterogeneity in cell size within a population of cells; and if this difference does exist, it is possible that the device will not function properly [316].

3.1.8 Acoustic Techniques. Compared to previously mentioned techniques, acoustic techniques are relatively new to the field of cell mechanics. In general, these systems employ acoustic waves to manipulate whole cells. Here, we discuss acoustic tweezers, ultrasound stimulation, and quartz crystal microbalance sensors.

Acoustic tweezers use standing surface acoustic waves (SSAW) to translate or stretch cells and microparticles, [327]. A surface acoustic wave (SAW) is a sound wave that travels along the top surface of an elastic material [328]. These devices are commonly fabricated by placing a PDMS microchannel above a piezoelectric substrate with two interdigital transducers (IDTs) [327,329]. For one-dimensional manipulation, these transducers are placed in parallel, and for two-dimensional control, they are oriented orthogonal to one another. To use this device, cells are dispersed within the microchannel via pressure-driven flow, until the distribution of cells is stable. If the IDTs are placed in parallel, and an identical RF signal is applied to each, then the interference of the opposing propagating waves leads to SSAW motion in the perpendicular direction. Alternatively, if the IDTs are placed orthogonal to one another, then cell motion can be controlled in two-dimensions by altering the RF signal applied to each IDT [327]. In either case, this motion is driven by a periodic distribution of pressure nodes within the fluid.

Alternatively, ultrasound stimulation can be used to apply mechanical forces to cells by inducing acoustic vibrations within a fluid environment containing the cells [330]. This can be achieved by culturing the cells in between two rigid substrates, and sinusoidally vibrating one of the plates with a piezoelectric transducer [330]. Alternatively, these vibrations can be limited to the surface of a piezoelectric material by converting an electrical signal into polarized waves via interdigital transducers [331].

Finally, quartz crystal microbalance is a surface-sensitive means of quantifying changes in the mechanical properties of cells. In this system, two electrodes are placed at the opposite ends of a thin quartz piezoelectric substrate [331]. Mechanical oscillations are then induced when a potential difference is created between these two surface electrodes. Using this technique, changes in cell mass or attachment are measured by observed shifts in the resonance frequency of the sensor crystal, and changes in the cell viscoelastic properties are measured by observing changes in the energy dissipation of the shear oscillation of the sensor [332].

Within the field of cell mechanics, ultrasound devices have been used to investigate the role of acoustic stimulation on cell proliferation [333–337], genetic activity [333,335,337], cell–cell interactions [338], and ECM organization [337], to induce the differentiation of various different cell types [337,339], as well as they have been used for cell manipulation and transport [330].

In general, acoustic systems are noninvasive, only introduce low-power mechanical vibrations to the sample (rather than heat or photodamage), have a much lower power requirement than their optical counterparts, and do not require cell pretreatment regardless of cell shape, size, electrical properties, or optical properties [327,329,330,333,340]. Additionally, these systems are fairly simple and inexpensive to use compared to optical and magnetic systems, are high throughput, and can be applied to individual cells or multiple cells at once. However, because these techniques are relatively new to the field of cell mechanics; thus far, they have only been employed for one and two-dimensional manipulation of cells on the micro and milli-scale.

3.1.9 Electrical Techniques. Recent advancements in micro-electromechanical systems (MEMS) technologies and electrical-stimulation devices have helped elucidate the effect of a cell's mechanical environment on its electrical properties, and vice versa.

As their name implies, MEMS combine mechanical and electrical components onto one microscale device, which are generally fabricated with standard micro and nanofabrication processes [341–343]. One of the more prominent MEMS techniques used within the field of cell mechanics is dielectrophoresis (DEP). Dielectrophoresis uses a nonuniform electrical field to induce the translational motion of particles. This is achieved by first inducing polarization of the cell (or cells) of interest via an applied electric field. Then, when a nonuniform electrical field is applied, the

disparity in the Coulombic forces pulling on each end of the cell dipole results in cell motion [344,345]. This motion is governed by the magnitude and polarity of the charges induced in the cell by the applied electrical field, which are dependent on the electrical properties of the cell, the size of the cell, the frequency of the applied field, and the conductivity and permittivity of the medium [343,346]. This technique can be used to stretch cells via electrical stresses generated by planar microelectrodes [342,343]. This is achieved by using DEP to trap individual cells at the tip of a microelectrode, or by chemically attaching cells to individual microelectrodes, and then applying an electrical potential between that and an opposing electrode via a signal generator. This potential results in an applied electric field, which deforms the trapped cells at a constant stress [342]. This deformation can then be observed and captured with standard optical imaging to determine approximations in the cell stress, strain, and viscoelastic material properties [342].

Recently, MEMS systems have gained more popularity within the field of cell mechanics, and have been designed to enable force sensing during or directly after mechanical actuation events [341,347], to simply apply mechanical strain to cells [345], to monitor cell attachment and spreading [332], to measure cell–ECM interactions [348,349], to quantify cell death [346], and to quantify cell mechanical properties [342,343,350].

One of the main advantages of MEMS devices is that they are designed to be all-inclusive systems, i.e., they generally do not require much external equipment to operate. Additionally, these devices can be designed to perform single or multicellular studies, and can also be used to perform parallel analysis [350]. However, fabrication of these devices is generally fairly expensive and complicated, and once fabricated, it is not easy to alter chip design. Furthermore, the fabrication of each new device generally takes a couple of days, and prior to their use, these devices often have to be calibrated, which can be a complicated process [341,344].

Alternatively, electrochemical gradients or stimulation can be applied to a population of cells in culture via metal electrodes or salt bridges. Electrical signals are involved in cell development, wound healing and migration, neuronal and cardiac action potentials, and the progression of disease [351]. Upon injury, wounds generate naturally occurring electric fields that guide cell migration [352,353]. This phenomenon is commonly referred to as electrotaxis or galvanotaxis, and can be recreated in vitro by applying an electrochemical field to cultured cells. Often, this electric field is delivered to the cells via agar salt bridges within the cell media, which are connected to two electrodes immersed in Steinberg's solution and stimulated with a DC field [354–356].

In the human body, cardiomyocytes and neurons are periodically exposed to ionic currents, and their continued function relies on the propagation of these currents. To elucidate the effect of electrical stimulation on cell mechanical properties, an electrical field can be administered to cultured cells by placing electrodes directly into the culture medium, and applying an AC field to these electrodes [351].

Within the field of cell mechanics, electrical fields have been used for the directed migration of fibroblasts [357–359], epithelial cells [356], endothelial cells [360,361], stem cells [354,355], white blood cells [362,363], and various different malignant cell types [364–366]. They have also been used to determine the effect of electrical gradients on cytoskeletal orientation and organization [358,361,366–368], as well as cellular contraction [367–370]. These electrical gradients are most often applied to cells cultured on flat substrates, but can also be applied to cells in three-dimensional scaffolds or tissues [364,368].

Overall, electrical stimulation techniques are relatively simple to implement, can be applied to multiple cells at a time, and are a widely standardized and established method for cell stimulation. However, these apparatuses can be bulky, expensive, and can result in nonuniform electrical fields.

3.1.9.1 Material Constants Obtained via Experimentation. The experimental techniques highlighted in Sec. 3.1 of this review have been useful in estimating material constants for cells. However, the reported values for different cellular material properties can be influenced quite strongly by the experimental technique used to obtain them, as well as by the particular type of cell being investigated (Table 2). For instance, the constants resulting from techniques that require a physical adherence between the cell and the test equipment will depend upon the shape and overall size of the contact area between the cell and equipment, as well as on the point of adherence within the cell. Furthermore, because the cytoplasm is nonhomogeneous and is consistently remodeling, e.g., changes during migration or spreading, the material properties obtained are an approximate average of a cell's components at a particular instant in time. However, these approximate values have proven to be very useful in defining computational models of cell mechanics. This idea will be further expanded upon in the following sections of this review.

3.2 Force-Sensing Techniques. The other class of tools used for cell mechanics are used to measure the forces produced by cells during development, contraction, migration, and other commonly occurring cell processes (Fig. 6). These techniques can be used to measure cell forces within a static environment, or they can be combined with one of the previously mentioned techniques to investigate the effect of externally applied forces on cell-produced forces.

3.2.1 Wrinkling Membranes. Albert Harris developed the first technique used to measure the traction forces produced by cells [371]. These forces were observed by seeding cells onto a thin, flexible membrane of silicone rubber. As these cells contracted, they pulled on the silicone membrane, causing wrinkles to form. The lengths of these wrinkles, as well as the number of wrinkles surrounding a cell, can be used to estimate the amount of force produced by the cells [372].

Studies utilizing wrinkling membranes for traction force measurements have yielded information regarding the relative magnitude of forces exerted by different cell types and how these forces serve to remodel the extracellular matrix [373]. The main advantage of this method is its ability to assess whether a particular area of a cell is under tension or compression. However, this technique is not able to determine the exact location, direction, or magnitude of traction forces, as the wrinkles produced by the cell are a result of multiple individual traction forces. Furthermore, debris, surface defects, and nonuniformity in the thickness of in the membrane can incorrectly alter calculated traction forces, or complicate their quantification [374].

3.2.2 Traction Force Microscopy. Traction force microscopy was developed as a means for measuring cell traction forces in a quantitative manner. In traction force microscopy (also known as particle tracking), the cell of interest is seeded onto or within a polymeric gel substrate, along with a large number of micro-scale fiduciary beads [250]. Given a value for the elastic stiffness of the substrate, traction forces can be estimated by tracking the displacement of the beads [53]. Assuming that an elastic, homogeneous, isotropic, and linear material is used as the particle substrata, the relationship between the displacement field and traction field can be determined from the material properties of the substrate material using Green's function [375].

Traction force microscopy has been used to measure the forces produced by a vast number of different cell types [254,367,376–379], to determine the contribution of active cytoskeletal contraction to these traction forces [377,380,381], and to elucidate the effects of pathological events on these forces [382–384]. It has also been used to measure forces at focal adhesions [385], to determine traction forces during migration [380,386,387] and development [388,389], elucidate the effect of cell shape [390] and electrical stimulation on traction forces

[367], and to determine the effect of certain gene upregulation on traction forces [383]. More recently, this technique has been combined with laser scanning confocal microscopy to allow for the measurement of traction forces in three dimensions [391–395]. Furthermore, when combined with force-application techniques, traction force microscopy has yielded information regarding the effect of applied forces on cell traction forces [396,397].

This technique has a number of advantages. For instance, because the cells of interest can be seeded on top or within the gel material, this technique can be used with both adherent and non-adherent cell types. Additionally, the material properties of the gel can be altered to expose the cells to testing environments of different stiffness. Furthermore, the variety of different bead types and sizes available for these experiments allows researchers to control the area over which the force is applied, as well as the vast range of different bead coatings that can be used for these experiments allows for strict control over cell-bead attachment. However, there are also a number of negative aspects associated with particle tracking. Namely, the accuracy of this technique is limited by a number of different properties. First, force resolution is based on optical resolution; therefore, forces that are resolved using a low resolution imaging technique will be inherently inaccurate. Second, determined cell forces are based on the accuracy of the cell's assumed stiffness, which is often based on indirect measurements. And lastly, resolved forces are strongly influenced by the size of the particle and fluctuations in temperature. Furthermore, since bead deflections are due to the summation of multiple different point forces, traction force microscopy only gives an estimation of the directionality and magnitude of a cell's traction force at one particular point in space [78].

3.2.3 Cantilever Sensing. Cantilever beams are essentially long, slender structures, whose deflections are used to measure the traction forces produced of cells. The first incarnation of this tool was an array of horizontal cantilever beams built underneath flat surfaces that the cell can come into contact with [398,399]. As a cell migrates across these surfaces, it bends the cantilever to a degree that is proportional to the traction force applied to this region by the cell. This relationship is governed by Hooke's law [400]. Alternatively, if the cantilever beam is fabricated on the end of a sensory probe, it can be used to apply a discrete force to the cell, while simultaneously measuring changes in cell contractile forces [401].

Studies employing these cantilevers have found that the front of migrating fibroblasts produce intermittent rearward forces, while the tail region produces forward-directed forces of larger magnitude, and both these forces have periodic fluctuations [398]. However, in general, cellular deflections are linear in nature [402]. In addition to yielding contractile forces, cantilever beams have also been used to elicit information regarding the effect of lateral indentation or tugging on cell morphology [401,403–407], the role that tension plays in neurotransmission [408], and cell material properties [409–411].

The main advantage of this technique is its ability to elicit discrete traction force measurements. More specifically, this technique is able to determine the magnitude and direction of the traction force experienced by a subcellular region of interest below the cell. Furthermore, fabrication of multiple cantilevers in series allows the measurement of forces in multiple locations over time [410]. However, these cantilever arrays are relatively expensive, difficult to fabricate, and are limited to the measurement of forces along two axes [409]. After the introduction of large arrays of horizontal cantilever beams, technological advances within the field of soft lithography allowed for the production of vertical arrays of cantilevers, also known as micropost arrays. These tools are described in further detail in Sec. 4 of this paper.

3.2.4 Bioreactors. A bioreactor is essentially an apparatus in which cell cultures can be maintained and simultaneously subject to externally applied stimuli. Recently, these systems have gained

more popularity within the field of cell mechanics, and have been designed to enable the measurement of multicellular forces in three-dimensional environments [412,413], as well as the forces produced by microtissues during or directly after mechanical actuation events [414–417].

One of the main benefits of these systems is their ability to allow for the measurement of multicellular forces within a physiologically relevant environment. Additionally, because these systems are able to simultaneously apply external stimuli to cells and measure cell properties, they allow for stricter control over the cellular culture environment, and enable more complex experimental studies. However, further development and use of these systems is limited by the cost and complication associated with their fabrication. That said, if the cost of these systems can be lowered, or they become commercially available for purchase, they have the ability to serve as a standard, all-inclusive, cell-mechanics testing platform.

4 Focus on Micropost Arrays

Micropost arrays, also known as microfabricated post array detectors (mPADs) or micropillars, are arrays of vertical cantilevers, which are used to spatially track the traction forces produced by cells attached to their tips. This section of the paper will outline micropost fabrication, how they are used to measure cell forces, the advantages and disadvantages associated with using micropost arrays, and current knowledge that has been obtained from their use.

4.1 Fabrication. Before making the silicon micropost arrays, master cantilever templates are made from silicon or photoresist using photolithography techniques. During this process, a photosensitive photoresist (generally SU-8) is exposed by UV light through a photomask (generally made out of chrome and glass). This UV treatment cross-links the exposed material, which makes it insoluble to the developer solution. Therefore, when the substrate is immersed in the developer, the remaining regions will wash away, leaving only the exposed structures (Fig. 7). This master can be fabricated as either a positive (silicon microposts)

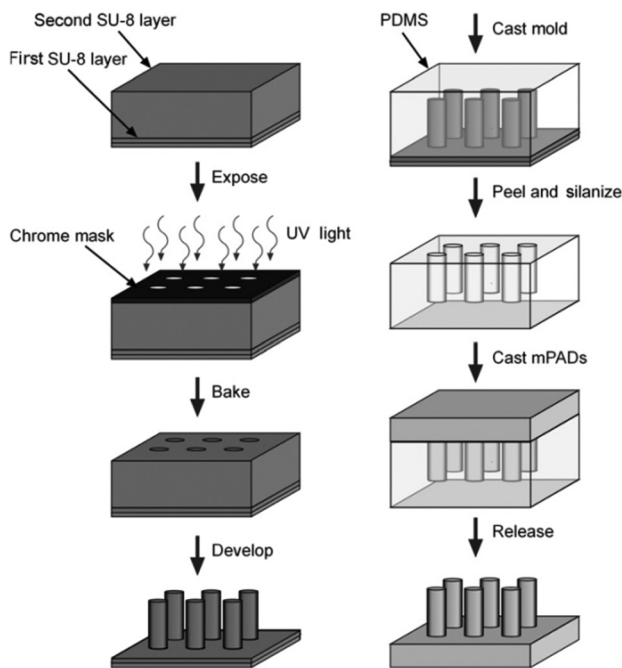


Fig. 7 Micropost array fabrication steps. (Reprinted from Ref. [394] with permission from Elsevier.)

or a negative replica (silicon substrate with micro-sized holes) of the post arrays.

After this silicon master, micropost arrays can be created by casting replicas of this master mold, using a silicone or thermoplastic material. Generally, micropost arrays are formed out of polydimethylsiloxane (PDMS), but they have also been fabricated out of polymethylmethacrylate (PMMA) [418]. When using a positive master, two casting steps are required. First, the silicone or plastic is cast off of the silicon master to create a negative mold. A second casting is then made from this negative mold to make the mPAD. Alternatively, when using a negative master, the silicone or plastic can be cast onto the silicon master to form the microposts in one step. While this single-step process eliminates the need for a second casting procedure, it has previously been found that the silicone material can become clogged within silicon holes, which leads to micropost arrays with defective posts. In order to prevent the casting material from sticking to the master wafer or negative mold, these structures must be silyanized prior to these casting steps.

After making the micropost arrays, cells are attached to the tops of the posts by coating an extracellular matrix protein on their tips via a process called microcontact printing (Fig. 8). In the initial steps of this process, an ECM protein is allowed to absorb on a block of silicone material (called a “stamp”), while the micropost arrays are treated with UV ozone to make them hydrophilic. When these two surfaces are placed in contact, the protein is transferred from the stamp to the tips of the microposts. Once the ECM protein has been absorbed to the post tips, the posts are fluorescently stained such that their locations can be determined during fluorescence microscopy. After staining, the remaining surfaces of the microposts are treated with Pluronic to ensure that cell attachment is limited to the tips of the microposts, and not along their sides or base. At this point, the substrates are ready for cell seeding and experimentation [418].

4.2 Determining Cell Forces and Examining Cell Structure. To determine a cell’s traction forces, the deflection of each post that the cell is attached to is determined by comparing images of the top plane of the posts to the bottom plane. Knowing the Young’s modulus and dimensions of the posts, linear elastic beam theory can then be used to determine the cell’s traction forces using the following equation:

$$F = \left(\frac{3ED^4}{64L^3} \right) \delta \quad (1)$$

where E is the Young’s modulus of the silicone, D is the diameter of the cantilever post, L is its length, and δ is the horizontal deflection of the post. If the height-to-diameter ratio of the posts is low,

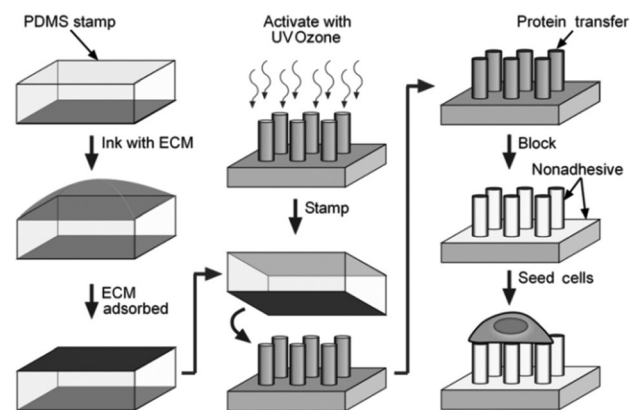


Fig. 8 Steps performed for micropost array functionalization. (Reprinted from Ref. [418] with permission from Elsevier.)

the spring constant used for these force calculations need to be adjusted to account for rotation at the base of the microposts [419].

If a static experiment is being performed, the cells can simply be fixed and fluorescently stained on top of the posts following experimentation. Alternatively, in order to visualize cell structures during a live experiment, the cells should be transfected with a fluorescent protein, such as green fluorescent protein. Fluorescently staining cells prior to live-cell experimentation has been found to result in cell death and can interfere with their normal behavior. However, following live experimentation, the cells can be fixed and fluorescently stained for other cell structures of interest.

4.3 Applications and Limitations of Micropost Arrays.

Micropost arrays can be used to measure local traction forces, multicellular forces, cell–cell forces, and any changes to these forces due to externally applied stimuli. Furthermore, since cell structures can be visualized via fluorescence imaging, changes to these structures can be simultaneously investigated. With regard to their spatial resolution, microposts have dimensions that are on the microscale, which results in a high density of force sensors beneath a single cell. Additionally, these posts can be fabricated in a cost effective manner, as multiple identical arrays can be made from a single silicon master, and PDMS is a relatively cheap material.

However, since post deflections are optically observed using microscopy, the range of materials that the posts can be fabricated out of is limited to those that are transparent. In addition, during experimentation, the researcher must choose between observing one cell with high accuracy or multiple cells with low accuracy due to limited field of view with microscopy at high magnification. Furthermore, the nonphysiological form of these substrates could stimulate cell responses that are elicited by the topology and adhesion area of the micropost landscape. Lastly, tapered side walls and/or top surfaces, posts sticking in the holes, and posts coming out of the molds with greatly reduced dimensions are some of the difficulties that can arise during the fabrication of these microposts [420].

4.4 Studies on the Utility of Microposts for Cell Mechanics. Since their induction into the world of cellular mechanics, micropost array sensors have been used to study changes to cellular forces experienced during various different cellular processes, and within a wide variety of different test environments. This section of the paper will review some of the experiments that have utilized micropost arrays and their major findings.

4.4.1 Cell Spreading. When cells are initially seeded onto a surface, they are generally characterized by a rounded morphology. After cells have adhered to the underlying substrate, they begin to spread. In the first experiments employing micropost arrays, cell traction forces and focal adhesion area were quantified for unspread and spread bovine pulmonary artery smooth muscle cells [421]. These experiments found that both the focal adhesion area and the amount of cell spreading were proportional to contractile force production. These results were expanded upon in further experiments by the same group, which showed that the spread area of cells seeded on micropost arrays was similar to that for cells on glass slides, glass slides coated with fibronectin, and the total cell force increased with increasing cell spread area (Fig. 9) [422].

4.4.2 Cellular Migration. Micropost arrays have been used to study cellular forces during the processes of planar migration, as well as the transmigration of single cells. In a study on Madin Darby canine kidney (MDCK) epithelial cells, du Roure et al. found that during the process of migration, maximum traction forces are concentrated at the edge of the cell, and that epithelial

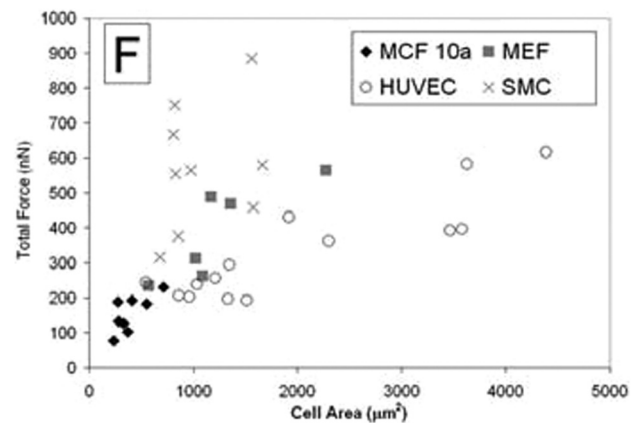


Fig. 9 Force as a function of spread area for mouse embryo fibroblasts (MEF); human umbilical vein endothelial cells (HUVEC); human mammary epithelial cells (MCF10a); and bovine aortic smooth muscle cells (SMC) [422].

cells within monolayers create higher traction forces than individual cells alone [423]. More recently, Sochol et al. found that when micropost arrays are fabricated with variable amounts of spacing, bovine aortic endothelial cells (BAECs) will migrate in the direction of decreasing post-to-post spacing [424]. Additionally, a group out of the University of Pennsylvania used micropost arrays to show that the migration of primary murine dendritic cells is driven by traction forces at their leading edge, and the orientation of these traction forces can be used to predict the direction of dendritic cell motion [425].

In the realm of transmigration studies, Rabodzey et al. demonstrated that the tangential forces exerted by neutrophils during transendothelial migration, significantly increase as they penetrate into the intercellular space [426]. This study also found that the traction forces exerted by the endothelial monolayer through which the neutrophils migrated, also increased. This increase in traction forces was seen to coincide with the disruption of VE-cadherins at the endothelial cell–cell boundary. More recently, Liu et al. [427] performed a study in which micropost arrays were used to determine the cell forces created by a monolayer of endothelial cells during monocyte adhesion and transmigration. This study found that the average traction forces within the monolayer increased during both of these processes, and that the endothelial cell(s) in direct contact with the adhered monocyte experienced the largest traction forces, which were aligned in a centripetal orientation (Fig. 10) [427].

4.4.3 Cell Contractile Power. Micropost arrays also have the ability to yield information regarding the velocity—and thus power—of cellular contractile events. Using an enhanced optical tracking technique that records micropost deflections in high spatiotemporal resolution, Rodriguez et al. found that cardiomyocyte twitch power increased with increasing substrate rigidity, while twitch velocity decreased (Fig. 11) [428]. Cells with increased twitch power were also found to have improved myofibril structure and increased intracellular calcium levels.

4.4.4 Cell–Cell Forces. In general, the majority of studies that employ micropost arrays to study cell mechanics measure traction forces experienced by focal adhesion complexes, i.e., zyxin [429] and FAK [430]. In these studies, the tips of the microposts are coated with an extracellular matrix protein. Alternatively, the tips of the microposts can be stamped with a cadherin ligand, in order to quantify the magnitude of forces experienced by these complexes. Experiments employing this technique have found that the forces experienced by cadherin complexes are on the same order as those found for focal adhesion complexes [431].

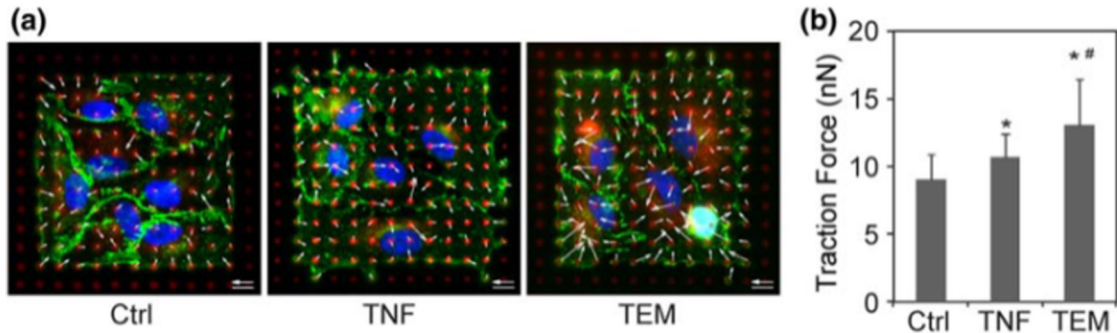


Fig. 10 (a) Fluorescent images and traction forces for control (Ctrl), TNF α -treated (TNF), and monocyte migrating (TEM) monolayers of human pulmonary artery endothelial cells (HPAECs). Structures stained are: β -catenin (cell border), monocytes (light patch), nuclei (ovals), and microposts (dots). Scale bars indicate 10 μ m; the white arrow bar indicates a vector traction force of 32 nN. (b) Bar graph indicating average tractions for these monolayers; where * $p < 0.05$ indicates comparison between TEM and Ctrl, and # $p < 0.05$ indicates comparison between TEM and TNF. (Reprinted from [427], with kind permission from Springer Science and Business Media.)

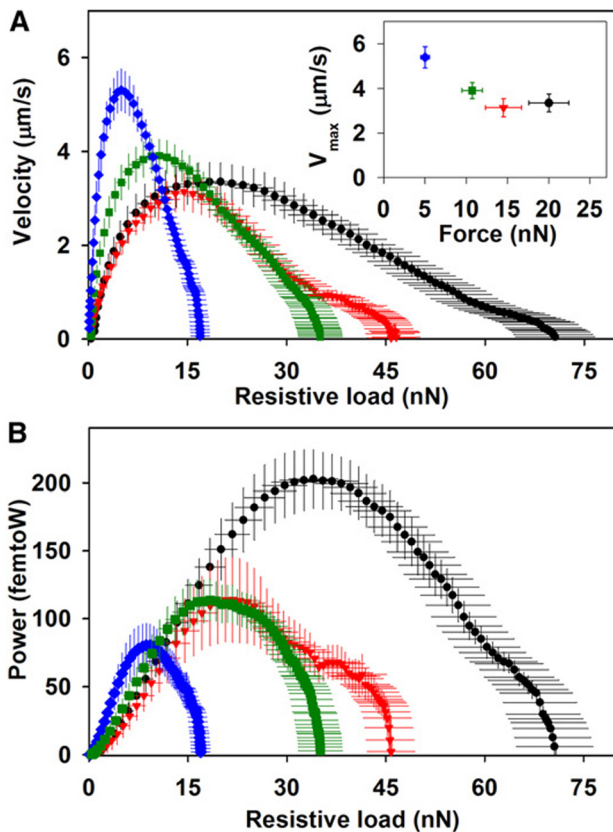


Fig. 11 Contractile velocity (A) and power (B) of cardiomyocytes from newborn Fischer 344 rats on substrates of different stiffnesses: 3 kPa (diamonds), 8 kPa (squares), 10 kPa (triangles), and 15 kPa (circles). (Reprinted from [428], with permission from Elsevier.)

Similarly, if two cells are patterned on top of the micropost arrays such that their contact area is limited, the traction force experienced by this interface can be elicited. In a recent study performed by Liu et al., changes to adherens junction size and the traction force existing at this junction were recorded. These experiments found that adherens junction size is regulated by the cell–cell tugging force, and that both quantities will increase with increasing myosin activation (Fig. 12) [432].

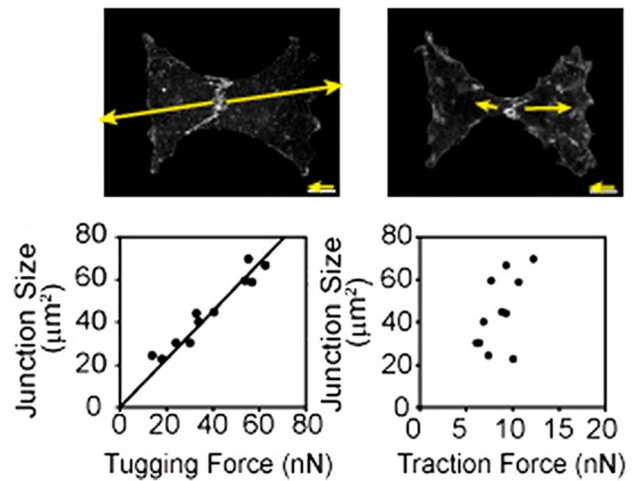


Fig. 12 Top: Tugging forces (arrows) exerted by human pulmonary artery endothelial cells (HPAECs); where adherens junctions are fluorescently stained with anti- α -catenin (cell–cell boundary). Bottom: Relationship between tugging force and junction size, as well as traction force and junction size. (Reprinted from [432], with permission from the National Academy of Sciences.)

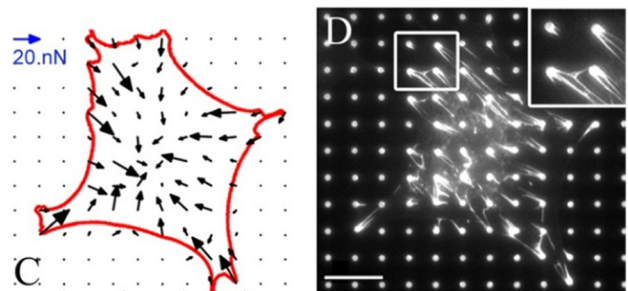


Fig. 13 (c) Traction force vector map of a representative NIH 3T3 cell, with the cell perimeter shown in red. (d) Immunofluorescence images of fibronectin (white). Scale bar represents 20 μ m. (Reprinted from Ref. [433] with permission from Elsevier.)

4.4.5 Forces Involved in Cell–Matrix Assembly. Micropost arrays have also been used to investigate the role of traction forces in extracellular matrix assembly. In experiments performed by Lemmon et al. (Fig. 13) [433], the contractile forces produced by NIH3T3 cells on microposts were recorded, while simultaneously

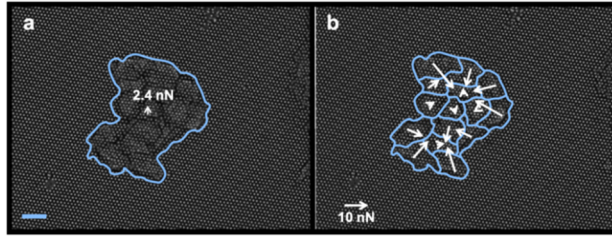


Fig. 14 (a) Average traction force vector for monolayer of by Madin–Darby canine kidney epithelial cells on a micropillar array. Scale bar = $20\ \mu\text{m}$ (b) Average reaction force vector for each individual cell [435]. (Reproduced by permission of IOP Publishing.)

measuring fibronectin fibril growth. Results indicated that individual fibril growth occurs in the direction of the traction force applied to that fibril and that fibrillogenesis is driven by the spatial redistribution of traction forces from the cell periphery toward the cell center.

4.4.6 Monolayer Forces. The ability to print large patterns of extracellular matrix proteins on the tips of the microposts enables the spatial characterization of the traction forces exerted by cell populations of various sizes. In studies performed by Saez et al., sheets of epithelial cells were cultured on top of micropost arrays. Upon investigating monolayer traction forces, it was found that the largest traction forces were created by cells along the edge of the monolayer [434]. Furthermore, cell growth was shown to align with respect to the direction of highest traction forces (Fig. 14) [435].

4.4.7 3D Configurations for Cellular Force Measurements. While various studies have shown the benefit of using micropost arrays to study the mechanics of planar cells or cell monolayers, a small number have also demonstrated the ability of micropost arrays to elicit information regarding the mechanics of three-dimensional cell populations. For example, experiments performed by Liang et al. revealed that the contractile forces produced by microthrombi increase with increasing thrombin concentration and activation time (Fig. 15) [436].

Alternatively, larger scale silicone structures can be made via the same fabrication techniques to allow for contractility measurements of multicellular tissue constructs [437]. These devices, which are commonly referred to as microfabricated tissue gauges, were pioneered by the Chen Lab at UPenn, and have been used to measure the contractility of skeletal muscle [438], cardiac muscle (Fig. 16) [439], smooth muscle [440], and fibroblast [441] tissues. Recently, Zhao et al. demonstrated the ability of this device to measure the contractility of multicellular tissues under applied force [442]. This was accomplished by attaching a nickel sphere to the top of one pillar, and then using a magnetic tweezer to actuate the sphere.

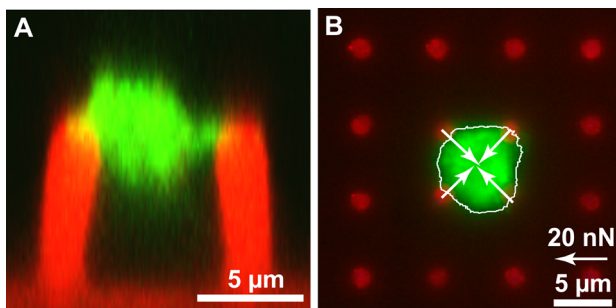


Fig. 15 Traction forces exerted by a human platelet aggregate [436]

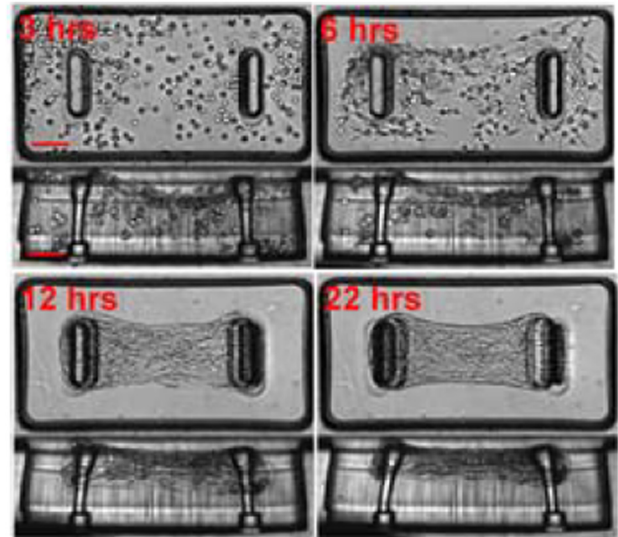


Fig. 16 Measuring the contraction of cardiac microtissues with the μTUG system. (Reprinted from Ref. [437] with permission from the National Academy of Sciences.)

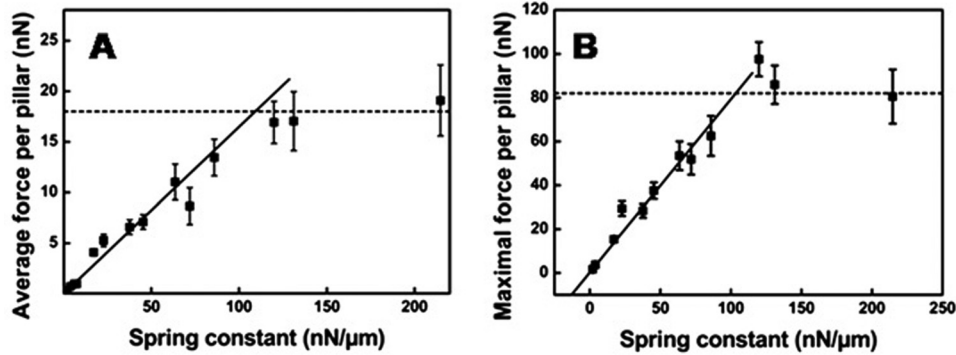
4.4.8 Effect of Micropost Stiffness. As discussed earlier, the stiffness of the entire micropost array can be altered by changing the dimensions of the microposts. In a study performed by Saez et al., it was found that the traction forces exerted by MDCK epithelial cells were proportional to the spring constant of the micropost pillars on which they were seeded [443]. This result was also found in subsequent studies performed by Ghibaudo et al. using 3T3 fibroblastic and MDCK epithelial cells. However, in these experiments, it was noted that there is a plateau of substrate rigidity, past which increases in post stiffness do not result in increases in traction forces (Fig. 17) [444].

Micropost substrate rigidity has also been found to affect cell morphology, focal adhesion area, cytoskeletal contractility, and stem cell differentiation. Han et al. found that the traction forces and focal adhesion area human pulmonary artery endothelial cells (HPAECs), 3T3 fibroblasts, and human aortic smooth muscle cells can be altered by controlling the cell spread area and density of microposts under the cell [445]. Alternatively, a study performed by Fu et al. found that stem cells seeded on rigid microposts were more spread out, displayed more highly organized cytoskeletal proteins, and had larger focal adhesion complexes than cells on soft microposts, which agrees with previous studies [444]. Furthermore, rigid microposts elicited differentiation into osteogenic cell lines, while softer microposts lead to adipogenic differentiation (Fig. 18) [446]. Simultaneous experiments showed that increases in substrate stiffness can also increase cortical cell stiffness [147]. Furthermore, Sun et al. showed that very rigid substrates are able to maintain human embryonic stem cell (hESC) pluripotency, as well as that differentiated hESCs can be distinguished from nondifferentiated hESCs via their traction forces; differentiated hESCs create much stronger traction forces, regardless of the stiffness of the underlying substrate [447].

Alternatively, micropost arrays can be fabricated such that specific regions within an individual array are stiffer than others, by designing these regions to have larger diameter posts. In experiments performed by Saez et al., MDCK epithelial cells were found to migrate in the direction of highest stiffness [448]. The same result was found in subsequent experiments with 3T3 fibroblasts and MDCK epithelial cells [444], as well as for BAECs [449]. Furthermore, it was also discovered that cellular traction forces also tend to align in the direction of highest stiffness [444].

4.4.9 Effect of Applied Mechanical Force. Due to their elastic material properties, silicone micropost arrays can be subject to a

MDCK cells



FIBROBLASTS

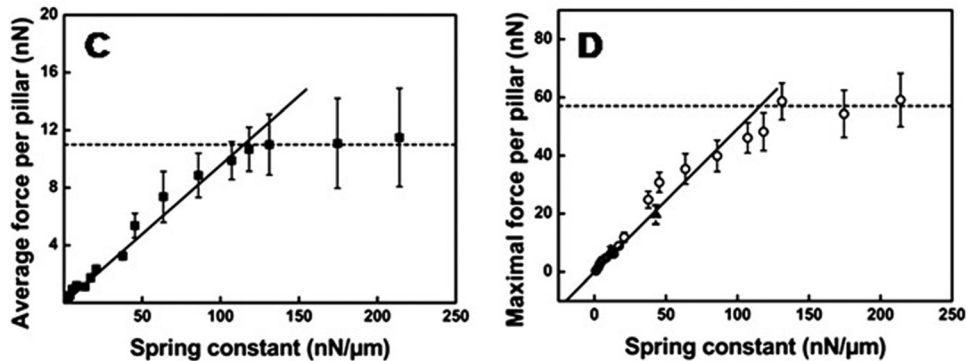


Fig. 17 Average traction force of (a) MDCK and (b) fibroblasts as a function of substrate stiffness [444]. (Reproduced by permission of The Royal Society of Chemistry.)

wide variety of high-magnitude mechanical forces without losing structural integrity. Such mechanical forces can be applied to whole cells—using techniques such as shear flow or whole membrane stretching—or to individual cell structures via individual post deflections.

To assess the effect of applying external force to individual focal adhesions on cellular traction forces, magnetic nanowires can be implanted into individual microposts and then subject to an applied magnetic field. This technique, has demonstrated that the application of concentrated forces to focal adhesions causes a decrease in cell traction forces (Fig. 19) [450], that force leads to an increase in focal adhesion assembly at the site of force application, and that multiple force applications result in greater focal adhesion growth [451].

Another realm of these studies involves the application of shear flow to cells seeded on top of microposts. In a recent study, monolayers of endothelial cells were grown on arrays of microposts and exposed to laminar or disturbed flow. These studies found that cells experiencing laminar flow had higher traction forces, higher intercellular forces, and larger focal adhesions than those under static conditions, while cells exposed to disturbed flow had lower traction forces, lower intercellular forces, and smaller focal adhesions (Fig. 20) [452]. In a similar study [453], shear flow was found to realign endothelial cells in the direction of flow, while maintaining their same spread area. In this study, the cell's contractile forces were found to instantaneously increase at the onset of flow but ultimately decrease to baseline levels.

Additionally, Mann et al. recently demonstrated the ability to mechanically strain cells on microposts by fabricating the posts on top of a thin, stretchable, PDMS membrane. This system enabled the measurement of real-time live-cell contractility during stretch events [454]. The results of this study demonstrated that

when exposed to equibiaxial stretch, vascular smooth muscle cells initially enhanced their contractile forces to resist cell deformation, and then, as the cytoskeleton reorganized, these forces were slowly reduced.

5 Computational Descriptions of Whole-Cell Mechanics

Computational models provide us with the ability to interpret experimental measurements. Depending on the complexity of the model, this interpretation can be as simple as calibrating the passive elastic stiffness of the cytoplasm and nucleus, or as complex as uncovering rate constants for the process of cytoskeletal remodeling within an active model. Single cell experimentation does not offer a clear interpretation of cell mechanical properties or substantial insight into the contribution of key biomechanical processes to cellular events without the parallel use of computational modeling. Additionally, mechanical measurement alone is limited due to complex cell geometries, complex boundary conditions, the inhomogeneous nature of a cell's materials and structures, cell remodeling over time (the initial conditions are critical), and the active response of the cell to mechanical stimuli that are applied as part of the measurement process [455].

Cells are active entities that respond to mechanical stimuli. Therefore, the application of a mechanical stimulus to a cell during an experiment is likely to result in active remodeling of that cell. Consequently, an experimentally observed response to an applied force may be in part a passive response and in part an active response. In order to correctly interpret experimental data using a model, the model should contain a description of the active mechanisms of the cell in addition to the passive

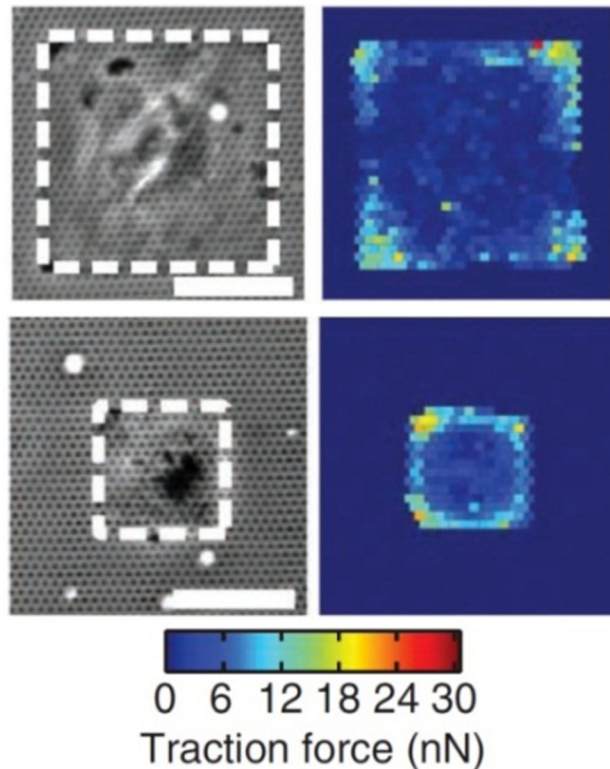


Fig. 18 Brightfield micrographs and corresponding traction force maps for micropatterned single human mesenchymal stem cells (hMSCs) exposed to (top) osteogenic differentiation medium (OM) or (bottom) adipogenic differentiation medium (AM). Scale bars, 50 μm . (Reprinted by permission from Macmillan Publishers Ltd: Nature Methods [446].)

mechanical behavior, so that the passive and active responses can be parsed.

Additionally, in order for a model to be completely encompassing of a cell's biomechanical behavior, it needs to be able to predict the response of a cell to its physical surroundings. Such active models could, for example, uncover the mechanisms by which a cell seeded on stiffer substrates exhibits a higher apparent stiffness [147,444,456,457]. Therefore, in order to be truly predictive, a constitutive framework must include the key mechanisms by which a cell responds to its physical environment in order to

interpret and predict experimentally measured responses to AFM, micropipette aspiration, compression, etc. In a sense, a truly predictive model must first be able to predict the initial conditions that exist in the cell at the beginning of an experiment so that the active behavior of a cell during the experiment can then be simulated.

The main drawback with computational models is that they require complex mechanics in order to capture the essential features of active cell biomechanical behavior. Such constitutive formulations require a large number of parameters that are highly nonlinear and consequently computationally expensive. The real challenge is that a model should be able to robustly predict a vast array of experiments. Several frameworks have fallen short in accomplishing this task, but we believe that the framework used for the bio-chemo-mechanical model discussed in a later section of this paper proves quite successful in this respect.

The main category of computational models used to represent cellular mechanics is continuum models. Continuum models are generally solved using the finite element method. This method, which has been implemented in various different commercially available software platforms, incorporates material and geometrical nonlinearities into a simulation for the mechanical response of geometrically complex entities, as well as it is able to accurately simulate contact and boundary conditions. Several studies have used well established elastic, hyperelastic, or viscoelastic material formulations to model cells. These constitutive formulations are readily available in commercial software. However, as previously mentioned, the ability of these passive models to replicate cell behavior is limited. In order to model active cellular behavior, material formulations incorporating biomechanical processes must be incorporated into finite element solvers.

In this section of the paper, we will review several commonly used whole-cell models for cell mechanics, including both passive and active models. Passive models assume that a cell will respond passively to mechanical stimuli whereas active models incorporate key biomechanical processes that underlie cell behavior. By extension, active models possess the ability to simulate the remodeling of cells when exposed physical stimuli.

5.1 Liquid Drop Models. A fundamental category of passive models encompasses the Newtonian liquid drop model, compound Newtonian liquid drop model, shear-thinning liquid drop model, and the Maxwell liquid drop model. In general, these models assume that cells are composed of one or more layers of cytoplasmic fluids, surrounded by prestressed cortical shells. These formulations were mainly developed to account for the rheological response of leukocytes during micropipette aspiration [458].

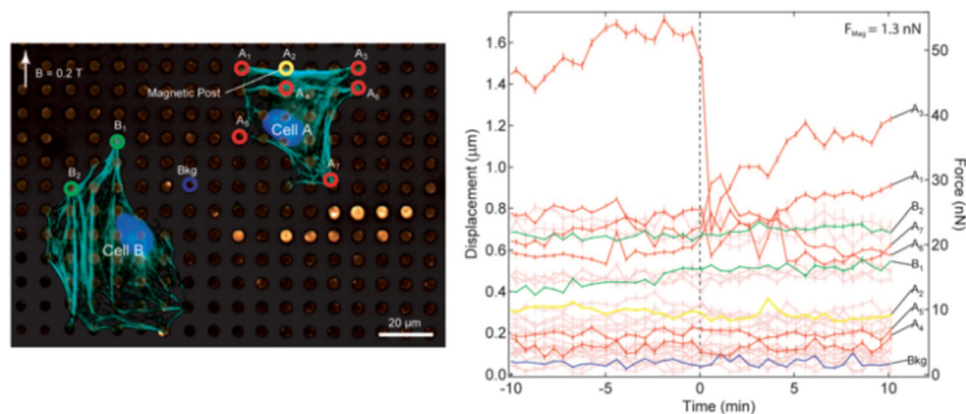


Fig. 19 (A) Immunofluorescent staining of cell A, force-stimulated with a magnetic post, and cell B, unstimulated control. Stained structures are: actin (cell cytoskeleton), nuclei (ovals), and PDMS (dots). (B) Plot of displacement and force versus time for all posts for cell A. Onset of force stimulation is indicated by dashed line ($t = 0$). (Reprinted from [450], National Academy of Sciences, U.S.A.)

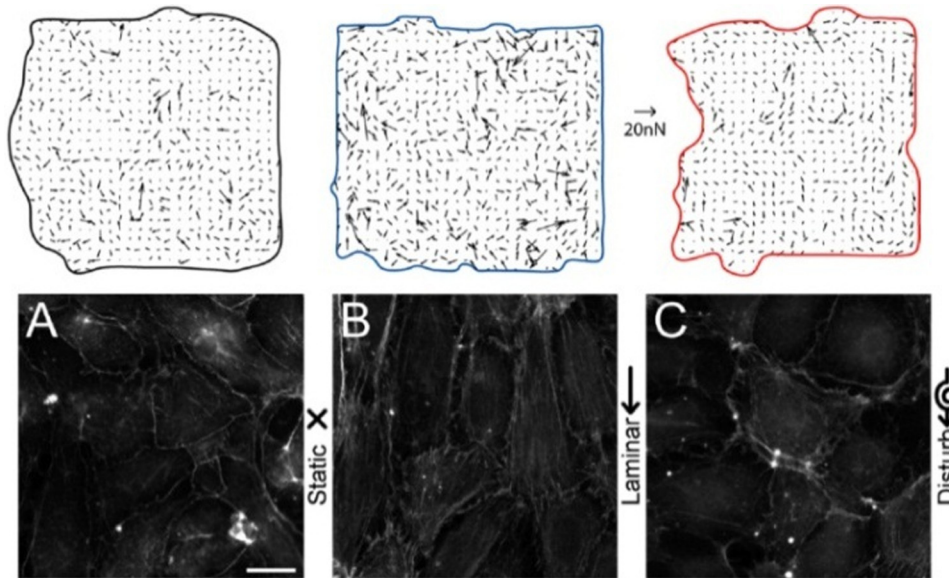


Fig. 20 Top row: vector maps of traction forces measured from microposts for static (left), laminar (center), and disturbed (right) monolayers. Bottom row: β -catenin staining for monolayers on flat substrates exposed to static (A), laminar (B), or disturbed flow (C). Scale bar $20\ \mu\text{m}$ [452].

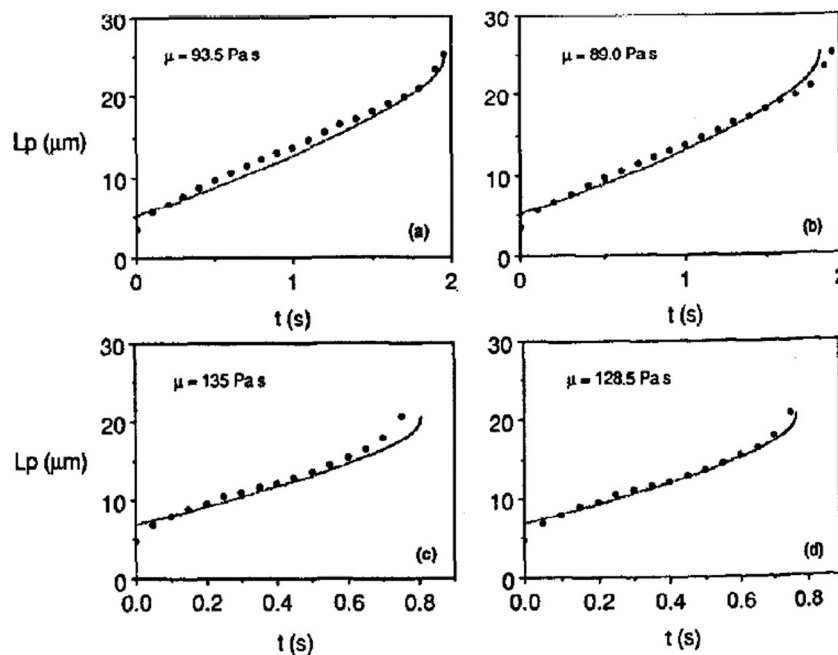


Fig. 21 Comparison between experimental (dots) and computational (line) results for the micropipette aspiration of neutrophils. Top: data for an aspiration pressure of $1\ \text{kPa}$, and Bottom: data for an aspiration pressure of $2\ \text{kPa}$. The viscosities in panels on the left were determined using a slope-matching technique, while those in the panels on the right were determined using a best fit between the computed and experimental data [461].

5.1.1 Newtonian Liquid Drop Model. In the Newtonian liquid drop model, the cell's interior is assumed to be a homogenous, viscous, Newtonian liquid. Alternatively, the cell's cortex is represented by a layer of isotropic, viscous fluid with static tension and no bending resistance [458,459].

The Newtonian liquid drop model is able to predict the overall deformation of a cell and its recovery behavior during micropipette aspiration (Fig. 21). However, it is unable to capture the initial rapid entry behavior of the cell into the pipette, and its

immediate morphological changes after ejection from the pipette [458,460–462].

5.1.2 Compound Newtonian Liquid Drop Model. In order to account for some of the discrepancies between experimental and numerical results found when using the Newtonian liquid drop model, a compound Newtonian liquid drop model was developed. This model defines cells to be composed of two different layers: the cytoplasm, and the nucleus [458]. Essentially, the compound

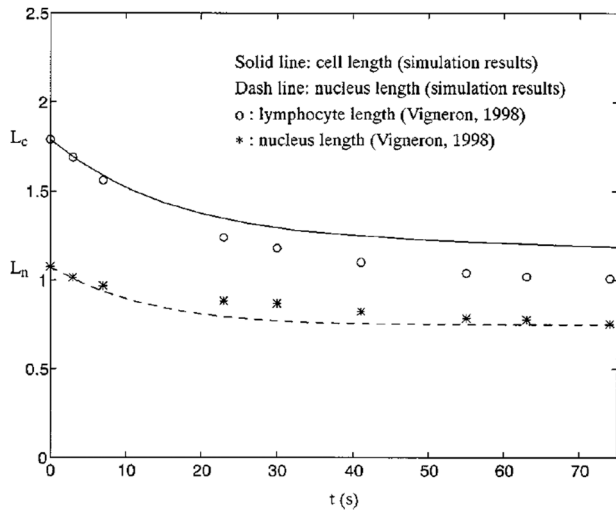


Fig. 22 Recovery curves for whole cell and nucleus aspiration length versus recovery time for lymphocytes. Solid and dashed lines represent computed recovery lengths for the cell and nucleus, respectively. Open circles and asterisks correspond to the experimental data for the cell and nucleus, respectively. (Reprinted from Ref. [464], with permission from Springer Science and Business Media.)

drop can be thought of as three incompressible, Newtonian fluid layers of different densities and viscosities, separated by layers of constant surface tension [463]. Following these definitions, the momentum continuum equations for the cell can be described by the velocity and pressure of the material within each region, the viscosities of the three fluids, and the forces transmitted through the interfaces between the different fluid regions [463].

Simulations conducted using the compound Newtonian liquid drop model have found that it is able to predict a cell's initial deformation behavior more accurately than its predecessor (Fig. 22) [463]. This model is also able to predict cell ejection recovery behavior to a certain extent [464]. However, this ejection behavior is largely dependent on the material values chosen to represent the surface tension and viscosity of the different cell layers, and these values can be combined in a number of different ways to yield a particular rheological behavior [465]. Therefore, correct predictions of ejection behavior necessitate the performance of a large number of calibration experiments.

5.1.3 Shear-Thinning Liquid Drop Model. The shear-thinning liquid drop model assumes that the cytoplasm of a cell acts as non-Newtonian fluid. This model accounts for changes in cytoplasmic viscosity with applied shear rates. Specifically, there is a decrease in cytoplasm viscosity with increasing aspiration pressure, i.e., shear rate [461,466], which follows a power-law relationship. When this relationship is substituted into the constitutive relationship for a liquid drop, the result is the governing equation for the shear-thinning liquid drop model.

When compared to the Newtonian model, the shear-thinning liquid drop model shows an improved ability to capture the non-linear deformation behavior of a cell as it enters a micropipette. This model can also describe the dependence of aspiration rate on pipette diameter and can describe a cell's ejection behavior [467]. However, it is unable to reproduce the rapid entry behavior of a cell into the micropipette (Fig. 23) [465]. Furthermore, the concept of shear-thinning for cells has its drawbacks. Specifically, dynamic measurements of cells subjected to small strain deformations using magnetic twisting cytometry have seen that a large number of cell types—smooth muscle cells, neutrophils, epithelial cells, carcinoma cells, and macrophages—fail to exhibit shear-thinning behavior [468].

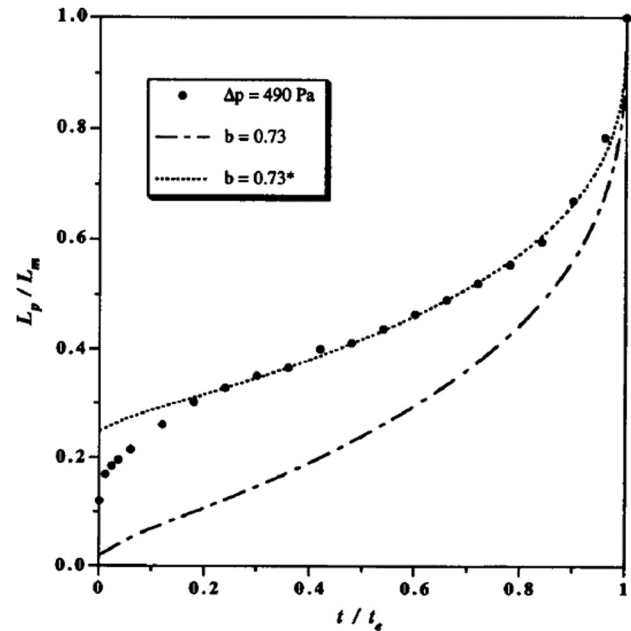


Fig. 23 Comparison between the shear thinning model and experimental results for a neutrophil entering a $4\ \mu\text{m}$ diameter pipette. Where dark circles indicate the experimental results, dashes indicate the model results, and small dots indicate model results when the cell is given an initial cell projection length. (Reprinted from Ref. [466] with permission from Elsevier.)

5.1.4 Maxwell Liquid Drop Model. The Maxwell liquid drop model was developed in order to capture the rapid entry of cells into a micropipette at the beginning of an aspiration test. This model is defined in the same manner as the Newtonian liquid drop model, but assumes that the cytoplasm acts as a Maxwell element (elastic spring in series with a dashpot).

It has been shown that the Maxwell model is able to predict the rapid entry and recovery behavior of leukocytes subject to small strains from micropipette aspiration [469]. However, when this same model was used for the finite element simulations of large deformations by micropipette aspiration, it was unable to replicate the experimental results without applying a shear-thinning behavior to a cell's viscosity and elasticity (Fig. 24) [470,471]. The inability of the Maxwell and Newtonian models to accurately simulate both small and large scale cell deformation without adjustments of the material parameters highlights the need for nonclassical models and/or active models that incorporate dynamic remodeling of the cell in response to mechanical stimuli.

5.2 Solid Elastic Models. Solid elastic models assume that the cell is composed of one or more homogenous material layers. In general, there are two kinds of elastic solid models: the linear-elastic model and linear-viscoelastic model.

5.2.1 Linear-Elastic Solid Models. In the linear-elastic solid model, the cell is defined to be a solid with homogenous, elastic properties governed by Hooke's law. Therefore, the elasticity of the cell can be determined from experimentally obtained values of stress and strain. However, more often than not, the techniques used to determine cell material properties, apply shear forces to the cell (or cells) of interest. In such cases, the shear modulus of the cell can be determined from shear stress and strain measurements, and the elastic modulus of the cell can be calculated from the Poisson's ratio of the cell.

While linear elastic models are useful for determining estimates of cell material properties, they are greatly oversimplified when compared to living cells. As discussed in the introductory section of this chapter, living cells are surrounded by a lipid membrane,

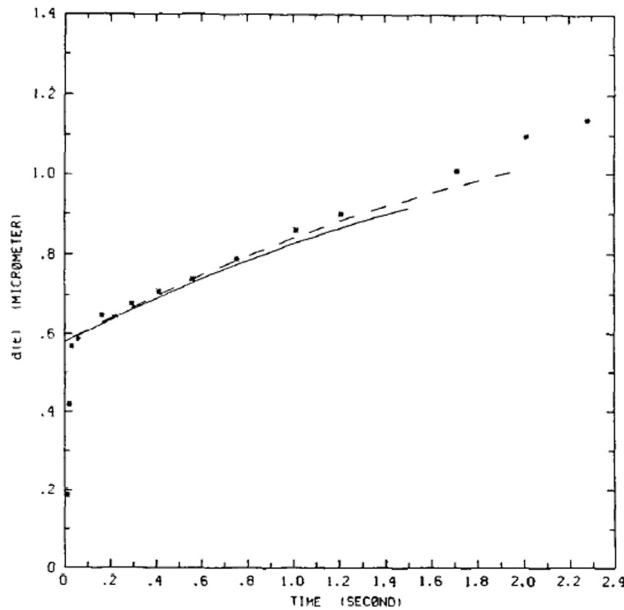


Fig. 24 Comparison of leukocyte displacements during micropipette aspiration to series (dashed) and FEA (solid) solutions of the Maxwell liquid drop model [469]

which is filled with fluid (cytosol), and supported by the cell cytoskeleton. Therefore, it is expected that the cell would have both fluidlike and solidlike properties. In order to account for this, linear-viscoelastic solid models were developed as a means of capturing both of these material phase properties.

5.2.2 Linear-Viscoelastic Solid Models. In a linear-viscoelastic model, the normal stress experienced by the cell is assumed to be linearly related to the strain rate in the normal direction via the normal viscosity of the cell. This is equivalent to a Maxwell model in parallel with a spring element. Like the linear solid model, this relationship can be rewritten with shear terms to yield a constitutive equation for this model [458].

Both the linear-elastic and linear-viscoelastic solid models have been used to determine the material properties of chondrocytes (Fig. 25) [64,288,472], endothelial cells [70,473], and leukocytes [474]. They have also been coupled with other models to investigate changes to cellular mechanics during migration [475] and cellular deformation [79,105,476,477]. Recently, realistic three-dimensional finite element models of osteocytes were derived from confocal imaging of the lacunar-canalicular network, and used to predict the loading conditions experienced by osteocytes during normal physiological activities [478]. Simulations revealed that these passive linear-elastic models predicted 350–400% greater strain amplification experienced by osteocytes compared to an idealized cell model (Fig. 26).

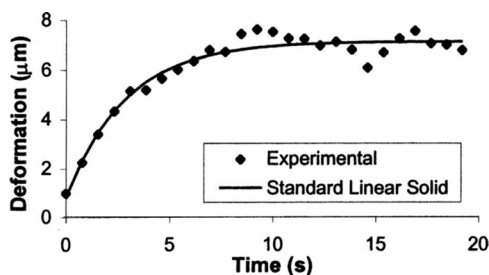


Fig. 25 Comparison between experimental and computational results for bovine articular chondrocytes subject to creep indentation [106]

A significant limitation of elastic and viscoelastic cell models is that a unique set of material properties cannot be used to accurately simulate the behavior of round and spread cells. An artificial elevation of elastic moduli for spread cells is required to capture the reduction in deformability due to the alteration in the cell cytoskeletal structures [479,480]. This important consideration can be addressed by simulation of the active bio-chemo-mechanical processes that govern cytoskeletal remodeling, as discussed in Sec. 6.

5.3 Power-Law Rheology Model. This modeling approach was developed to account for the responses of adherent cells that are subjected to time-varying forces. It is based on empirical observations that a large number of “soft” materials exhibit similar rheological properties. One of the most central of these rheological properties is that these materials have microscopic constituents, which, like glass, are unable to equilibrate thermodynamically. Because of this property, these materials are sometimes called soft-glassy materials. It has been proposed that models applicable to such materials are also able to describe the frequency-dependent rheology of cells that follows a power-law trend [481]. Expanding upon this idea, various experiments have shown that cells can demonstrate dynamical heterogeneity, physical aging, and shear-induced rejuvenation, which further support the concept that a cell is a soft-glassy rheological material [482]. The material law given for power-law, frequency-dependent, soft glassy materials is as follows [483]:

$$G'(\omega) = G_0(\omega/\omega_0)^{x-1} \cos\left[\frac{(x-1)\pi}{2}\right] \quad (2)$$

$$G''(\omega) = \eta G'(\omega) \quad (3)$$

$$\eta = \tan\left[\frac{(1-x)\pi}{2}\right] \quad (4)$$

where $G'(\omega)$ and $G''(\omega)$ are the frequency-dependent storage and loss moduli of the material, respectively, ω is the frequency of excitation, x is the temperature ($1 \leq x < 2$), G_0 is the shear storage modulus of the material at the glass transition temperature ($x = 1$), ω_0 is the reference frequency, and η is the structural damping coefficient. Assuming that a cell has reached its steady-state response after experiencing an applied shear strain given by $\gamma(t) = \gamma_0 e^{i\omega t}$, then the shear stress will be [483]

$$\tau(t) = G(\omega)\gamma_0 e^{i\omega t} \quad (5)$$

where $G(\omega) = G'(\omega) + iG''(\omega)$ is the complex shear modulus of the material. Thus, the magnitude of the shear stress can be given by

$$|\tau_0| = |\gamma_0| \sqrt{[G'(\omega)]^2 + [G''(\omega)]^2} \quad (6)$$

The power law model differs from spring-dashpot models, like the Newtonian and Maxwell models, in its ability to account for frequency-dependent cellular responses [458]. This model has been used to simulate the response of cells to magnetic twisting cytometry (Fig. 27) [468,481,484,485] and AFM [486].

5.4 Biphasic Models. The biphasic model accounts for the liquid and solid composition of the cytoplasm by treating it as a combination of a solid phase, and a fluid phase that is able to diffuse through the solid phase. Momentum exchange occurs through friction between the two phases. In the general definition of a biphasic model, the solid phase is treated as a linear-elastic material, while the fluid phase is assumed to be an inviscid fluid

$$\sigma_s = -\phi_s p \mathbf{I} + \lambda_s \text{tr}(\epsilon) \mathbf{I} + 2\mu_s \epsilon \quad (7)$$

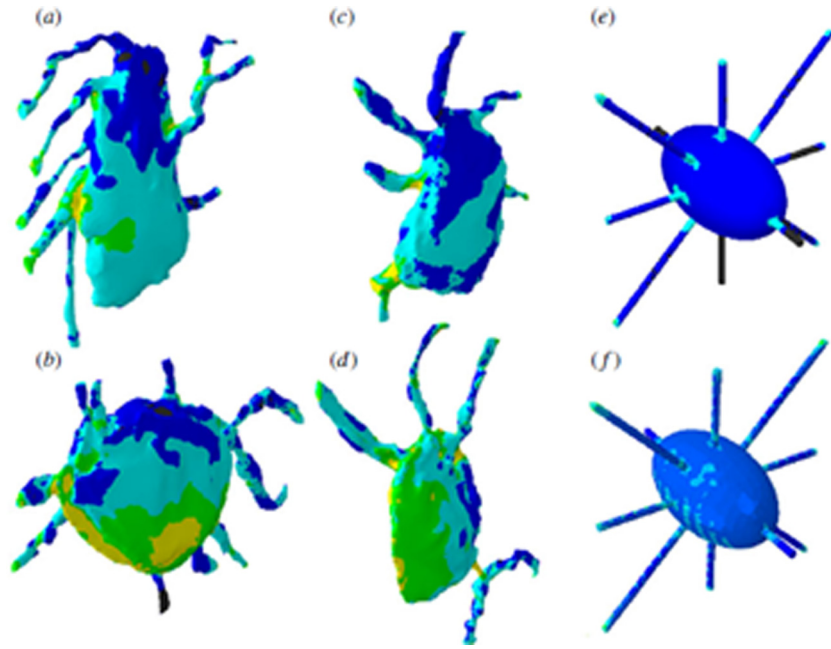


Fig. 26 Strain distribution in four confocal image-derived models of osteocytes (a)–(d) and idealized osteocytes without ECM projections (e), and with ECM projections included (f) under global loading of $3000 \mu\epsilon$. (Figure adapted from Ref. [478] with permission from The Royal Society.)

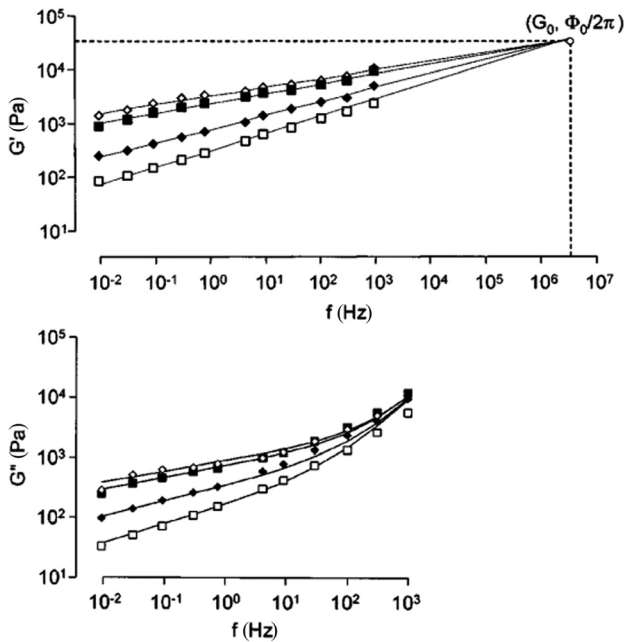


Fig. 27 G' and G'' versus f in HASM cells under control conditions (black square); and after 10 min treatment with the contractile agonist histamine (white diamond), the relaxing agonist DBcAMP (black diamond) and the actin-disrupting drug cytochalasin D (white square). (Figure reprinted with permission from Ref. [468] by the American Physical Society.)

$$\sigma_f = -\phi_f p \mathbf{I} \quad (8)$$

where the subscripts s and f indicate the solid phase and fluid phase, respectively, σ is the Cauchy stress tensor, ϵ is Cauchy's infinitesimal strain tensor, \mathbf{I} is the identity tensor, p is the fluid pressure, ϕ_s and ϕ_f are the solid and fluid volume fractions,

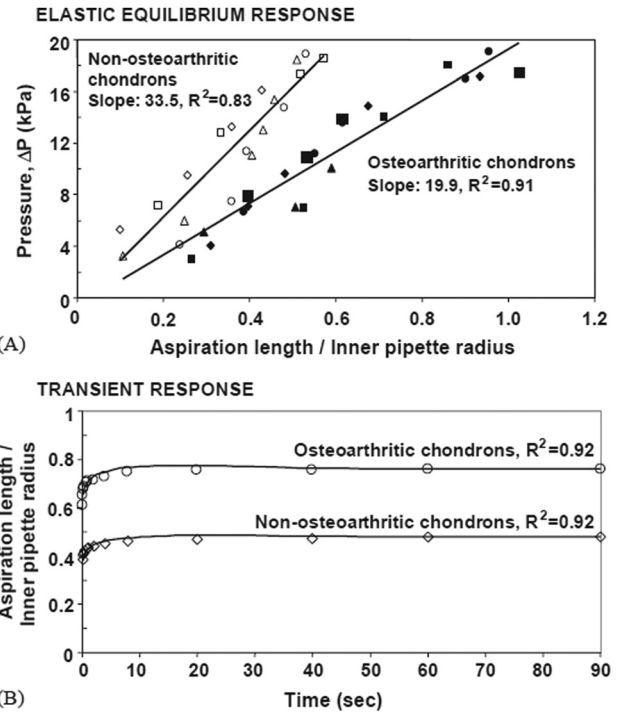


Fig. 28 Comparison between equilibrium (a) and creep (b) responses of osteoarthritic and nonosteoarthritic chondrons subject to aspiration pressure ΔP , to the biphasic model. (Reprinted from Ref. [487] with permission from Elsevier.)

respectively, and λ_s and μ_s are the Lamé constants for the solid phase [458].

Simulations of this model, and its derivatives, have been particularly useful in determining the mechanics of chondrons (Fig. 28) [487–494]. It has also been adapted for three-dimensional simulations [495,496], and has been used in concurrence with other standard models [497]. However, some studies have shown that

the biphasic model is unable to capture initial deformation characteristics of cells under compression [488].

5.5 Tensegrity. The tensegrity model represents the cell as a mechanically stable structure, composed of compression-bearing struts and tension-bearing cables [498]. The cables create an initial prestress in the cell model, which is resisted by the struts, in order to maintain a system in mechanical equilibrium [499]. The physiological parallels to these compressive elements are microtubules or highly bundled actin filaments, which resist compressive loads, while stress fibers, actin filaments, and intermediate filaments are a physiological representation of the cables, which resist tensional loads [32,499–501]. These elements are connected through pin-joints, which represent cross-linking or molecular binding, and frictionless loops, which represent connections that allow for sliding of these structures past one another [502]. Closely related to the tensegrity model are open lattice models, which assume that the cell is composed of compression members, surrounding an open area of fluid cytosol [503,504].

The tensegrity model has been shown to have the ability to predict the linear relationship between cellular prestress and cell stiffness seen in experiments [28,505,506], the frequency dependence of a cell's rheological properties (Fig. 29) [507,508], and stress-dependent spatial rearrangement of cell structures [509,510]. These models have also been used to elucidate mechanotransduction pathways [511–513], and have been adapted to allow for tensegrity structures of higher complexity and enhanced physiological relevance, i.e., models that incorporate different material properties for distinct cell structures, that have nonlinear tensegrity components, and that incorporate molecular motor movements [502,514–520]. However, the tensegrity model predicts a limited frequency dependence due to its simplistic representation of cytoskeletal structure. Additionally, in this model, cell components are arranged in an idealized fashion, which is very organized when compared to actual cells. Furthermore, a large percentage of the cell is a fluid, so compressive loads can also be supported by hydrostatic pressures, which the tensegrity model does not capture [51].

5.6 Semiflexible Chain Model. The semiflexible chain model was developed as a means to explain how tension enables

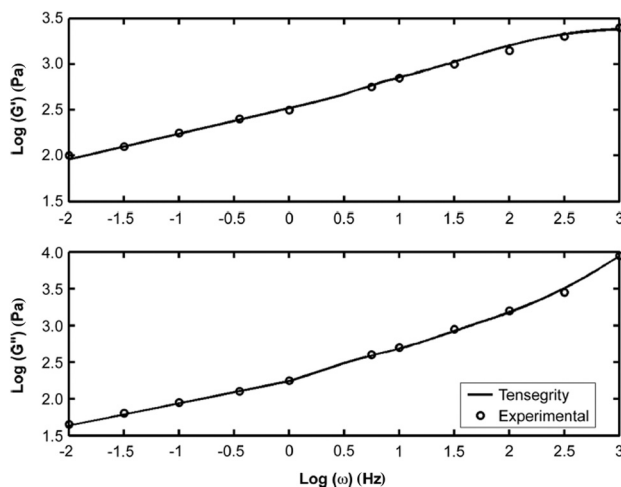


Fig. 29 Comparison between model predictions of elastic (G') and frictional (G'') moduli dependence on frequency (ω) for a heterogeneous tensegrity structure and experimental results from human airway smooth muscle cells. Circles represent experimental data replotted from Fabry et al. [481]; lines indicate data generated by the tensegrity model. (Reprinted from Ref. [507] with permission from Springer Science and Business Media.)

cells to maintain mechanical stability. This model is based on the idea that when a thermally fluctuating chain (like a cytoskeletal filament) is stretched, the number of possible chain configuration states is reduced. In addition, a reduction in the number of configuration states is associated with lower entropy in the chain and stiffening of the chain.

In the semiflexible chain model, actin filament links are classified by their persistence length l_p , which is the length above which bending due to thermal fluctuations becomes significant [28]. The elastic response of the network results from tension in these chain segments, which is a function of the extension $L - L_0$, where L_0 is the unstretched length of the segment. When this network is stretched by a tension τ , the energy per unit length of the chain is defined by changes in the bending of the chain and the work that the chain does in contracting against the applied tension. This energy per unit length can be written as [521]

$$H = \frac{1}{2} \kappa (\nabla^2 u)^2 + \frac{1}{2} \tau (\nabla u)^2 \quad (9)$$

where $\kappa \cong l_p kT$ is the chain bending modulus, k is the Boltzmann constant, T is the temperature, and u is the transverse deviation of the chain away from its straight conformation. For this definition, the shear modulus can be estimated from $G' \sim kT/\xi^3$, where ξ is the characteristic mesh size of the chain network. For a network of stiff chains, this mesh size is given by $\sim 1/\sqrt{ac_A}$, where c_A is the concentration of actin monomers of size a .

This representation has been found to be good for describing actin filament organization and the dependence of cell material properties on actin concentration (Fig. 30), but is unable to deliver information regarding the effect of alterations to the cell's external mechanical environment on the cell.

5.7 Dipole Polymerization Model. The dipole polymerization model represents the active remodeling of the cytoskeleton as actin–myosin dipoles, which are defined by their orientation, as well as the magnitude of the forces that they exert. This model is used to characterize a cell shortly after it has adhered to a substrate. In this state, actin filaments in the cytoskeleton are assumed to be isotropic, and then develop into anisotropic stress fibers over time. When actin–myosin dipoles are oriented in the direction of an applied tensile stress, a contractile force opposes this stretch and restores the system to equilibrium. In this manner, actin–myosin dipoles polarize in response to the anisotropy of applied elastic stress [28]. When a force is applied to a cell population, the polarization of the cells in the direction of the principal strain can be written as [522]

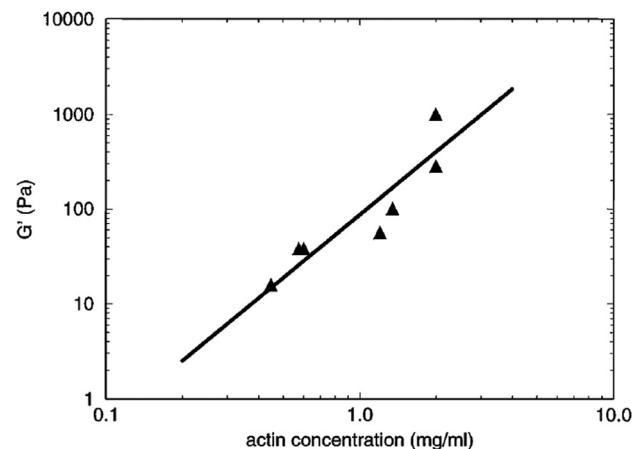


Fig. 30 The shear modulus G' of actin networks as a function of concentration; based upon the semiflexible chain model. (Figure reprinted with permission from Ref. [521] by the American Physical Society.)

$$P_{ij} = \rho (\langle p_{ij} \rangle - \langle p_{ij} \rangle_0) \quad (10)$$

where P_{ij} is the polarization tensor, ρ is the number of cells per unit volume, and $\langle p_{ij} \rangle_0$ and $\langle p_{ij} \rangle$ are the average cell polarization tensors before and after the force is applied, respectively. The total excess stress due to the applied stress σ_{ij}^a and the polarization stress P_{ij} is the sum of these two values. The applied stress is given by $\sigma_{ij}^a = \epsilon C u_{ij}$, where ϵ is the elastic permittivity tensor, C is the elastic moduli of the system, and u_{ij} is the excess strain in the system. From this definition, the optimal orientation of a cell in the presence of an elastic strain can be predicted by minimizing the interaction energy W between the cellular dipole p_{ij} with the local strain u_{ij}^{loc}

$$W = \frac{a_s p T}{2\mu} \cos^2 \theta + \left(\frac{a_v}{9\kappa} - \frac{a_s}{6\mu} \right) \quad (11)$$

$$a_v = \frac{\epsilon_v \kappa}{\tilde{s}_v (\kappa - \tilde{\kappa}) + \tilde{\kappa}} \quad \text{where} \quad \tilde{s}_v = \frac{1 + \tilde{\nu}}{3(1 - \tilde{\nu})} \quad (12)$$

$$a_s = \frac{\epsilon_s \mu}{\tilde{s}_s (\mu - \tilde{\mu}) + \tilde{\mu}} \quad \text{where} \quad \tilde{s}_s = \frac{2(4 - 5\tilde{\nu})}{15(1 - \tilde{\nu})} \quad (13)$$

In these equations, κ is the bulk modulus, μ is the shear modulus, T is the uniaxial tension, and $\tilde{\nu}$ is the effective Poisson's ratio.

This model was originally developed to account for experimental variations in the sizes of cells seeded on substrates or matrices of different rigidities (Fig. 31), and was used to evaluate the average cell orientation, the mean polarization stress, and the effective elastic constants of the material [522]. It has the ability to predict the monotonic increase in cellular forces with increases to matrix rigidity in one-, two-, or three-dimensional simulations, and alignment of stress fibers parallel to the long axis of cells [522–525]. However, it does not account for the molecular mechanism of stress-fiber formation [28].

5.8 Brownian Ratchet Models. Brownian ratchet models are a group of active models based upon the idea that chemical reactions generate cellular protrusive forces during actin and microtubule polymerization, via rectifying Brownian motion. The elastic Brownian ratchet model is a generalized form of the Brownian ratchet model which defines the polymer as an elastic material, and allows for the relaxation of the growing polymer tips. Generally, these models are used to describe adherent cells [28].

5.8.1 Brownian Ratchet Model. In the Brownian ratchet model, the ratchet velocity is given by [526]

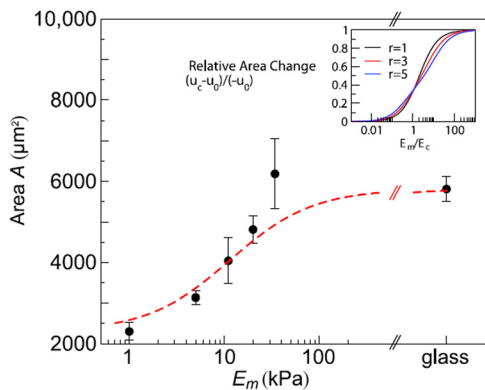


Fig. 31 Modulation of cell spreading area with matrix rigidity. The main panel shows a quantitative fit of the dipole polymerization model to experimentally measured values for human mesenchymal stem cells [524]. (Reproduced by permission of IOP Publishing).

$$v = \delta \frac{\alpha \int_{\delta}^{\infty} c(x) dx - \beta \int_0^{\infty} c(x) dx}{\int_0^{\infty} c(x) dx} \quad (14)$$

where $c(x)$ is the density of polymerized actin fibers at the location x , α , and β are polymerization and depolymerization constants, respectively, and δ is the half size of an actin monomer. When depolymerization is negligible ($\beta \rightarrow 0$), the relationship for velocity v and load ω can be described by

$$v = \frac{2D}{\delta} \left[\frac{(\mu - \omega) \left(\frac{\omega^2}{2} \right)}{\omega^2 + \mu(e^{\omega} - \omega - 1)} \right] \quad (15)$$

$$\mu - \omega = \frac{\alpha \delta^2}{D} \left(\frac{1 - e^{-\mu}}{\mu} \right) \quad (16)$$

$$\omega = \frac{f \delta}{k_B T} \quad (17)$$

where D is the diffusion coefficient for the actin monomers, f is the applied load, k_B is Boltzmann's constant, T is the absolute temperature, ω is the dimensionless work done against the load in adding one monomer, and μ is a dummy variable, which can be determined by solving Eq. (16). When the polymerization velocities are very slow in comparison to the ratchet velocity, then this simplifies to $v = \delta(\alpha e^{-\omega} - \beta)$ (Fig. 32).

5.8.2 Elastic Brownian Ratchet. Alternatively, the load-velocity relationship for the elastic Brownian ratchet, as well as the optimal filament angle, are dependent on the length of the filaments and the magnitude of the applied force [527] (Table 3). In this table, ω has the same definition as was given for the Brownian ratchet model, $\epsilon = \kappa_0 \delta^2 / 2k_B T$, $\hat{f} = \omega / 2\epsilon = f / \kappa_0 \delta$, δ is the bending distance of the filament, λ is the persistence length of the filament, l is the filament's fixed length, k_{on} and k_{off} are equivalent to α and β , and M is the concentration of actin monomers. Recently, Lin et al. refined this model to include bonding between actin filaments and the load surface, actin fiber nucleation, and actin filament tip capping (Fig. 33) [529].

Both the Brownian Ratchet model and the Elastic Brownian Ratchet model are able to account for dynamic force production-driven propulsions, have proven accurate in eliciting protrusion dynamics, and derivatives of these models have been used to describe the protrusive motion developed by lamellar [530] and

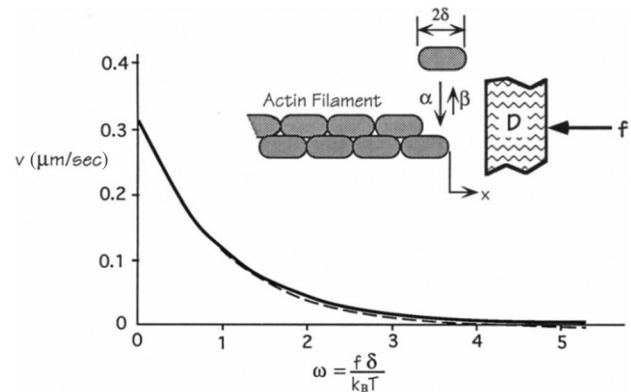


Fig. 32 Speed of the polymerization ratchet v driven by a single actin filament as a function of dimensionless load force ω . The solid line represents the ratchet speed when depolymerization is negligible, while the dashed line is valid when polymerization is much slower than diffusion. (Reprinted from Ref. [526] with permission from Elsevier.)

Table 3 Optimal velocity and angle equations for elastic Brownian Ratchet model

Condition	Meaning	Optimal angle	Optimal velocity
$\varepsilon \ll 1$	Flexible filaments	$\theta_c \sim 0$	$V \approx \delta k_{on} M$ (18)
$\hat{f} \ll 1$	Small applied force		
$\varepsilon \ll 1$	Flexible filaments	$\theta_c \approx \cos^{-1}\left(\frac{1}{\omega}\right)$	$V \approx \frac{k_B}{T} \left(\frac{k_{on} M}{e} - k_{off}\right)$ (19)
$\omega \gg 1$	Large applied force		
$\varepsilon \sim 1$ or $\varepsilon \gg 1$	Stiff filaments	$\theta_c \approx \tan^{-1}\left(\frac{2\delta\sqrt{\lambda}}{\beta^{3/2}}\right)$	$V \approx \delta \cos \theta_c (k_{on} M - k_{off})$ (20)
$\omega \ll 1$	Small applied load		
$\varepsilon \approx 1$ or $\varepsilon \gg 1$	Stiff filaments	$\theta_c \approx \cos^{-1}\left(\frac{1}{\omega}\right)$	$V \approx \frac{k_B}{T} \left(\frac{k_{on} M}{e} - k_{off}\right)$ (21)
$\hat{f} \gg 1$	Large applied load		

filopodial [531–533] structures during cellular migration. Additionally, the elastic Brownian model accounts for force production from thermal motions of polymerizing actin filaments. However, both models have yet to be implemented for the whole cell [526,527], and they cannot be solved without a priori load, i.e., a designated initial loading state [534].

5.9 Stress-Fiber Reorganization Model. This model, which was developed by Kaunas et al., was originally developed to describe the reorganization of stress fibers following mechanical stretch. It is based on the observation that stress fibers are pre-extended at a “homeostatic” level under static conditions, and that externally applied changes in stress fiber length results in the dissociation of stress fibers [535]. In this model, the rate of stress fiber assembly is defined as follows:

$$\frac{d\Phi^i}{dt} = -k^i \Phi^i \quad (22)$$

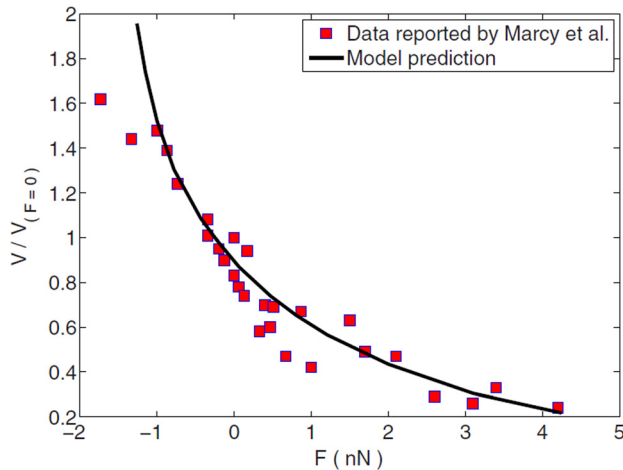


Fig. 33 Comparison between the model prediction [529] and the experimental data [528] for normalized ratchet speed V versus load force F . (Figure reprinted with permission from Ref. [529] by the American Physical Society.)

where Φ^i is the mass fraction of stress fiber i and k^i is its reaction rate constant, which is a function of the fiber stretch α^i :

$$k^i = k_0 \left[1 + k_1 \left(\frac{\alpha^i - \alpha_0}{\alpha_0} \right)^2 \right] = k_0 [1 + k_1 (\Delta\alpha^i)] \quad (23)$$

where k_0 and k_1 are constants, and α_0 is the homeostatic stretch level.

This model accurately captures the experimental observation that stress fibers align parallel to the direction of stretching under uniaxial stretch conditions whereas fibers are remain unaligned in response equibiaxial stretching (Fig. 34).

Recently, Kaunas et al. refined this model definition to include a relationship between fiber dissociation and fiber strain rate [537]. In this refined model, if a stress fiber strain rate is too high, then it is assumed that actin–myosin interactions cannot occur and the stress fiber force is obtained from the elastic properties of the stress fiber. If the strain rate is sufficiently low then actin–myosin

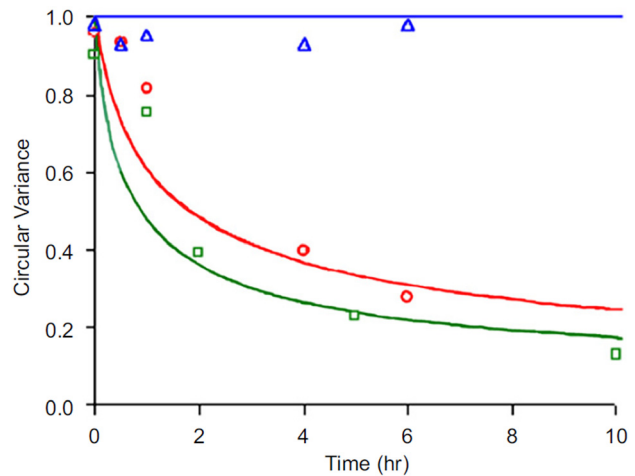


Fig. 34 Predicted (solid lines) and experimentally reported [536] (symbols) response to equibiaxial stretch (10% strain at 1 Hz - triangles) and uniaxial stretch (10% strain at 1 Hz - circles; 10% strain at 0.5 Hz - squares). (Reprinted from [535] with permission from Elsevier.)

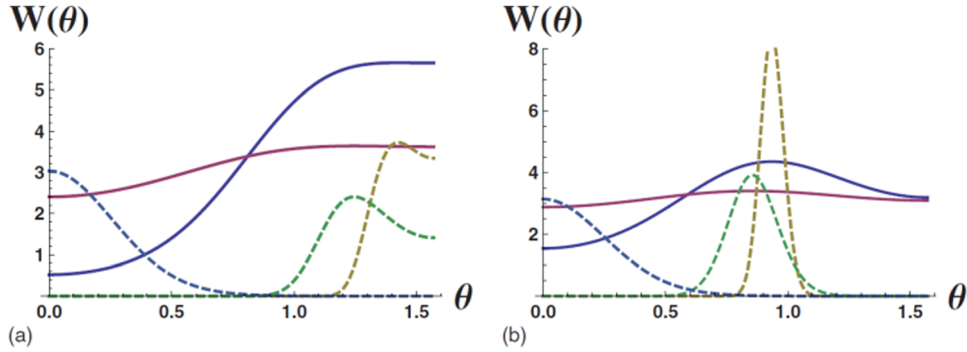


Fig. 35 $W(\theta)$, the distribution of angles versus angle (in radians) of cells controlled by stress (a) and strain (b). The dashed curves are for $Ts = 0.001$ (scaled temperature) and scaled frequencies $\omega = 10, 0.5, 0.001$ (uppermost right, lower right, and left, respectively). The solid curves are for $Ts = 0.1$ with $\omega = 10, 0.5$ (upper right and lower right, respectively); for the solid curves, we show 5 $W(\theta)$ for clarity. The distributions are normalized to unity in the physical interval from $\theta = 0$ to $\theta = \pi/2$. (Figure reprinted with permission from Ref. [538] by the American Physical Society.)

force generation follows a linear version of the Hill force–velocity relationship. This model predicts that a decrease in the frequency of cyclic stretching results in a decrease in the alignment of stress fibers.

5.10 Dynamic Stochastic Model. The dynamic stochastic model (also known as the active elastic dipole model) is an active model which represents a cell as an elastic force dipole that changes its orientation and magnitude in response to external forces (Fig. 35). It was originally developed to explain why cells orient their stress fibers parallel or perpendicular to an applied force. This model operates on the idea that a cell will reorganize its stress fibers in the direction that maintains an optimal stress or strain within the cell, and any deviance from this orientation will result in internal forces which restore this optimal state of stress or strain.

The force dipole is characterized by a cell's stress fiber activity. Specifically, the cell is modeled as an anisotropic force dipole tensor: $P_{ij} = l_i f_j$, where l_i is the distance between the forces, and f_j is the magnitude of the forces. These forces are derived from the gradients of the effective free energy, F_c , which is a function of the dipole magnitude and direction. The free energy of a cell with bipolar morphology, and an external uniaxial stress σ_a applied at an angle θ relative to the cell's central axis, can be written as follows:

$$F_c = \frac{1}{2} \chi (P^*)^2 [-p + p_a(t)(\phi - \phi_1) - 1]^2 \quad (24)$$

where χ is a measure of cell activity, P^* is the optimal force dipole, $p = P/P^*$ and $p_a(t) = P_a(t)/(\alpha_o P^*)$ are dimensionless variables (α_o is a function of ν), and $\phi_1 = \cos^2 \theta_o = \nu/(1 + \nu)$ is the cellular dipole (θ_o is the zero strain direction). Alternatively, the free energy of the matrix is written as

$$F_m = P_{ij} u_{ij}^a \quad (25)$$

where u_{ij}^a is the external strain field. The effective free energy is $F = F_c + F_m$, and the equations for the dipole magnitude and orientation are given by

$$\frac{dP}{dt} = \frac{1}{\tau_p} \frac{\partial F}{\partial P} \quad (26)$$

$$\frac{d\theta}{dt} = \frac{1}{\tau_\theta} \frac{\partial F}{\partial \theta} \quad (27)$$

where τ_p and τ_θ are the times that it takes for the orientation and magnitude of the force dipole to reach their optimal states, respectively [28].

Not only is this model relatively simple—in that it only has two degrees of freedom (dipole magnitude and orientation)—but it also incorporates components of active cellular forces created by cytoskeletal remodeling, and elastic forces created by cell–ECM interactions. Additionally, it is a relatively generic description of a contractile cell, since it lumps several molecular processes into two variables.

5.11 Constrained Mixture Models. Using this model, the mechanics of a cell are assumed to be governed by four primary events: the diffusion of actin monomers within the cell, the formation of a network of stress fibers from these monomers, biomechanical contraction of these stress fibers, and dissociation of the fibers into actin monomers [539]. This model was developed to address a number of key physical principals that are generally neglected in whole-cell computational models, namely, the dependency of contractility on substrate stiffness and ligand density, mass conservation, osmotic loading, and transport phenomena.

For this model, the cell is defined to have four distinct, yet coupled types of structures: a solid cytoskeleton (s), a fluid cytosol (c), a network of stress fibers (p), and a mass of actin monomers (m). The cytoskeleton, which is assumed to be porous and passive, is included within this definition in order to assess cell deformation, and acts as an intermediary space between the cytosol and the extracellular matrix. Alternatively, the cytosol, which is presumed to be composed of an incompressible fluid, allows for actin monomer transport and resists the cell's internal pressure. Lastly, the stress fibers constitute the cell's actin cytoskeleton, and are required for contraction.

The formation of these stress fibers is limited by the amount of available actin monomers present in the cytoplasm, and the rate of both the formation and the disassociation processes for an individual stress fiber are dependent on the contractile tension in that stress fiber

$$\Gamma_\theta^p = \left(k^f \frac{\phi_m^m}{\phi_f^f} - k^d \phi_\theta^p \right) \quad (28)$$

where Γ_θ^p is the rate of stress fiber polymerization, ϕ_m is the availability of actin monomers, ϕ_f is the volume fraction of the fluid cytosol, ϕ_θ^p is the variation in stress fiber density with direction θ , and k^f and k^d are the formation and dissociation constants for F-actin. The density of these stress fibers is assumed to have a von Mises distribution

$$\phi_\theta^p = \phi_p \left\{ \frac{\exp[b \cos(2\theta - \theta_0)]}{I_0(b)} \right\} \quad (29)$$

where b is the degree of anisotropy of the stress fibers, θ_0 is the direction of largest fiber density, and $I_0(b)$ is the zero-order Bessel's function of the first kind

$$I_0(b) = \frac{1}{\pi} \int_0^\pi \exp(b \cos \theta) d\theta \quad (30)$$

$$\frac{T^p}{T} = T^*(\epsilon, \dot{\epsilon}) \quad (31)$$

Stress fiber contraction is governed by classical length-tension and velocity tension characteristics

$$T^* = \begin{cases} \left(1 + \frac{\dot{\epsilon}/\dot{\epsilon}_0}{\sqrt{(\dot{\epsilon}/\dot{\epsilon}_0)^2 + 1}} \right) e^{-\left(\frac{\epsilon}{\epsilon_0}\right)^2} & \epsilon < 0 \\ \left(1 + \frac{\dot{\epsilon}/\dot{\epsilon}_0}{\sqrt{(\dot{\epsilon}/\dot{\epsilon}_0)^2 + 1}} \right) \left[e^{-\left(\frac{\epsilon}{\epsilon_0}\right)^2} + \left(\frac{\epsilon}{\epsilon_1}\right)^2 \right] & \epsilon \geq 0 \end{cases} \quad (32)$$

where T^p is the tension in the stress fibers, ϵ is the strain in a stress fiber, $\dot{\epsilon}$ is the strain rate of the stress fiber, T is the isometric contraction for the stress fiber in its original length ($\epsilon = 0$) assuming no strain rate ($\dot{\epsilon} = 0$), ϵ_0 is a constant which describes how quickly contraction decreases as strain deviates from zero, and ϵ_1 is a characterizing constant for the passive strain hardening of the stress fibers. When results obtained using this model are compared to those obtained experimentally, it has been found that this model is able to accurately capture the relationship between cell contraction and substrate stiffness in addition to capturing stress fiber alignment along a free edge of a cell between two discrete attachments (Fig. 36) [539]. More recently, this model has been used to predict the formation and orientation of stress fibers in cells subjected to constant or cyclic stretch and for cells on substrates with different stiffnesses [540].

6 Focus on Bio-Chemo-Mechanical Model

The bio-chemo-mechanical model was first proposed by Deshpande et al. in 2006 [16]. This model describes the biochemistry of stress fiber remodeling with a biomechanical description of stress fiber contractility. The biochemistry of stress fiber formation is based on two key observations: (i) stress fibers assemble due to activation of proteins or signaling molecules in the cell, such as RhoA/Ca²⁺ [23] and (ii) stress fibers dissociate when there is a reduction in tension in the cytoskeleton [23]. Based on experimental observation [541], an exponentially decaying signal is typically assumed. This activation signal is represented by the nondimensional signal intensity C :

$$C = \exp(-t_i/\theta) \quad (33)$$

where θ is the decay constant of the signal, and t_i is the time measured from the onset of the i th activation signal. A first-order kinetic equation describes the rate of stress fiber assembly

$$\frac{d\eta}{dt} = [1 - \eta] \frac{Ck_f}{\theta} - \left[1 - \frac{T}{T_0} \right] \frac{\eta k_b}{\theta} \quad (34)$$

where η is the nondimensional assembly level of stress fibers, k_f is the forward rate constant, k_b is the backward rate constant, and T_0 is the isometric tension. The first term in this equation describes the rate of stress fiber formation, which increases with the activation level C in a cell and decreases with the assembly level η . The second term describes the rate of stress fiber disassembly, which increases with the assembly level η and decreases with increasing tension T in the stress fiber.

Due to similarities between stress fibers and myofibrils, the contractile behavior of a nonmuscle cell is assumed to have similar isotonic and isometric relationships as skeletal muscle. This relationship is represented by Hill's equation, which was linearized to the following form:

$$\frac{T}{T_0} = 1 + \frac{\bar{k}_v}{\eta} \left(\frac{\dot{\epsilon}}{\dot{\epsilon}_0} \right) \quad (35)$$

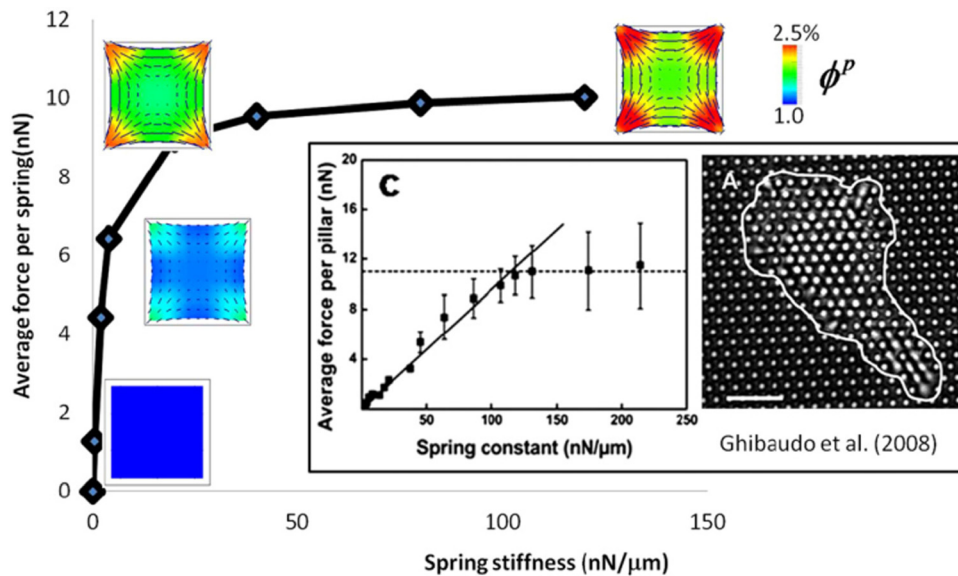


Fig. 36 Steady-state contractile force as a function of support stiffness predicted with the constrained mixture model. The steady-state morphology and corresponding stress fiber distributions are shown for select values of substrate stiffness. For comparison, experimental results from Ghibaudo et al. [444] are also reported. (Reprinted from Ref. [539] with permission from Elsevier.)

where $\dot{\epsilon}$ is the strain rate, $\dot{\epsilon}_0$ is the maximum strain rate, and \bar{k}_v is the Hill-type constant that relates the reduction in tension due to the strain rate. In experiments performed by Mitrossilis et al., this tension-strain rate relationship was found to be valid for myoblast cells [542]. It is important to note that stress fiber shortening, i.e. strain rate, leads to a reduction in tension, which in turn, results in stress fiber disassembly. The loss in assembled stress fibers leads to reduced tension production and the cell eventually reaches a steady state level of contraction.

6.1 Computational Implementation of the Bio-Chemo-Mechanical Model. To use this model, a representative volume element (RVE) is defined such that 2D finite element implementation allows for a fully predictive framework in terms of stress fiber distribution and contractility through the cell cytoplasm [16,543]. Essentially, at each integration point in a finite element mesh, Eqs. (33)–(35) are solved in a large number of directions so that the stress fiber distribution at this point depends on the local stress state and cell signaling. Theoretically, stress fibers can form in any direction in a RVE, but it has been numerically demonstrated that solving these equations in 72 discrete, evenly spaced, directions provides a converging solution. A 3D implementation has recently been developed by Ronan et al. where these equations are solved in 400 evenly distributed directions in a spherical RVE [544]. This active stress fiber formulation then is placed in parallel with a passive material component (generally a hyperelastic formulation), which represents the noncontractile components of the cell cytoplasm such as microtubules, intermediate filaments, and organelles.

6.2 Applications and Limitations of the Bio-Chemo-Mechanical Model. The main advantage of this model is that it accounts for dynamic reorganization of the cytoskeleton in response to changes in the intracellular stress state. This model is also entirely predictive, with the ability predict stress fiber formation in all directions at all points throughout the cell cytoplasm so that initial conditions regarding stress fiber distribution and orientation are not required. Furthermore, this model represents stress fiber contractility via the Hill model—which embodies the interaction between actin and myosin—and represents stress fiber assembly and dissociation via the kinetic equation. Therefore, it is phenomenological, but based on experimental observation.

The bio-chemo-mechanical model also has the ability to accurately predict the influence of substrate compliance on cellular traction forces, the dependence of cell size on forces, and the influence of cell shape, boundary conditions, and forces on the orientation of stress fibers and distribution of focal adhesions. Some of these results have been discussed in previous reviews [543,545], and are further discussed in the following section of this review. Most importantly, this framework has been shown to accurately simulate the response of cells to a wide variety of different boundary conditions and loading scenarios, demonstrating the robustness of the formulation.

However, while this model has many advantages over others, it still has room for improvement. Physiologically, cells are composed by a large number of different structures, each with their own mechanical properties, and their own effect on the average whole-cell mechanics. In order to account for the individual contributions of these structures to whole-cell mechanics, the passive hyperelastic component of the model could potentially be replaced with more complex constitutive formulations to represent the biomechanical behavior of microtubules and intermediate filaments. Additionally, 2D and 3D implementations of the model have assumed that the activation signal within the model is not spatially dependent.

6.3 Studies Confirming the Validity of the Bio-Chemo-Mechanical Model. This formulation has been implemented in one-, two-, and three-dimensional simulations of a wide variety of

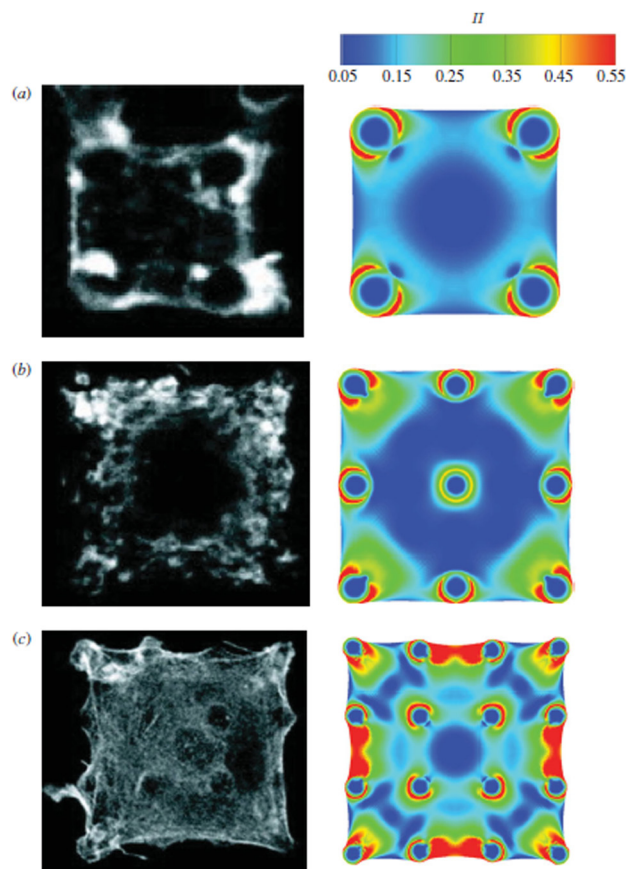


Fig. 37 Experimental (left) and computationally predicted (right) concentrations of stress fiber assembly for a square cell attached to posts at its corners [455]

experiments; and has been found to capture a large number of key cellular responses that cannot be captured by passive models. Some of these findings are discussed in the following sections of this review.

6.3.1 Predictions of Contractility and Spreading. The first paper that reported upon the use of this framework demonstrated the model's ability to predict changes in stress fiber formation for square cells seeded on top of supports with different magnitudes of stiffness [16], which was previously seen in experiments of the same nature [421].

Subsequent simulations by the same authors found that, for a single stress fiber on top of a one-dimensional row of microposts, the model predicts an increase in the fiber's average traction force with increasing post stiffness, and a decrease in the fiber's average traction force with an increased number of support posts [543]. In this same study, the corners of a square-shaped virtual cell were attached to the tops of square posts for two-dimensional simulations. These simulations showed that the model accurately predicts the development of cytoskeletal anisotropy with changes to cell shape and boundary conditions (cytoskeletal anisotropy under uniaxial loading and structural isotropy under biaxial loading), a high concentration of stress fibers in the vicinity of the attachment points, increased stress fiber assembly at points of force application, and enhanced stress fiber development with multiple activation signals (Fig. 37). These findings are consistent with previous experimental results [421].

In further conformational studies, 2D simulations of the bio-chemo-mechanical model were compared to experiments employing micropost arrays [455]. In these simulations, the contractile responses of smooth muscle cells, fibroblasts, and mesenchymal stem cells were investigated for various different micropost array

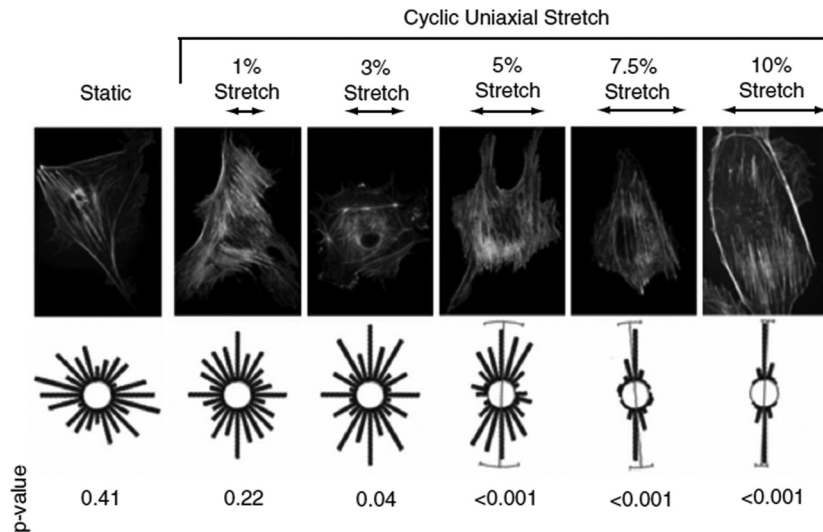


Fig. 38 Comparison experimental and simulated stress fiber alignment in response to applied uniaxial strain of varying magnitudes [546]

sizes. These simulations showed that the bio-chemo-mechanical model was able to consistently yield results seen in previous experimental studies [15,420,450,457]. These results included changes in traction forces exerted by cells on different numbers of microposts, the alignment and distribution of actin stress fibers, the curvature of the cell boundaries between the microposts, higher traction forces at the cell periphery, and larger-magnitude forces for cells with higher post stiffness and/or cell area.

6.3.2 Response of a Cell Exerted to External Force. In a separate set of simulations, a two-dimensional cell was subject to uniaxial and equibiaxial strain in order to determine the model's ability to predict changes in stress fiber orientation and assembly due to the application of cyclic strains (Fig. 38) [546]. These simulations found that uniaxial cyclic straining of a cell resulted in the alignment of stress fibers perpendicular to the direction of stretching. Additionally, higher alignment was seen with increased magnitude and frequency of the applied stretch, while transverse contraction of the cell substrate was found to result in an alignment of stress fibers at approximately 70 deg to the direction of stretching. Alternatively, equibiaxial cyclic strain was shown to result in a uniform distribution of stress fiber alignment. Stress fiber alignment is a result of the dissociation of fibers aligned in the stretching direction as a result of fiber shortening and consequent tension reduction during unloading half-cycles. These predictions are consistent with experimental observations for fibroblasts and endothelial cells seeded on silicone substrates that are subjected to cyclic stretching [547–550].

6.3.3 Cellular Migration. In recent simulations, this model was employed to elicit information regarding changes in traction forces during one and two-dimensional cellular migration (Fig. 39) [551]. Here a single migration cycle—contraction of the cytoskeleton, extension of the leading cell edge, and release of the rear adhesions—was investigated. These studies found that this model was able to predict the spatial distribution of traction forces elicited by previous experiments [16,386,398,543]. These experiments also revealed that the formation of a new adhesion leads to the immediate reorganization of cytoskeletal stress fibers, and that the strain energy of a cell's traction forces undergoes a cyclic pattern that rises during adhesion formation and falls during adhesion release.

6.3.4 Incorporation of Focal Adhesion Assembly. In further studies, a focal adhesion model was incorporated into the bio-chemo-mechanical definition to account for the effect that

cytoskeletal contractile forces have on the assembly of focal adhesion protein complexes. This model is based on three key assumptions: (i) low and high affinity integrins coexist in thermodynamic equilibrium, (ii) low affinity integrins within the plasma membrane are mobile, and (iii) the contractile forces generated by stress fibers are in mechanical equilibrium and change the free energies of the integrins [552]. In a one-dimensional simulation of this new model, it was found that focal adhesions concentrate around the periphery of a cell, the percentage of the cell with focal adhesions decreases with decreasing cell size (while the total amount of focal adhesion area increases), and that the total number of focal adhesions decrease when the cell is unable to produce contractile forces.

Another set of simulations used this same focal adhesion model to investigate the effects that a cell's shape have on focal adhesion assembly, as well as cytoskeletal organization (Fig. 40) [553]. In these simulations, two-dimensional cells having V, T, Y, and U shapes were compared to experimental results using cells patterned onto substrates of these same geometries [554]. The results of these simulations demonstrated that the coupled cytoskeleton-focal adhesion model was able to accurately predict: (i) the enhanced formation of highly aligned stress fibers along the non-adherent edges of the cells on concave patterns, (ii) high concentrations of focal adhesion formation along the edges of concave

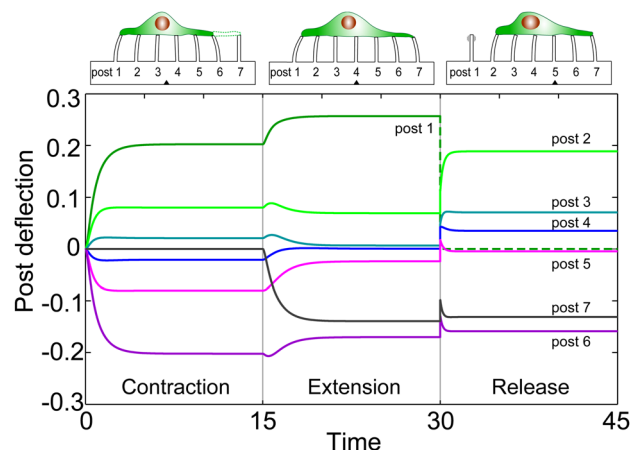


Fig. 39 Spatial mapping of simulated one-dimensional cellular traction forces for a migrating cell [551]

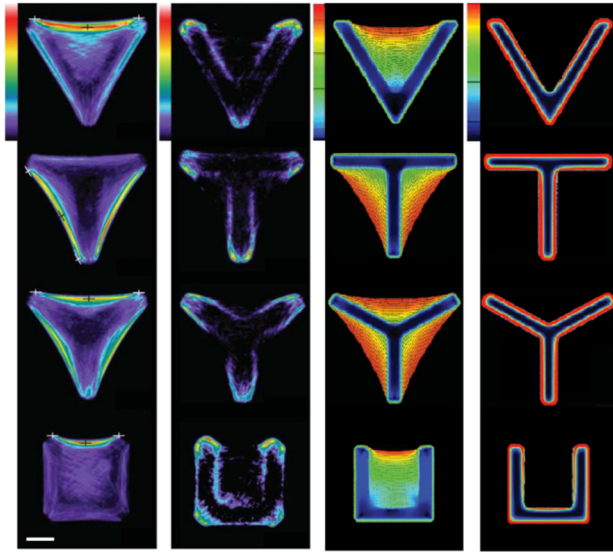


Fig. 40 Comparison of experimental (rows 1 and 2) and simulated (rows 3 and 4) stress fiber and focal adhesion assembly for cells of various shapes. (Figure adapted from Ref. [553] with permission from The Royal Society.)

patterns, and (iii) large populations of stress fibers and focal adhesions at the periphery of convex patterns.

6.3.5 Incorporation of Intracellular Signaling. Recently, this bio-chemo-mechanical model was further refined to include a signaling model, which is defined based on the assumption that IP_3 molecules—messenger molecules used in signal transduction—are generated when focal adhesions grow, due to the clustering of high affinity integrins (Fig. 41) [555]. These IP_3 molecules then lead to the activation of the contractility model by diffusing into the cell and triggering the activation signal that initiates cellular contractility. In simulations performed using this new coupled model, a one-dimensional cell was pulled at one end, and changes to stress fiber activation, focal adhesion distributions, and activation level were recorded. The model predicted similar results to previous simulations with regard to stress fiber orientation and concentration, as well as focal adhesion distributions. Furthermore, it was found that the activation signal is dependent on the rate of the applied mechanical load, but not the net displacement of the cell due to that load. More specifically, when the rate of the applied load is higher, the maximum value of activation within the cell grows at an increasing rate and the time that it takes the cell to reach this maximum value decreases. These findings are consistent with previously obtained experimental results [556,557].

6.3.6 Role of Contractility in the Compression Resistance of Cells. Using a 3D implementation of the active framework, a recent study of Ronan et al. reveals that polarized and axisymmetric spread cells contain stress fibers which form dominant bundles that are stretched during compression (Fig. 42) [558]. These dominant fibers exert tension, causing an increase in computed compression forces compared to round cells. Fewer stress fibers are predicted for round cells, leading to a lower resistance to compression. Most importantly, it is demonstrated that highly contractile cells provide greater resistance to compression. Computed predictions using this model correlate strongly with published experimentally observed trends of compression resistance [289,559] and offer an insight into the link between cell geometry, stress fiber distribution and contractility, and cell deformability. This framework was recently used to determine the contractile properties of osteoblasts using AFM compression data and

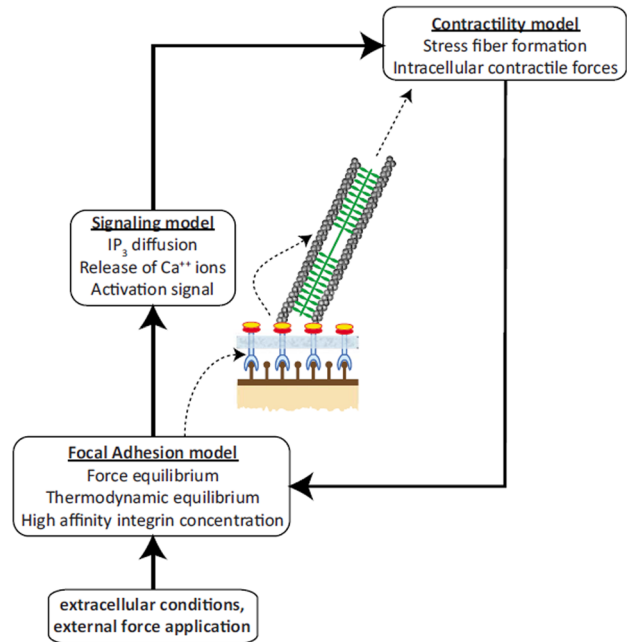


Fig. 41 Relationship between the contractility model, signaling model, and focal adhesion model within the bio-chemo-mechanical modeling framework [555]

imaging of deformed cell and nucleus geometries [560]. Additionally, in conjunction with a mixed-mode implementation of the aforementioned focal adhesion assembly model, this 3D implementation was used to predict cell response to substrate stiffness, with results strongly correlating with experimental measurements [561].

6.3.7 Role of the Actin Cytoskeleton in the Shear Resistance. A recent computational-experimental study by Dowling et al. demonstrates the importance of actin cytoskeleton remodeling and contractility in the shear resistance of chondrocyte cells (Fig. 43) [562]. These studies found that the active modeling framework must be used to capture the distinctive yielding behavior of the experimental force-indentation curve for untreated control cells. Alternatively, passive hyperelastic models are shown to only capture the behavior of cells in which the actin cytoskeleton has been disrupted with the chemical agent cytochalasin D (cytoD).

6.3.8 Three-Dimensional Simulations. Using calibrated bio-chemo-mechanical model parameters for chondrocytes, Dowling et al. also developed a micro-mechanical model of cartilage tissue, including an actively contractile chondrocyte, a peri-cellular matrix and an anisotropic extracellular matrix [562]. Simulations of this model predict that in vivo dynamic loading of cells leads to a continuous dissociation of the actin cytoskeleton in contrast to static loading (Fig. 44). This prediction correlates with 3D cell experiments performed by Knight et al., using chondrocytes in agarose gels [563,564] and demonstrates the potential of the modeling framework to guide strategies to maintain the chondrocyte phenotype in vivo.

6.4 Parameters Previously Employed for Simulations of the Bio-Chemo-Mechanical Model. As discussed earlier, the constants and parameters associated with this model are generally obtained by using canonical experimental techniques and from comparing the results of these experiments with computational predictions [545]. The reported parameters used for the previously-mentioned simulations of the bio-chemo-mechanical model are shown in the Table 4.

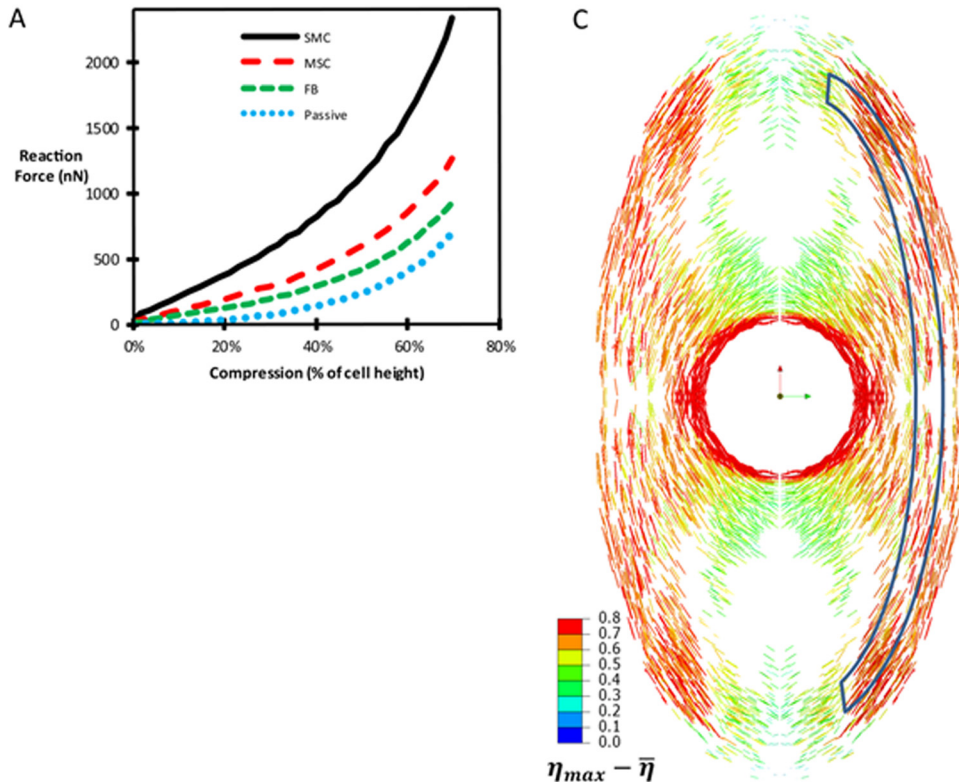


Fig. 42 Role of contractility on the compression resistance of cells. (a) Relationship between cell contractility and compression resistance; (c) aligned axial stress fibers in 3D polarized cell. (Reprinted from Ref. [558] with permission from Elsevier.)

7 Future Directions in Cell Mechanics

To this date, much has been accomplished within the fields of experimental techniques for cell mechanics, as well as computational modeling of cell mechanics. However, there are still a number of improvements that can be made to enhance these techniques and models for a better understanding of basic biology and disease states. Potential improvements to both fields are discussed in the following, closing sections of this work.

7.1 Future of Tools for Cell Mechanics. In order for these tools to serve as an effective means to uncover the bio-chemo-mechanical behavior of cells, standard experimental techniques and methodologies should be established to inform future model

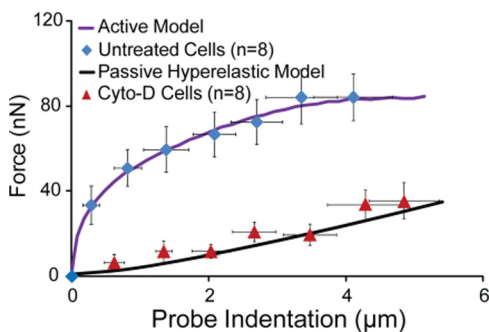


Fig. 43 Prediction of active modeling framework for the shear resistance of untreated contractile cells, capturing a distinctive yield behavior. In contrast, the linear response predicted by passive hyperelastic material modeling is appropriate only for cells in which the actin cytoskeleton has been removed. (Reprinted from Ref. [562] with permission from Elsevier.)

development. Additionally, the development of experimental techniques that are capable of parsing the active mechanical contribution of cells in response to applied loading, accounting for cell remodeling due to the applied stimulus, will allow for a greater understanding of the biomechanisms by which cells respond to their physical environment, with significant implications in terms of mechanotransduction, homeostasis, and disease progression. Furthermore, because cells are truly three-dimensional in nature, techniques that are able to uncover cell biomechanical behavior in three dimensions will enable more accurate approximations of cellular function in vivo.

With regard to potential improvements to micropost arrays, the development of nanopost-dimension arrays would not only allow for the spatial improvement in traction force measurements, but it would enable the use of individual posts to measure forces of cell structures that are on the nano length scale. Furthermore, the incorporation of microposts into complex mechanical environments would allow for the measurement of cell traction forces

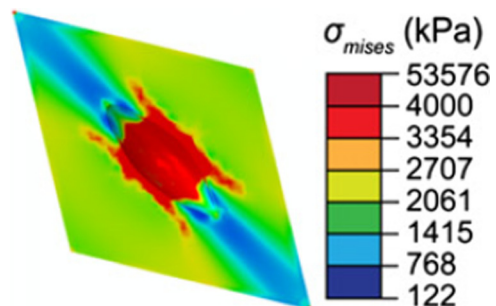


Fig. 44 Stress distribution in cartilage tissue due to physiological loading and chondrocyte contractility. (Reprinted from Ref. [562] with permission from Elsevier.)

Table 4 Reported parameters used for simulations of the bio-chemo-mechanical model

Valid cell type (s)	θ (s)	E (kPa)	ν	k_f	k_b	k_v	σ_{\max} (kPa)	$\dot{\epsilon}_o$ (s ⁻¹)	Ref
Fibroblasts	720	0.077	0.3	10	1	10	3.9	2.8×10^{-4}	[543]
hTERT-RPE1	720	0.08	0.3	10	1	6	4	2.8×10^{-4}	[553]
Fibroblasts and Endothelial cells	100	0.08	0.3	0.04	4	0.25	4	1	[546]
Smooth muscle cells, fibroblasts, and mesenchymal stem cells	70	0.4	0.3	10	1	7	25	0.003	[455]
						7	3.25		
						12	8		
Arbitrary 1D migration	1	0.25	0.36	3	2	1.5	1	0.4	[551]
Arbitrary 2D migration				5	3		0.025	0.2	
General	–	0.08	0.3	1.4×10^{-3}	1.4×10^{-3}	6	3.9	2.8×10^{-4}	[555]
Shearing of chondrocytes	70	4*	0.4	10	1	6	0.85	0.003	[544]
		1.5**							
Compression of spread cells	70	4*	0.3-0.4	–	1	7	3.5	0.003	[558]
							8		
		0.4**					25		

References cited in the table are [455,543,544,546,551,553,555,558].

Note: a single asterisk indicates material properties of the cell nucleus and two asterisks indicate material properties of the cell cytoplasm

within environments that are more physiologically relevant. For example, in the body, endothelial cells are subject to stretching and fluid shear stresses. Therefore, it is safe to assume that a system which is able to mimic these environmental conditions is more likely to give valid results than one that does not. Moreover, while the current method for determining post deflections is sound, optical microscopy is limited by the ability of the optical equipment to capture events on short time scales. Improvements to this temporal resolution would allow for the use of micropost arrays to study the forces involved in events that take place very rapidly.

Experimentally, there are also still a number of different studies that have yet to be investigated in great detail with regard to cell mechanics. Many of these experiments have the potential to be studied using the micropost platform, including multicellular studies, the investigation of developmental biomechanics, mechanotransduction, and three-dimensional mechanics. Investigating the forces within cell monolayers, at cell–cell junctions, and at cell–ECM junctions for different force environments would allow for the investigation of how the mechanics of a single cell is translated into a group of cells. Studying developmental biomechanics by measuring force production of cells during different stages of development would enable researchers to determine the role that forces play while cells structurally mature, as well as their role in disease progression. Furthermore, studying mechanotransduction with microposts would elucidate the specific structures and chemical pathways involved in mechanotransduction, and using this platform in three dimensions would allow for the determination of cellular forces in a more physiologically relevant framework.

7.2 Future of Computational Models. In order for these computational models to be universally established and accepted as a standard means for determining the mechanical responses of different cells, they should be general enough such that a single model could be used to accurately describe the response of (almost) any cell type to any applied mechanical stimulus. Such a universal model could be used to describe a variety of different cells by using distinct material constants and parameters for each cell type, since most cells have similar mechanical parts but may express different amounts of isoforms of these proteins.

It is also important to develop multiscale models, which would serve to bridge the gap between microscopic and macroscopic simulations and yield a more complete characterization of molecular, single-cell, monolayer, or even tissue level mechanics. In these models, separate calculations would be carried out at different length scales, and then combined, to produce models capable of describing the biological, chemical, and mechanical outcomes of different experimental conditions. The main challenge involved

in developing these models would be the correct coupling of these individual scale computations [545]. Not only do these events take place at different length scales, but they also occur on different time scales; the outcomes of these events affect multiple processes on these other scales [565].

Another key direction for the future of this field is to develop models based on molecular processes that underlie the mechanotransduction processes of cells. Such constitutive formulations must be implemented in computational simulations for a wide variety of single cell experiments. The validity of a phenomenological implementation of such mechanisms could then be determined by the ability of the model to predict and interpret experimental observation. This will also be facilitated by the determination of other important molecular mechanisms and signaling pathways that occur in the cell, and representing these events in a continuum sense in finite element models. These models would then have to be confirmed based on existing or new experimental data. Additionally, future development should entail the use of these models for complex cells with physiologically realistic geometries and loading modes in three dimensions.

Ultimately, the improvements in computational models within the field of cell mechanics could lead to improvements in human health. For instance, the mechanical behavior of certain cells can potentially be used to quantify the cell’s health, which could lead to the diagnosis of certain diseases that affect cell function. Also, information regarding the difference between the mechanical behavior of “healthy” and “unhealthy” cells can be used to predict whether therapeutic treatments will be effective in treating certain diseases. Additionally, a better knowledge of cell biomechanics will enable an improved approximation of the biomechanical behavior of tissues, which is essential in tissue engineering. These and other such potential applications of cell mechanics make it a very important topic of study, both currently, and for years to come.

References

- [1] Bershadsky, A., Kozlov, M., and Geiger, B., 2006, “Adhesion-Mediated Mechanosensitivity: A Time to Experiment, and a Time to Theorize,” *Curr. Opin. Cell Biol.*, **18**(5), pp. 472–481.
- [2] Krishnan, R., Park, C. Y., Lin, Y. C., Mead, J., Jaspers, R. T., Trepats, X., Lenormand, G., Tambe, D., Smolensky, A. V., Knoll, A. H., Butler, J. P., and Fredberg, J. J., 2009, “Reinforcement Versus Fluidization in Cytoskeletal Mechanoresponsiveness,” *PLoS One*, **4**(5), e5486.
- [3] Moore, S. W., Roca-Cusachs, P., and Sheetz, M. P., 2010, “Stretchy Proteins on Stretchy Substrates: The Important Elements of Integrin-Mediated Rigidity Sensing,” *Dev. Cell*, **19**(2), pp. 194–206.
- [4] Ingber, D. E., 2003, “Mechanobiology and Diseases of Mechanotransduction,” *Ann. Med.*, **35**(8), pp. 564–577.
- [5] Affonce, D. A., and Lutchen, K. R., 2006, “New Perspectives on the Mechanical Basis for Airway Hyperreactivity and Airway Hypersensitivity in Asthma,” *J. Appl. Physiol.*, **101**(6), pp. 1710–1719.

- [6] Klein-Nulend, J., Bacabac, R. G., Veldhuijzen, J. P., and Van Loon, J. J., 2003, "Microgravity and Bone Cell Mechanosensitivity," *Adv. Space Res.*, **32**(8), pp. 1551–1559.
- [7] Vollrath, M. A., Kwan, K. Y., and Corey, D. P., 2007, "The Micromachinery of Mechanotransduction in Hair Cells," *Ann. Rev. Neurosci.*, **30**, pp. 339–365.
- [8] Gimbrone, M. A., Jr., Topper, J. N., Nagel, T., Anderson, K. R., and Garcia-Cardena, G., 2000, "Endothelial Dysfunction, Hemodynamic Forces, and Atherogenesis," *Ann. NY Acad. Sci.*, **902**, pp. 230–239.
- [9] Paszek, M. J., Zahir, N., Johnson, K. R., Lakins, J. N., Rozenberg, G. I., Gefen, A., Reinhart-King, C. A., Margulies, S. S., Dembo, M., Boettiger, D., Hammer, D. A., and Weaver, V. M., 2005, "Tensional Homeostasis and the Malignant Phenotype," *Cancer Cells*, **8**(3), pp. 241–254.
- [10] Judex, S., Gross, T. S., Bray, R. C., and Zernicke, R. F., 1997, "Adaptation of Bone to Physiological Stimuli," *J. Biomech.*, **30**(5), pp. 421–429.
- [11] Tan, J. C., Kalapesi, F. B., and Coroneo, M. T., 2006, "Mechanosensitivity and the Eye: Cells Coping with the Pressure," *Br. J. Ophthalmol.*, **90**(3), pp. 383–388.
- [12] Heydemann, A., and McNally, E. M., 2007, "Consequences of Disrupting the Dystrophin-Sarcoglycan Complex in Cardiac and Skeletal Myopathy," *Trends Cardiovasc. Med.*, **17**(2), pp. 55–59.
- [13] Di Carlo, D., Wu, L. Y., and Lee, L. P., 2006, "Dynamic Single Cell Culture Array," *Lab Chip*, **6**(11), pp. 1445–1449.
- [14] Anderson, A. E., Ellis, B. J., and Weiss, J. A., 2007, "Verification, Validation and Sensitivity Studies in Computational Biomechanics," *Comput. Methods Biomech. Biomed. Eng.*, **10**(3), pp. 171–184.
- [15] Tan, J. L., Tien, J., Pirone, D. M., Gray, D. S., Bhadriraju, K., and Chen, C. S., 2003, "Cells Lying on a Bed of Microneedles: An Approach to Isolate Mechanical Force," *Proc. Natl. Acad. Sci. U.S.A.*, **100**(4), pp. 1484–1489.
- [16] Deshpande, V. S., McMeeking, R. M., and Evans, A. G., 2006, "A Bio-Chemo-Mechanical Model for Cell Contractility," *Proc. Natl. Acad. Sci. U.S.A.*, **103**(38), pp. 14015–14020.
- [17] Karp, G., 2002, *Cell and Molecular Biology*, John Wiley and Sons, Inc., New York.
- [18] Bo, L., and Waugh, R. E., 1989, "Determination of Bilayer Membrane Bending Stiffness by Tether Formation from Giant, Thin-Walled Vesicles," *Biophys. J.*, **55**(3), pp. 509–517.
- [19] Alberts, B., Johnson, A., Lewis, J., Raff, M., Roberts, K., and Walter, P., 2002, *Molecular Biology of the Cell*, Garland Science, New York.
- [20] Lammerding, J., 2011, *Mechanics of the Nucleus: Comprehensive Physiology*, American Physiological Society, Cambridge, MA.
- [21] Dahl, K. N., Ribeiro, A. J., and Lammerding, J., 2008, "Nuclear Shape, Mechanics, and Mechanotransduction," *Circ. Res.*, **102**(11), pp. 1307–1318.
- [22] Guilak, F., Tedrow, J. R., and Burgkart, R., 2000, "Viscoelastic Properties of the Cell Nucleus," *Biochem. Biophys. Res. Commun.*, **269**(3), pp. 781–786.
- [23] Wang, N., Tytell, J. D., and Ingber, D. E., 2009, "Mechanotransduction at a Distance: Mechanically Coupling the Extracellular Matrix With the Nucleus," *Nat. Rev. Mol. Cell Biol.*, **10**, pp. 75–82.
- [24] Pullarkat, P. A., Fernández, P. A., and Ott, A., 2007, "Rheological Properties of the Eukaryotic Cell Cytoskeleton," *Phys. Rep.*, **449**(1–3), pp. 29–53.
- [25] Panorchan, P., Lee, J. S., Kole, T. P., Tseng, Y., and Wirtz, D., 2006, "Microrheology and Rock Signaling of Human Endothelial Cells Embedded in a 3D Matrix," *Biophys. J.*, **91**(9), pp. 3499–3507.
- [26] Tseng, Y., Kole, T. P., and Wirtz, D., 2002, "Micromechanical Mapping of Live Cells by Multiple-Particle-Tracking Microrheology," *Biophys. J.*, **83**(6), pp. 3162–3176.
- [27] Zimmerman, S. B., and Minton, A. P., 1993, "Macromolecular Crowding: Biochemical, Biophysical, and Physiological Consequences," *Ann. Rev. Biophys. Biomol. Struct.*, **22**, pp. 27–65.
- [28] De, R., Zemel, A., and Safran, S. A., 2010, "Theoretical Concepts and Models of Cellular Mechanosensing," *Methods Cell Biol.*, **98**, pp. 143–175.
- [29] Fletcher, D. A., and Mullins, R. D., 2010, "Cell Mechanics and the Cytoskeleton," *Nature*, **463**(7280), pp. 485–492.
- [30] De Forges, H., Bouissou, A., and Perez, F., 2012, "Interplay between Microtubule Dynamics and Intracellular Organization," *Int. J. Biochem. Cell Biol.*, **44**(2), pp. 266–274.
- [31] Kristofferson, D., Mitchison, T., and Kirschner, M., 1986, "Direct Observation of Steady-State Microtubule Dynamics," *J. Cell Biol.*, **102**(3), pp. 1007–1019.
- [32] Brangwynne, C. P., Mackintosh, F. C., Kumar, S., Geisse, N. A., Talbot, J., Mahadevan, L., Parker, K. K., Ingber, D. E., and Weitz, D. A., 2006, "Microtubules Can Bear Enhanced Compressive Loads in Living Cells Because of Lateral Reinforcement," *J. Cell Biol.*, **173**(5), pp. 733–741.
- [33] Hirokawa, N., 1998, "Kinesin and Dynein Superfamily Proteins and the Mechanism of Organelle Transport," *Science*, **279**(5350), pp. 519–526.
- [34] Sharp, D. J., Rogers, G. C., and Scholey, J. M., 2000, "Microtubule Motors in Mitosis," *Nature*, **407**(6800), pp. 41–47.
- [35] Lodish, H., Berk, A., Zipursky, S. L., Matsudaira, P., Baltimore, D., and Darnell, J., 2000, *Molecular Cell Biology*, W. H. Freeman, New York.
- [36] Herrmann, H., Bar, H., Kreplak, L., Strelkov, S. V., and Aebi, U., 2007, "Intermediate Filaments: From Cell Architecture to Nanomechanics," *Nat. Rev. Mol. Cell Biol.*, **8**(7), pp. 562–573.
- [37] Goley, E. D., and Welch, M. D., 2006, "The Arp2/3 Complex: An Actin Nucleator Comes of Age," *Nat. Rev. Mol. Cell Biol.*, **7**(10), pp. 713–726.
- [38] Welch, M. D., 1999, "The World According to Arp: Regulation of Actin Nucleation by the Arp2/3 Complex," *Trends Cell Biol.*, **9**(11), pp. 423–427.
- [39] Pellegrin, S., and Mellor, H., 2007, "Actin Stress Fibres," *J. Cell Sci.*, **120**(20), pp. 3491–3499.
- [40] Finer, J. T., Simmons, R. M., and Spudich, J. A., 1994, "Single Myosin Molecule Mechanics: Piconewton Forces and Nanometre Steps," *Nature*, **368**(6467), pp. 113–119.
- [41] Bershadsky, A. D., Balaban, N. Q., and Geiger, B., 2003, "Adhesion-Dependent Cell Mechanosensitivity," *Ann. Rev. Cell Dev. Biol.*, **19**, pp. 677–695.
- [42] Gomez, G. A., Mclachlan, R. W., and Yap, A. S., 2011, "Productive Tension: Force-Sensing and Homeostasis of Cell-Cell Junctions," *Trends Cell Biol.*, **21**(9), pp. 499–505.
- [43] Jaalouk, D. E., and Lammerding, J., 2009, "Mechanotransduction Gone Awry," *Nat. Rev. Mol. Cell Biol.*, **10**(1), pp. 63–73.
- [44] Tarbell, J. M., Weinbaum, S., and Kamm, R. D., 2005, "Cellular Fluid Mechanics and Mechanotransduction," *Ann. Biomed. Eng.*, **33**(12), pp. 1719–1723.
- [45] Janmey, P. A., and McCulloch, C. A., 2007, "Cell Mechanics: Integrating Cell Responses to Mechanical Stimuli," *Ann. Rev. Biomed. Eng.*, **9**, pp. 1–34.
- [46] Haswell, E. S., Phillips, R., and Rees, D. C., 2011, "Mechanosensitive Channels: What Can They Do and How Do They Do It?," *Structure*, **19**(10), pp. 1356–1369.
- [47] Arnadottir, J., and Chalfie, M., 2010, "Eukaryotic Mechanosensitive Channels," *Ann. Rev. Biophys.*, **39**, pp. 111–137.
- [48] Sachs, F., 2010, "Stretch-Activated Ion Channels: What Are They?," *Physiol. (Bethesda)*, **25**(1), pp. 50–56.
- [49] Vogel, V., and Sheetz, M., 2006, "Local Force and Geometry Sensing Regulate Cell Functions," *Nat. Rev. Mol. Cell Biol.*, **7**(4), pp. 265–275.
- [50] Loh, O., Vaziri, A., and Espinosa, H. D., 2009, "The Potential of MEMS for Advancing Experiments and Modeling in Cell Mechanics," *Exp. Mech.*, **49**, pp. 105–124.
- [51] Hochmuth, R. M., 2000, "Micropipette Aspiration of Living Cells," *J. Biomech.*, **33**(1), pp. 15–22.
- [52] Mitchison, J. M., and Swann, M. M., 1954, "The Mechanical Properties of the Cell Surface. II. The Unfertilized Sea-Urchin Egg," *J. Exp. Biol.*, **31**, pp. 461–472.
- [53] Van Vliet, K. J., Bao, G., and Suresh, S., 2003, "The Biomechanics Toolbox: Experimental Approaches for Living Cells and Biomolecules," *Acta Mater.*, **51**(19), pp. 5881–5905.
- [54] Sung, K. L., Dong, C., Schmid-Schonbein, G. W., Chien, S., and Skalak, R., 1988, "Leukocyte Relaxation Properties," *Biophys. J.*, **54**(2), pp. 331–336.
- [55] Ting-Beall, H. P., Needham, D., and Hochmuth, R. M., 1993, "Volume and Osmotic Properties of Human Neutrophils," *Blood*, **81**(10), pp. 2774–2780.
- [56] Liu, B., Goergen, C. J., and Shao, J. Y., 2007, "Effect of Temperature on Tether Extraction, Surface Protusion, and Cortical Tension of Human Neutrophils," *Biophys. J.*, **93**(8), pp. 2923–2933.
- [57] Herant, M., Heinrich, V., and Dembo, M., 2005, "Mechanics of Neutrophil Phagocytosis: Behavior of the Cortical Tension," *J. Cell Sci.*, **118**, pp. 1789–1797.
- [58] Evans, E., and Yeung, A., 1989, "Apparent Viscosity and Cortical Tension of Blood Granulocytes Determined by Micropipet Aspiration," *Biophys. J.*, **56**(1), pp. 151–160.
- [59] Evans, E. A., 1973, "New Membrane Concept Applied to the Analysis of Fluid Shear- and Micropipette-Deformed Red Blood Cells," *Biophys. J.*, **13**(9), pp. 941–954.
- [60] Hochmuth, R. M., 1993, "Measuring the Mechanical Properties of Individual Human Blood Cells," *ASME J. Biomech. Eng.*, **115**(4B), pp. 515–519.
- [61] Waugh, R., and Evans, E. A., 1979, "Thermoelasticity of Red Blood Cell Membrane," *Biophys. J.*, **26**(1), pp. 115–131.
- [62] Trickey, W. R., Baajens, F. P., Laursen, T. A., Alexopoulos, L. G., and Guilak, F., 2006, "Determination of the Poisson's Ratio of the Cell: Recovery Properties of Chondrocytes after Release from Complete Micropipette Aspiration," *J. Biomech.*, **39**(1), pp. 78–87.
- [63] Trickey, W. R., Vail, T. P., and Guilak, F., 2004, "The Role of the Cytoskeleton in the Viscoelastic Properties of Human Articular Chondrocytes," *J. Orthop. Res.*, **22**(1), pp. 131–139.
- [64] Trickey, W. R., Lee, G. M., and Guilak, F., 2000, "Viscoelastic Properties of Chondrocytes from Normal and Osteoarthritic Human Cartilage," *J. Orthop. Res.*, **18**(6), pp. 891–898.
- [65] Guilak, F., Jones, W. R., Ting-Beall, H. P., and Lee, G. M., 1999, "The Deformation Behavior and Mechanical Properties of Chondrocytes in Articular Cartilage," *Osteoarthritis Cartilage*, **7**(1), pp. 59–70.
- [66] Haga, J. H., Beaudoin, A. J., White, J. G., and Strony, J., 1998, "Quantification of the Passive Mechanical Properties of the Resting Platelet," *Ann. Biomed. Eng.*, **26**(2), pp. 268–277.
- [67] White, J. G., Burris, S. M., Tukey, D., Smith, C., II, and Clawson, C. C., 1984, "Micropipette Aspiration of Human Platelets: Influence of Microtubules and Actin Filaments on Deformability," *Blood*, **64**(1), pp. 210–214.
- [68] McGrath, B., Mealing, G., and Labrosse, M. R., 2011, "A Mechanobiological Investigation of Platelets," *Biomech. Model. Mechanobiol.*, **10**(4), pp. 473–484.
- [69] Burris, S. M., Smith, C. M., II, Tukey, D. T., Clawson, C. C., and White, J. G., 1986, "Micropipette Aspiration of Human Platelets after Exposure to Aggregating Agents," *Arteriosclerosis*, **6**(3), pp. 321–325.
- [70] Sato, M., Theret, D. P., Wheeler, L. T., Ohshima, N., and Nerem, R. M., 1990, "Application of the Micropipette Technique to the Measurement of Cultured Porcine Aortic Endothelial Cell Viscoelastic Properties," *ASME J. Biomech. Eng.*, **112**(3), pp. 263–268.
- [71] Sato, M., Ohshima, N., and Nerem, R. M., 1996, "Viscoelastic Properties of Cultured Porcine Aortic Endothelial Cells Exposed to Shear Stress," *J. Biomech.*, **29**(4), pp. 461–467.

- [72] Dahl, K. N., Scaffidi, P., Islam, M. F., Yodh, A. G., Wilson, K. L., and Misteli, T., 2006, "Distinct Structural and Mechanical Properties of the Nuclear Lamina in Hutchinson-Gilford Progeria Syndrome," *Proc. Natl. Acad. Sci. U.S.A.*, **103**(27), pp. 10271–10276.
- [73] Vaziri, A., and Mofrad, M. R., 2007, "Mechanics and Deformation of the Nucleus in Micropipette Aspiration Experiment," *J. Biomech.*, **40**(9), pp. 2053–2062.
- [74] Zwerger, M., Ho, C. Y., and Lammerding, J., 2011, "Nuclear Mechanics in Disease," *Ann. Rev. Biomed. Eng.*, **13**, pp. 397–428.
- [75] Pajewowski, J. D., Dahl, K. N., Zhong, F. L., Sammak, P. J., and Discher, D. E., 2007, "Physical Plasticity of the Nucleus in Stem Cell Differentiation," *Proc. Natl. Acad. Sci. U.S.A.*, **104**(40), pp. 15619–15624.
- [76] Chu, Y. S., Eder, O., Thomas, W. A., Simcha, I., Pincet, F., Ben-Ze'ev, A., Perez, E., Thiery, J. P., and Dufour, S., 2006, "Prototypical Type I E-Cadherin and Type II Cadherin-7 Mediate Very Distinct Adhesiveness through Their Extracellular Domains," *J. Biol. Chem.*, **281**(5), pp. 2901–2910.
- [77] Chu, Y. S., Thomas, W. A., Eder, O., Pincet, F., Perez, E., Thiery, J. P., and Dufour, S., 2004, "Force Measurements in E-Cadherin-Mediated Cell Doublets Reveal Rapid Adhesion Strengthened by Actin Cytoskeleton Remodeling through RAC and CDC42," *J. Cell Biol.*, **167**(6), pp. 118–194.
- [78] Pelling, A. E., and Horton, M. A., 2008, "An Historical Perspective on Cell Mechanics," *Pflugers Arch.*, **456**(1), pp. 3–12.
- [79] Shin, D., and Athanasiou, K., 1999, "Cytointentation for Obtaining Cell Biomechanical Properties," *J. Orthop. Res.*, **17**(6), pp. 880–890.
- [80] Daily, B., Elson, E. L., and Zahalak, G. I., 1984, "Cell Poking. Determination of the Elastic Area Compressibility Modulus of the Erythrocyte Membrane," *Biophys. J.*, **45**(4), pp. 671–682.
- [81] McConnaughey, W. B., and Petersen, N. O., 1980, "Cell Poking: An Apparatus for Stress-Strain Measurements on Living Cells," *Rev. Sci. Instrum.*, **51**(5), pp. 575–580.
- [82] Darling, E. M., Topel, M., Zauscher, S., Vail, T. P., and Guilak, F., 2008, "Viscoelastic Properties of Human Mesenchymally-Derived Stem Cells and Primary Osteoblasts, Chondrocytes, and Adipocytes," *J. Biomech.*, **41**(2), pp. 454–464.
- [83] Darling, E. M., Zauscher, S., Block, J. A., and Guilak, F., 2007, "A Thin-Layer Model for Viscoelastic, Stress-Relaxation Testing of Cells Using Atomic Force Microscopy: Do Cell Properties Reflect Metastatic Potential?," *Biophys. J.*, **92**(5), pp. 1784–1791.
- [84] Coughlin, M. F., Puig-De-Morales, M., Bursac, P., Mellema, M., Millet, E., and Fredberg, J. J., 2006, "Filamin-A and Rheological Properties of Cultured Melanoma Cells," *Biophys. J.*, **90**(6), pp. 2199–2205.
- [85] Jones, W. R., Ting-Beall, H. P., Lee, G. M., Kelley, S. S., Hochmuth, R. M., and Guilak, F., 1999, "Alterations in the Young's Modulus and Volumetric Properties of Chondrocytes Isolated from Normal and Osteoarthritic Human Cartilage," *J. Biomech.*, **32**(2), pp. 119–127.
- [86] Darling, E. M., Zauscher, S., and Guilak, F., 2006, "Viscoelastic Properties of Zonal Articular Chondrocytes Measured by Atomic Force Microscopy," *Osteoarthritis Cartilage*, **14**(6), pp. 571–579.
- [87] Byfield, F. J., Aranda-Espinoza, H., Romanenko, V. G., Rothblat, G. H., and Levitan, I., 2004, "Cholesterol Depletion Increases Membrane Stiffness of Aortic Endothelial Cells," *Biophys. J.*, **87**(5), pp. 3336–3343.
- [88] Costa, K. D., Sim, A. J., and Yin, F. C., 2006, "Non-Hertzian Approach to Analyzing Mechanical Properties of Endothelial Cells Probed by Atomic Force Microscopy," *ASME J. Biomech. Eng.*, **128**(2), pp. 176–184.
- [89] Laurent, V. M., Fodil, R., Canadas, P., Fereol, S., Louis, B., Planus, E., and Isabey, D., 2003, "Partitioning of Cortical and Deep Cytoskeleton Responses from Transient Magnetic Bead Twisting," *Ann. Biomed. Eng.*, **31**(10), pp. 1263–1278.
- [90] Hoffman, B. D., Massiera, G., Van Citters, K. M., and Crocker, J. C., 2006, "The Consensus Mechanics of Cultured Mammalian Cells," *Proc. Natl. Acad. Sci. U.S.A.*, **103**(27), pp. 10259–10264.
- [91] Wu, H. W., Kuhn, T., and Moy, V. T., 1998, "Mechanical Properties of L929 Cells Measured by Atomic Force Microscopy: Effects of Anticytoskeletal Drugs and Membrane Crosslinking," *Scanning*, **20**(5), pp. 389–397.
- [92] Mahaffy, R. E., Park, S., Gerde, E., Kas, J., and Shih, C. K., 2004, "Quantitative Analysis of the Viscoelastic Properties of Thin Regions of Fibroblasts Using Atomic Force Microscopy," *Biophys. J.*, **86**(3), pp. 1777–1793.
- [93] Mahaffy, R. E., Shih, C. K., Mackintosh, F. C., and Kas, J., 2000, "Scanning Probe-Based Frequency-Dependent Microrheology of Polymer Gels and Biological Cells," *Phys. Rev. Lett.*, **85**(4), pp. 880–883.
- [94] Jaasma, M. J., Jackson, W. M., and Keaveny, T. M., 2006, "The Effects of Morphology, Confluency, and Phenotype on Whole-Cell Mechanical Behavior," *Ann. Biomed. Eng.*, **34**(5), pp. 759–768.
- [95] Lee, J. S., Panorchan, P., Hale, C. M., Khatau, S. B., Kole, T. P., Tseng, Y., and Wirtz, D., 2006, "Ballistic Intracellular Nanorheology Reveals Rock-Hard Cytoplasmic Stiffening Response to Fluid Flow," *J. Cell Sci.*, **119**, pp. 1760–1768.
- [96] Fernandez, P., Pullarkat, P. A., and Ott, A., 2006, "A Master Relation Defines the Nonlinear Viscoelasticity of Single Fibroblasts," *Biophys. J.*, **90**(10), pp. 3796–3805.
- [97] Desprat, N., Richert, A., Simeon, J., and Asnacios, A., 2005, "Creep Function of a Single Living Cell," *Biophys. J.*, **88**(3), pp. 2224–2233.
- [98] Nagayama, K., Nagano, Y., Sato, M., and Matsumoto, T., 2006, "Effect of Actin Filament Distribution on Tensile Properties of Smooth Muscle Cells Obtained from Rat Thoracic Aortas," *J. Biomech.*, **39**(2), pp. 293–301.
- [99] Lieber, S. C., Aubry, N., Pain, J., Diaz, G., Kim, S. J., and Vatner, S. F., 2004, "Aging Increases Stiffness of Cardiac Myocytes Measured by Atomic Force Microscopy Nanoindentation," *Am. J. Physiol. Heart Circ. Physiol.*, **287**(2), pp. H645–H651.
- [100] Domke, J., Dannohl, S., Parak, W. J., Muller, O., Aicher, W. K., and Radmacher, M., 2000, "Substrate Dependent Differences in Morphology and Elasticity of Living Osteoblasts Investigated by Atomic Force Microscopy," *Colloids Surf., B*, **19**(4), pp. 367–379.
- [101] Charras, G. T., and Horton, M. A., 2002, "Determination of Cellular Strains by Combined Atomic Force Microscopy and Finite Element Modeling," *Biophys. J.*, **83**(2), pp. 858–879.
- [102] Pan, W., Petersen, E., Cai, N., Ma, G., Run Lee, J., Feng, Z., Liao, K., and Leong, K., 2005, "Viscoelastic Properties of Human Mesenchymal Stem Cells," *Conf. Proc. IEEE Eng. Med. Biol. Soc.*, **5**, pp. 4854–4857.
- [103] Yourek, G., Hussain, M. A., and Mao, J. J., 2007, "Cytoskeletal Changes of Mesenchymal Stem Cells During Differentiation," *ASAIO J.*, **53**(2), pp. 219–228.
- [104] Roca-Cusachs, P., Almendros, I., Sunyer, R., Gavara, N., Farre, R., and Navajas, D., 2006, "Rheology of Passive and Adhesion-Activated Neutrophils Probed by Atomic Force Microscopy," *Biophys. J.*, **91**(9), pp. 3508–3518.
- [105] Petersen, N. O., McConnaughey, W. B., and Elson, E. L., 1982, "Dependence of Locally Measured Cellular Deformability on Position on the Cell, Temperature, and Cytochalasin B," *Proc. Natl. Acad. Sci. U.S.A.*, **79**(17), pp. 5327–5331.
- [106] Koay, E. J., Shieh, A. C., and Athanasiou, K. A., 2003, "Creep Indentation of Single Cells," *ASME J. Biomech. Eng.*, **125**(3), pp. 334–341.
- [107] Zahalak, G. I., McConnaughey, W. B., and Elson, E. L., 1990, "Determination of Cellular Mechanical Properties by Cell Poking, With an Application to Leukocytes," *ASME J. Biomech. Eng.*, **112**(3), pp. 283–294.
- [108] Riveline, D., Zamir, E., Balaban, N. Q., Schwarz, U. S., Ishizaki, T., Narumiya, S., Kam, Z., Geiger, B., and Bershadsky, A. D., 2001, "Focal Contacts as Mechanosensors: Externally Applied Local Mechanical Force Induces Growth of Focal Contacts by an Mdia1-Dependent and Rock-Independent Mechanism," *J. Cell Biol.*, **153**(6), pp. 1175–1186.
- [109] Delanoë-Ayari, H., Al Kurdi, R., Vallade, M., Gulino-Debrac, D., and Riveline, D., 2004, "Membrane and Acto-Myosin Tension Promote Clustering of Adhesion Proteins," *Proc. Natl. Acad. Sci. U.S.A.*, **101**(8), pp. 2229–2234.
- [110] Maniotis, A. J., Chen, C. S., and Ingber, D. E., 1997, "Demonstration of Mechanical Connections between Integrins, Cytoskeletal Filaments, and Nucleoplasm That Stabilize Nuclear Structure," *Proc. Natl. Acad. Sci. U.S.A.*, **94**(3), pp. 849–854.
- [111] Hayakawa, K., Tatsumi, H., and Sokabe, M., 2008, "Actin Stress Fibers Transmit and Focus Force to Activate Mechanosensitive Channels," *J. Cell Sci.*, **121**, pp. 496–503.
- [112] Lamoureux, P., Zheng, J., Buxbaum, R. E., and Heidemann, S. R., 1992, "A Cytomechanical Investigation of Neurite Growth on Different Culture Surfaces," *J. Cell Biol.*, **118**(3), pp. 655–661.
- [113] Lamoureux, P., Ruthel, G., Buxbaum, R. E., and Heidemann, S. R., 2002, "Mechanical Tension Can Specify Axonal Fate in Hippocampal Neurons," *J. Cell Biol.*, **159**(3), pp. 499–508.
- [114] Ofek, G., Dowling, E. P., Raphael, R. M., McGarry, J. P., and Athanasiou, K. A., 2010, "Biomechanics of Single Chondrocytes Under Direct Shear," *Biomech. Model. Mechanobiol.*, **9**(2), pp. 153–162.
- [115] Krayer, J., Tatic-Lucic, S., and Neti, S., 2006, "Micro-Rheometer: High Throughput System for Measuring of Viscoelastic Properties of Single Biological Cells," *Sens. Actuators B*, **118**(1–2), pp. 20–27.
- [116] Kuznetsova, T. G., Starodubtseva, M. N., Yegorenkov, N. I., Chizhik, S. A., and Zhdanov, R. I., 2007, "Atomic Force Microscopy Probing of Cell Elasticity," *Micron*, **38**(8), pp. 824–833.
- [117] Binnig, G., Quate, C. F., and Gerber, C., 1986, "Atomic Force Microscope," *Phys. Rev. Lett.*, **56**(9), pp. 930–933.
- [118] Silva, L. P., 2005, "Imaging Proteins with Atomic Force Microscopy: An Overview," *Curr. Protein Pept. Sci.*, **6**(4), pp. 387–395.
- [119] Muller, D. J., 2008, "AFM: A Nanotool in Membrane Biology," *Biochemistry*, **47**(31), pp. 7986–7998.
- [120] Engel, A., and Gaub, H. E., 2008, "Structure and Mechanics of Membrane Proteins," *Ann. Rev. Biochem.*, **77**, pp. 127–148.
- [121] Hansma, H. G., Kasuya, K., and Orudjev, E., 2004, "Atomic Force Microscopy Imaging and Pulling of Nucleic Acids," *Curr. Opin. Struct. Biol.*, **14**(3), pp. 380–385.
- [122] Hirano, Y., Takahashi, H., Kumeta, M., Hizume, K., Hirai, Y., Otsuka, S., Yoshimura, S. H., and Takeyasu, K., 2008, "Nuclear Architecture and Chromatin Dynamics Revealed by Atomic Force Microscopy in Combination with Biochemistry and Cell Biology," *Pflugers Arch.*, **456**(1), pp. 139–153.
- [123] Rotsch, C., Jacobson, K., and Radmacher, M., 1999, "Dimensional and Mechanical Dynamics of Active and Stable Edges in Motile Fibroblasts Investigated by Using Atomic Force Microscopy," *Proc. Natl. Acad. Sci. U.S.A.*, **96**(3), pp. 921–926.
- [124] Pesen, D., and Hoh, J. H., 2005, "Micromechanical Architecture of the Endothelial Cell Cortex," *Biophys. J.*, **88**(1), pp. 670–679.
- [125] Hiratsuka, S., Mizutani, Y., Tsuchiya, M., Kawahara, K., Tokumoto, H., and Okajima, T., 2009, "The Number Distribution of Complex Shear Modulus of Single Cells Measured by Atomic Force Microscopy," *Ultramicroscopy*, **109**(8), pp. 937–941.
- [126] Cross, S. E., Jin, Y. S., Rao, J., and Gimzewski, J. K., 2007, "Nanomechanical Analysis of Cells from Cancer Patients," *Nat. Nanotechnol.*, **2**(12), pp. 780–783.

- [127] Cross, S. E., Jin, Y. S., Lu, Q. Y., Rao, J., and Gimzewski, J. K., 2011, "Green Tea Extract Selectively Targets Nanomechanics of Live Metastatic Cancer Cells," *Nanotechnology*, **22**(21), p. 215101.
- [128] Cross, S. E., Jin, Y. S., Tondre, J., Wong, R., Rao, J., and Gimzewski, J. K., 2008, "AFM-Based Analysis of Human Metastatic Cancer Cells," *Nanotechnology*, **19**(38), p. 384003.
- [129] Lekka, M., Laidler, P., Gil, D., Lekki, J., Stachura, Z., and Hryniewicz, A. Z., 1999, "Elasticity of Normal and Cancerous Human Bladder Cells Studied by Scanning Force Microscopy," *Eur. Biophys. J.*, **28**(4), pp. 312–316.
- [130] Maloney, J. M., Nikova, D., Lautenschlager, F., Clarke, E., Langer, R., Guck, J., and Van Vliet, K. J., 2010, "Mesenchymal Stem Cell Mechanics from the Attached to the Suspended State," *Biophys. J.*, **99**(8), pp. 2479–2487.
- [131] Solon, J., Levental, I., Sengupta, K., Georges, P. C., and Janmey, P. A., 2007, "Fibroblast Adaptation and Stiffness Matching to Soft Elastic Substrates," *Biophys. J.*, **93**(12), pp. 4453–4461.
- [132] Rotsch, C., and Radmacher, M., 2000, "Drug-Induced Changes of Cytoskeletal Structure and Mechanics in Fibroblasts: An Atomic Force Microscopy Study," *Biophys. J.*, **78**(1), pp. 520–535.
- [133] Rotsch, C., Braet, F., Wisse, E., and Radmacher, M., 1997, "AFM Imaging and Elasticity Measurements on Living Rat Liver Macrophages," *Cell Biol. Int.*, **21**(11), pp. 685–696.
- [134] Hofmann, U. G., Rotsch, C., Parak, W. J., and Radmacher, M., 1997, "Investigating the Cytoskeleton of Chicken Cardiocytes with the Atomic Force Microscope," *J. Struct. Biol.*, **119**(2), pp. 84–91.
- [135] Takai, E., Costa, K. D., Shaheen, A., Hung, C. T., and Guo, X. E., 2005, "Osteoblast Elastic Modulus Measured by Atomic Force Microscopy Is Substrate Dependent," *Ann. Biomed. Eng.*, **33**(7), pp. 963–971.
- [136] Sen, S., and Kumar, S., 2009, "Cell–Matrix De-Adhesion Dynamics Reflect Contractile Mechanics," *Cell Mol. Bioeng.*, **2**(2), pp. 218–230.
- [137] Radmacher, M., Fritz, M., Kacher, C. M., Cleveland, J. P., and Hansma, P. K., 1996, "Measuring the Viscoelastic Properties of Human Platelets with the Atomic Force Microscope," *Biophys. J.*, **70**(1), pp. 556–567.
- [138] Radmacher, M., Tillmann, R. W., and Gaub, H. E., 1993, "Imaging Viscoelasticity by Force Modulation With the Atomic Force Microscope," *Biophys. J.*, **64**(3), pp. 735–742.
- [139] Hoh, J. H., and Schoenberger, C. A., 1994, "Surface Morphology and Mechanical Properties of Mdk Monolayers by Atomic Force Microscopy," *J. Cell Sci.*, **107**, pp. 1105–1114.
- [140] Mathur, A. B., Collinsworth, A. M., Reichert, W. M., Kraus, W. E., and Truskey, G. A., 2001, "Endothelial, Cardiac Muscle and Skeletal Muscle Exhibit Different Viscous and Elastic Properties as Determined by Atomic Force Microscopy," *J. Biomech.*, **34**(12), pp. 1545–1553.
- [141] Collinsworth, A. M., Zhang, S., Kraus, W. E., and Truskey, G. A., 2002, "Apparent Elastic Modulus and Hysteresis of Skeletal Muscle Cells Throughout Differentiation," *Am. J. Physiol. Cell Physiol.*, **283**(4), pp. C1219–C1227.
- [142] Engler, A. J., Griffin, M. A., Sen, S., Bonnemann, C. G., Sweeney, H. L., and Discher, D. E., 2004, "Myotubes Differentiate Optimally on Substrates With Tissue-Like Stiffness: Pathological Implications for Soft or Stiff Micro-environments," *J. Cell Biol.*, **166**(6), pp. 877–887.
- [143] Lam, W. A., Rosenbluth, M. J., and Fletcher, D. A., 2007, "Chemotherapy Exposure Increases Leukemia Cell Stiffness," *Blood*, **109**(8), pp. 3505–3508.
- [144] Rosenbluth, M. J., Lam, W. A., and Fletcher, D. A., 2006, "Force Microscopy of Nonadherent Cells: A Comparison of Leukemia Cell Deformability," *Biophys. J.*, **90**(8), pp. 2994–3003.
- [145] Charras, G. T., Lehenkari, P. P., and Horton, M. A., 2001, "Atomic Force Microscopy Can Be Used to Mechanically Stimulate Osteoblasts and Evaluate Cellular Strain Distributions," *Ultramicroscopy*, **86**(1–2), pp. 85–95.
- [146] Charras, G. T., and Horton, M. A., 2002, "Single Cell Mechanotransduction and Its Modulation Analyzed by Atomic Force Microscope Indentation," *Biophys. J.*, **82**(6), pp. 2970–2981.
- [147] Tee, S. Y., Fu, J., Chen, C. S., and Janmey, P. A., 2011, "Cell Shape and Substrate Rigidity Both Regulate Cell Stiffness," *Biophys. J.*, **100**(5), pp. L25–L27.
- [148] Webster, K. D., Crow, A., and Fletcher, D. A., 2011, "An AFM-Based Stiffness Clamp for Dynamic Control of Rigidity," *PLoS One*, **6**(3), p. e17807.
- [149] Chaudhuri, O., Parekh, S. H., Lam, W. A., and Fletcher, D. A., 2009, "Combined Atomic Force Microscopy and Side-View Optical Imaging for Mechanical Studies of Cells," *Nat. Methods*, **6**(5), pp. 383–387.
- [150] Lim, C. T., Zhou, E. H., Li, A., Vedula, S. R. K., and Fu, H. X., 2006, "Experimental Techniques for Single Cell and Single Molecule Biomechanics," *Mater. Sci. Eng., C*, **26**(8), pp. 1278–1288.
- [151] Taubenberger, A., Cisneros, D. A., Friedrichs, J., Puech, P. H., Muller, D. J., and Franz, C. M., 2007, "Revealing Early Steps of Alpha2beta1 Integrin-Mediated Adhesion to Collagen Type I by Using Single-Cell Force Spectroscopy," *Mol. Biol. Cell*, **18**(5), pp. 1634–1644.
- [152] Hong, Z., Sun, Z., Li, Z., Mesquitta, W. T., Trzeciakowski, J. P., and Meininger, G. A., 2012, "Coordination of Fibronectin Adhesion with Contraction and Relaxation in Microvascular Smooth Muscle," *Cardiovasc. Res.*, **96**(1), pp. 73–80.
- [153] Puech, P. H., Poole, K., Knebel, D., and Muller, D. J., 2006, "A New Technical Approach to Quantify Cell–Cell Adhesion Forces by Afm," *Ultramicroscopy*, **106**(8–9), pp. 637–644.
- [154] Panorchan, P., Thompson, M. S., Davis, K. J., Tseng, Y., Konstantopoulos, K., and Wirtz, D., 2006, "Single-Molecule Analysis of Cadherin-Mediated Cell–Cell Adhesion," *J. Cell Sci.*, **119**, pp. 66–74.
- [155] Prass, M., Jacobson, K., Mogilner, A., and Radmacher, M., 2006, "Direct Measurement of the Lamellipodial Protrusive Force in a Migrating Cell," *J. Cell Biol.*, **174**(6), pp. 767–772.
- [156] Laurent, V. M., Kasas, S., Yersin, A., Schaffer, T. E., Catsicas, S., Dietler, G., Verkhovsky, A. B., and Meister, J. J., 2005, "Gradient of Rigidity in the Lamellipodia of Migrating Cells Revealed by Atomic Force Microscopy," *Biophys. J.*, **89**(1), pp. 667–675.
- [157] Rotsch, C., Jacobson, K., Condeelis, J., and Radmacher, M., 2001, "EGF-Stimulated Lamellipod Extension in Adenocarcinoma Cells," *Ultramicroscopy*, **86**(1–2), pp. 97–106.
- [158] Jeong, K. H., Lee, T. W., Ihm, C. G., Moon, J. Y., Lee, G. J., Park, H. K., and Lee, S. H., 2012, "Real-Time Monitoring of the Effects of Telmisartan on Angiotensin II-Induced Mechanical Changes in Live Mesangial Cells Using Atomic Force Microscopy," *Kidney Blood Pressure Res.*, **35**(6), pp. 573–582.
- [159] Liu, J., Sun, N., Bruce, M. A., Wu, J. C., and Butte, M. J., 2012, "Atomic Force Mechanobiology of Pluripotent Stem Cell-Derived Cardiomyocytes," *PLoS One*, **7**(5), p. e37559.
- [160] Upadhye, K. V., Candiello, J. E., Davidson, L. A., and Lin, H., 2011, "Whole-Cell Electrical Activity under Direct Mechanical Stimulus by Afm Cantilever Using Planar Patch Clamp Chip Approach," *Cell Mol. Bioeng.*, **4**(2), pp. 270–280.
- [161] Addae-Mensah, K. A., and Wikswo, J. P., 2008, "Measurement Techniques for Cellular Biomechanics In Vitro," *Exp. Biol. Med.*, **233**(7), pp. 792–809.
- [162] Ashkin, A., 1970, "Acceleration and Trapping of Particles by Radiation Pressure," *Phys. Rev. Lett.*, **24**(4), pp. 156–159.
- [163] Ashkin, A., 1980, "Applications of Laser Radiation Pressure," *Science*, **210**(4474), pp. 1081–1088.
- [164] Ashkin, A., and Dziedzic, J. M., 1987, "Optical Trapping and Manipulation of Viruses and Bacteria," *Science*, **235**(4795), pp. 1517–1520.
- [165] Ashkin, A., Dziedzic, J. M., and Yamane, T., 1987, "Optical Trapping and Manipulation of Single Cells Using Infrared Laser Beams," *Nature*, **330**(6150), pp. 769–771.
- [166] Block, S. M., 1992, "Making Light Work with Optical Tweezers," *Nature*, **360**(6403), pp. 493–495.
- [167] Svoboda, K., and Block, S. M., 1994, "Biological Applications of Optical Forces," *Ann. Rev. Biophys. Biomol. Struct.*, **23**, pp. 247–285.
- [168] Neuman, K. C., and Block, S. M., 2004, "Optical Trapping," *Rev. Sci. Instrum.*, **75**(9), pp. 2787–2809.
- [169] Fazal, F. M., and Block, S. M., 2011, "Optical Tweezers Study Life Under Tension," *Nat. Photonics*, **5**, pp. 318–321.
- [170] Neuman, K. C., Lionnet, T., and Allemand, J. F., 2007, "Single-Molecule Micromanipulation Techniques," *Ann. Rev. Mater. Res.*, **37**, pp. 33–67.
- [171] Zhang, H., and Liu, K. K., 2008, "Optical Tweezers for Single Cells," *J. R. Soc. Interface*, **5**(24), pp. 671–690.
- [172] Henon, S., Lenormand, G., Richert, A., and Gallet, F., 1999, "A New Determination of the Shear Modulus of the Human Erythrocyte Membrane Using Optical Tweezers," *Biophys. J.*, **76**(2), pp. 1145–1151.
- [173] Sleep, J., Wilson, D., Parker, K., Winlove, C. P., Simmons, R., and Gratzner, W., 1999, "Elastic Properties of the Red Blood Cell Membrane Measured Using Optical Tweezers: Relation to Haemolytic Disorders," *Biophys. J.*, **76**(1), pp. 3085–3095.
- [174] Lenormand, G., Henon, S., Richert, A., Simeon, J., and Gallet, F., 2001, "Direct Measurement of the Area Expansion and Shear Moduli of the Human Red Blood Cell Membrane Skeleton," *Biophys. J.*, **81**(1), pp. 43–56.
- [175] Dao, M., Lim, C. T., and Suresh, S., 2003, "Mechanics of the Human Red Blood Cell Deformed by Optical Tweezers," *J. Mech. Phys. Solids*, **51**(11–12), pp. 2259–2280.
- [176] Lim, C. T., Dao, M., Suresh, S., Sow, C. H., and Chew, K. T., 2004, "Large Deformation of Living Cells Using Laser Traps," *Acta Mater.*, **52**(7), pp. 1837–1845.
- [177] Suresh, S., Spatz, J., Mills, J. P., Micoulet, A., Dao, M., Lim, C. T., Beil, M., and Seufferlein, T., 2005, "Connections Between Single-Cell Biomechanics and Human Disease States: Gastrointestinal Cancer and Malaria," *Acta Biomater.*, **1**(1), pp. 15–30.
- [178] Gu, M., Kuriakose, S., and Gan, X. S., 2007, "A Single Beam near-Field Laser Trap for Optical Stretching, Folding and Rotation of Erythrocytes," *Optics Express*, **15**(3), pp. 1369–1375.
- [179] Park, S., Koch, D., Cardenas, R., Kas, J., and Shih, C. K., 2005, "Cell Motility and Local Viscoelasticity of Fibroblasts," *Biophys. J.*, **89**(6), pp. 4330–4342.
- [180] Ananthakrishnan, R., Guck, J., Wottawah, F., Schinkinger, S., Lincoln, B., Romeyke, M., Moon, T., and Kas, J., 2006, "Quantifying the Contribution of Actin Networks to the Elastic Strength of Fibroblasts," *J. Theor. Biol.*, **242**(2), pp. 502–516.
- [181] Guck, J., Schinkinger, S., Lincoln, B., Wottawah, F., Ebert, S., Romeyke, M., Lenz, D., Erickson, H. M., Ananthakrishnan, R., Mitchell, D., Kas, J., Ulvick, S., and Bilby, C., 2005, "Optical Deformability as an Inherent Cell Marker for Testing Malignant Transformation and Metastatic Competence," *Biophys. J.*, **88**(5), pp. 3689–3698.
- [182] Huang, W., Anvari, B., Torres, J. H., Lebaron, R. G., and Athanasiou, K. A., 2003, "Temporal Effects of Cell Adhesion on Mechanical Characteristics of the Single Chondrocyte," *J. Orthop. Res.*, **21**(1), pp. 88–95.
- [183] Curtis, J. E., and Spatz, J. P., 2004, "Getting a Grip: Hyaluronan-Mediated Cellular Adhesion," *Proceedings of the SPIE*, Vol. 5514, Denver, CO, pp. 455–466.
- [184] Walker, L. M., Holm, A., Cooling, L., Maxwell, L., Oberg, A., Sundqvist, T., and El Haj, A. J., 1999, "Mechanical Manipulation of Bone and Cartilage Cells with 'Optical Tweezers'," *FEBS Lett.*, **459**(1), pp. 39–42.

- [185] Titushkin, I., and Cho, M., 2006, "Distinct Membrane Mechanical Properties of Human Mesenchymal Stem Cells Determined Using Laser Optical Tweezers," *Biophys. J.*, **90**(7), pp. 2582–2591.
- [186] Bustamante, C., Bryant, Z., and Smith, S. B., 2003, "Ten Years of Tension: Single-Molecule DNA Mechanics," *Nature*, **421**(6921), pp. 423–427.
- [187] Allemand, J. F., Bensimon, D., and Croquette, V., 2003, "Stretching DNA and RNA to Probe Their Interactions with Proteins," *Curr. Opin. Struct. Biol.*, **13**(3), pp. 266–274.
- [188] Block, S. M., Goldstein, L. S., and Schnapp, B. J., 1990, "Bead Movement by Single Kinesin Molecules Studied With Optical Tweezers," *Nature*, **348**(6299), pp. 348–352.
- [189] Svoboda, K., and Block, S. M., 1994, "Force and Velocity Measured for Single Kinesin Molecules," *Cell*, **77**(5), pp. 773–784.
- [190] Svoboda, K., Schmidt, C. F., Schnapp, B. J., and Block, S. M., 1993, "Direct Observation of Kinesin Stepping by Optical Trapping Interferometry," *Nature*, **365**(6448), pp. 721–727.
- [191] Asbury, C. L., Fehr, A. N., and Block, S. M., 2003, "Kinesin Moves by an Asymmetric Hand-over-Hand Mechanism," *Science*, **302**(5653), pp. 2130–2134.
- [192] Mallik, R., Carter, B. C., Lex, S. A., King, S. J., and Gross, S. P., 2004, "Cytoplasmic Dynein Functions as a Gear in Response to Load," *Nature*, **427**(6975), pp. 649–652.
- [193] Knight, A. E., Veigel, C., Chambers, C., and Molloy, J. E., 2001, "Analysis of Single-Molecule Mechanical Recordings: Application to Acto-Myosin Interactions," *Prog. Biophys. Mol. Biol.*, **77**(1), pp. 45–72.
- [194] Block, S. M., Asbury, C. L., Shaevitz, J. W., and Lang, M. J., 2003, "Probing the Kinesin Reaction Cycle With a 2D Optical Force Clamp," *Proc. Natl. Acad. Sci. U.S.A.*, **100**(5), pp. 2351–2356.
- [195] Mehta, A. D., Rock, R. S., Rief, M., Spudich, J. A., Mooseker, M. S., and Cheney, R. E., 1999, "Myosin-V is a Processive Actin-Based Motor," *Nature*, **400**(6744), pp. 590–593.
- [196] Abbondanzieri, E. A., Greenleaf, W. J., Shaevitz, J. W., Landick, R., and Block, S. M., 2005, "Direct Observation of Base-Pair Stepping by Rna Polymerase," *Nature*, **438**(7067), pp. 460–465.
- [197] Wang, M. D., Schnitzer, M. J., Yin, H., Landick, R., Gelles, J., and Block, S. M., 1998, "Force and Velocity Measured for Single Molecules of Rna Polymerase," *Science*, **282**(5390), pp. 902–907.
- [198] Herbert, K. M., La Porta, A., Wong, B. J., Mooney, R. A., Neuman, K. C., Landick, R., and Block, S. M., 2006, "Sequence-Resolved Detection of Pausing by Single Rna Polymerase Molecules," *Cell*, **125**(6), pp. 1083–1094.
- [199] Neuman, K. C., Abbondanzieri, E. A., Landick, R., Gelles, J., and Block, S. M., 2003, "Ubiquitous Transcriptional Pausing is Independent of RNA Polymerase Backtracking," *Cell*, **115**(4), pp. 437–447.
- [200] Shaevitz, J. W., Abbondanzieri, E. A., Landick, R., and Block, S. M., 2003, "Backtracking by Single RNA Polymerase Molecules Observed at Near-Base-Pair Resolution," *Nature*, **426**(6967), pp. 684–687.
- [201] Liphardt, J., Onoa, B., Smith, S. B., Tinoco, I., Jr., and Bustamante, C., 2001, "Reversible Unfolding of Single RNA Molecules by Mechanical Force," *Science*, **292**(5517), pp. 733–737.
- [202] Kellermayer, M. S., Smith, S. B., Granzier, H. L., and Bustamante, C., 1997, "Folding-Unfolding Transitions in Single Titin Molecules Characterized with Laser Tweezers," *Science*, **276**(5315), pp. 1112–1116.
- [203] Cecconi, C., Shank, E. A., Bustamante, C., and Marqusee, S., 2005, "Direct Observation of the Three-State Folding of a Single Protein Molecule," *Science*, **309**(5743), pp. 2057–2060.
- [204] Thoumine, O., Kocian, P., Kottelat, A., and Meister, J. J., 2000, "Short-Term Binding of Fibroblasts to Fibrinectin: Optical Tweezers Experiments and Probabilistic Analysis," *Eur. Biophys. J.*, **29**(6), pp. 398–408.
- [205] Litvinov, R. I., Bennett, J. S., Weisel, J. W., and Shuman, H., 2005, "Multi-Step Fibrinogen Binding to the Integrin $\alpha_{IIb}\beta_3$ Detected Using Force Spectroscopy," *Biophys. J.*, **89**(4), pp. 2824–2834.
- [206] Fontes, A., Barjas Castro, M. L., Brandao, M. M., Fernandes, H. P., Thomaz, A. A., Huruta, R. R., Pozzo, L. Y., Barbosa, L. C., Costa, F. F., Saad, S. T. O., and Cesar, C. L., 2011, "Mechanical and Electrical Properties of Red Blood Cells Using Optical Tweezers," *J. Opt.*, **13**(4), pp. 1–8.
- [207] Mohanty, S. K., Uppal, A., and Gupta, P. K., 2008, "Optofluidic Stretching of RBCs Using Single Optical Tweezers," *J. Biophotonics*, **1**(6), pp. 522–525.
- [208] Fallman, E., and Axner, O., 1997, "Design for Fully Steerable Dual-Trap Optical Tweezers," *Appl. Opt.*, **36**(10), pp. 2107–2113.
- [209] Chiou, A. E., 1997, "Interferometric Optical Tweezers," *Optics Commun.*, **133**(1–6), pp. 7–10.
- [210] Macdonald, M. P., Spalding, G. C., and Dholakia, K., 2003, "Microfluidic Sorting in an Optical Lattice," *Nature*, **426**(6965), pp. 421–424.
- [211] Guck, J., Ananthkrishnan, R., Mahmood, H., Moon, T. J., Cunningham, C. C., and Kas, J., 2001, "The Optical Stretcher: A Novel Laser Tool to Micro-manipulate Cells," *Biophys. J.*, **81**(2), pp. 767–784.
- [212] Flynn, R. A., Birkbeck, A. L., Gross, M., Ozkan, M., Shao, B., Wang, M. M., and Esener, S. C., 2002, "Parallel Transport of Biological Cells Using Individually Addressable Vesel Arrays as Optical Tweezers," *Sens. Actuators B*, **87**(2), pp. 239–243.
- [213] Eriksen, R. L., Daria, V. R., and Gluckstad, J., 2002, "Fully Dynamic Multiple-Beam Optical Tweezers," *Optics Express*, **10**(14), pp. 597–602.
- [214] Rodrigo, P. J., Eriksen, R. L., Daria, V. R., and Gluckstad, J., 2003, "Shack-Hartmann Multiple-Beam Optical Tweezers," *Optics Express*, **11**(3), pp. 208–214.
- [215] Rodrigo, P. J., Perch-Nielsen, I. R., and Gluckstad, J., 2006, "Three-Dimensional Forces in Gpc-Based Counterpropagating-Beam Traps," *Optics Express*, **14**(12), pp. 5812–5822.
- [216] Bronkhorst, P. J. H., Streekstra, G. J., Grimbergen, J., Nijhof, E. J., Sixma, J. J., and Brakenhoff, G. J., 1995, "A New Method to Study Shape Recovery of Red Blood Cells Using Multiple Optical Trapping," *Biophys. J.*, **69**(5), pp. 1666–1673.
- [217] Hormeno, S., and Arias-Gonzalez, J. R., 2006, "Exploring Mechanochemical Processes in the Cell With Optical Tweezers," *Biol. Cell*, **98**(12), pp. 679–695.
- [218] Lincoln, B., Wottawah, F., Schinkinger, S., Ebert, S., and Guck, J., 2007, "High-Throughput Rheological Measurements With an Optical Stretcher," *Cell Mech.*, **83**, pp. 397–423.
- [219] Mohanty, S., 2012, "Optically-Actuated Translational and Rotational Motion at the Microscale for Microfluidic Manipulation and Characterization," *Lab Chip*, **12**(19), pp. 3624–3636.
- [220] Sraj, I., Eggleton, C. D., Jimenez, R., Hoover, E., Squier, J., Chichester, J., and Marr, D. W., 2010, "Cell Deformation Cytometry Using Diode-Bar Optical Stretchers," *J. Biomed. Opt.*, **15**(4), p. 047010.
- [221] Kreysing, M. K., Kiessling, T., Fritsch, A., Dietrich, C., Guck, J. R., and Kas, J. A., 2008, "The Optical Cell Rotator," *Optics Express*, **16**(21), pp. 16984–16992.
- [222] Ziemann, F., Radler, J., and Sackmann, E., 1994, "Local Measurements of Viscoelastic Moduli of Entangled Actin Networks Using an Oscillating Magnetic Bead Micro-Rheometer," *Biophys. J.*, **66**(6), pp. 2210–2216.
- [223] Bausch, A. R., Moller, W., and Sackmann, E., 1999, "Measurement of Local Viscoelasticity and Forces in Living Cells by Magnetic Tweezers," *Biophys. J.*, **76**, pp. 573–579.
- [224] Bausch, A. R., Ziemann, F., Boulbitch, A. A., Jacobson, K., and Sackmann, E., 1998, "Local Measurements of Viscoelastic Parameters of Adherent Cell Surfaces by Magnetic Bead Microrheometry," *Biophys. J.*, **75**(4), pp. 2038–2049.
- [225] Crick, F. H. C., 1950, "The Physical Properties of Cytoplasm. A Study by Means of the Magnetic Particle Method. Part 2. Theoretical Treatment," *Exp. Cell Res.*, **1**, pp. 505–533.
- [226] Crick, F. H. C., and Hughes, A. F. W., 1950, "The Physical Properties of the Cytoplasm. A Study by Means of the Magnetic Particle Method. Part 1," *Exp. Cell Res.*, **1**, pp. 37–80.
- [227] Strick, T. R., Allemand, J. F., Bensimon, D., Bensimon, A., and Croquette, V., 1996, "The Elasticity of a Single Supercoiled DNA Molecule," *Science*, **271**(5257), pp. 1835–1837.
- [228] Smith, S. B., Finzi, L., and Bustamante, C., 1992, "Direct Mechanical Measurements of the Elasticity of Single DNA Molecules by Using Magnetic Beads," *Science*, **258**(5085), pp. 1122–1126.
- [229] Strick, T. R., Croquette, V., and Bensimon, D., 2000, "Single-Molecule Analysis of DNA Uncoiling by a Type II Topoisomerase," *Nature*, **404**(6780), pp. 901–904.
- [230] Heinrich, V., and Waugh, R. E., 1996, "A Piconewton Force Transducer and its Application to Measurement of the Bending Stiffness of Phospholipid Membranes," *Ann. Biomed. Eng.*, **24**(5), pp. 595–605.
- [231] Mannix, R. J., Kumar, S., Cassiola, F., Montoya-Zavala, M., Feinstein, E., Prentiss, M., and Ingber, D. E., 2008, "Nanomagnetic Actuation of Receptor-Mediated Signal Transduction," *Nat. Nanotechnol.*, **3**(1), pp. 36–40.
- [232] Danilowicz, C., Greenfield, D., and Prentiss, M., 2005, "Dissociation of Ligand-Receptor Complexes Using Magnetic Tweezers," *Anal. Chem.*, **77**(10), pp. 3023–3028.
- [233] Glogauer, M., Arora, P., Yao, G., Sokholov, I., Ferrier, J., and McCulloch, C. A., 1997, "Calcium Ions and Tyrosine Phosphorylation Interact Coordinately With Actin to Regulate Cytoprotective Responses to Stretching," *J. Cell Sci.*, **110**, pp. 11–21.
- [234] Del Rio, A., Perez-Jimenez, R., Liu, R., Roca-Cusachs, P., Fernandez, J. M., and Sheetz, M. P., 2009, "Stretching Single Talin Rod Molecules Activates Vinculin Binding," *Science*, **323**(5914), pp. 638–641.
- [235] Matthews, B. D., Overby, D. R., Alenghat, F. J., Karavitis, J., Numaguchi, Y., Allen, P. G., and Ingber, D. E., 2004, "Mechanical Properties of Individual Focal Adhesions Probed With a Magnetic Microneedle," *Biochem. Biophys. Res. Commun.*, **313**(3), pp. 758–764.
- [236] D'addario, M., Arora, P. D., Ellen, R. P., and McCulloch, C. A., 2003, "Regulation of Tension-Induced Mechanotranscriptional Signals by the Microtubule Network in Fibroblasts," *J. Biol. Chem.*, **278**(52), pp. 53090–53097.
- [237] Browe, D. M., and Baumgarten, C. M., 2003, "Stretch of Beta 1 Integrin Activates an Outwardly Rectifying Chloride Current via FAK and SRC in Rabbit Ventricular Myocytes," *J. Gen. Physiol.*, **122**(6), pp. 689–702.
- [238] D'addario, M., Arora, P. D., Ellen, R. P., and McCulloch, C. A., 2002, "Interaction of P38 and SP1 in a Mechanical Force-Induced, Beta 1 Integrin-Mediated Transcriptional Circuit That Regulates the Actin-Binding Protein Filamin-A," *J. Biol. Chem.*, **277**(49), pp. 47541–47550.
- [239] D'addario, M., Arora, P. D., Fan, J., Ganss, B., Ellen, R. P., and McCulloch, C. A. G., 2001, "Cytoprotection Against Mechanical Forces Delivered Through β_1 Integrins Requires Induction of Filamin A," *J. Biol. Chem.*, **276**(34), pp. 31969–31977.
- [240] Glogauer, M., Arora, P., Chou, D., Janney, P. A., Downey, G. P., and McCulloch, C. A., 1998, "The Role of Actin-Binding Protein 280 in Integrin-Dependent Mechanoprotection," *J. Biol. Chem.*, **273**(3), pp. 1689–1698.
- [241] Mack, P. J., Kaazempour-Mofrad, M. R., Karcher, H., Lee, R. T., and Kamm, R. D., 2004, "Force-Induced Focal Adhesion Translocation: Effects of

- Force Amplitude and Frequency," *Am. J. Physiol. Cell Physiol.*, **287**(4), pp. C954–C9562.
- [242] Shifrin, Y., Arora, P. D., Ohta, Y., Calderwood, D. A., and McCulloch, C. A., 2009, "The Role of Filgap-Filamin A Interactions in Mechanoprotection," *Mol. Biol. Cell*, **20**(5), pp. 1269–1279.
- [243] Balasubramanian, L., Ahmed, A., Lo, C. M., Sham, J. S., and Yip, K. P., 2007, "Integrin-Mediated Mechanotransduction in Renal Vascular Smooth Muscle Cells: Activation of Calcium Sparks," *Am. J. Physiol. Regul. Integr. Comput. Physiol.*, **293**(4), pp. R1586–R1594.
- [244] Glogauer, M., Ferrier, J., and McCulloch, C. A., 1995, "Magnetic Fields Applied to Collagen-Coated Ferric Oxide Beads Induce Stretch-Activated Ca²⁺ Flux in Fibroblasts," *Am. J. Physiol.*, **269**, pp. C1093–C1104.
- [245] Wu, Z., Wong, K., Glogauer, M., Ellen, R. P., and McCulloch, C. A. G., 1999, "Regulation of Stretch-Activated Intracellular Calcium Transients by Actin Filaments," *Biochem. Biophys. Res. Commun.*, **261**(2), pp. 419–425.
- [246] Kris, A. S., Kamm, R. D., and Sieminski, A. L., 2008, "Vasp Involvement in Force-Mediated Adherens Junction Strengthening," *Biochem. Biophys. Res. Commun.*, **375**(1), pp. 134–138.
- [247] Tseng, P., Judy, J. W., and Di Carlo, D., 2012, "Magnetic Nanoparticle-Mediated Massively Parallel Mechanical Modulation of Single-Cell Behavior," *Nat. Methods*, **9**(11), pp. 1113–1119.
- [248] Kim, D. H., Wong, P. K., Park, J., Levchenko, A., and Sun, Y., 2009, "Microengineered Platforms for Cell Mechanobiology," *Ann. Rev. Biomed. Eng.*, **11**, pp. 203–233.
- [249] Neuman, K. C., and Nagy, A., 2008, "Single-Molecule Force Spectroscopy: Optical Tweezers, Magnetic Tweezers and Atomic Force Microscopy," *Nat. Methods*, **5**(6), pp. 491–505.
- [250] Sen, S., and Kumar, S., 2010, "Combining Mechanical and Optical Approaches to Dissect Cellular Mechanobiology," *J. Biomech.*, **43**(1), pp. 45–54.
- [251] Lele, T. P., Sero, J. E., Matthews, B. D., Kumar, S., Xia, S., Montoya-Zavala, M., Polte, T., Overby, D., Wang, N., and Ingber, D. E., 2007, "Tools to Study Cell Mechanics and Mechanotransduction," *Methods Cell Biol.*, **83**, pp. 443–472.
- [252] Wang, N., Butler, J. P., and Ingber, D. E., 1993, "Mechanotransduction Across the Cell Surface and Through the Cytoskeleton," *Science*, **260**(5111), pp. 1124–1127.
- [253] Fabry, B., Maksym, G. N., Shore, S. A., Moore, P. E., Panettieri, R. A., Jr., Butler, J. P., and Fredberg, J. J., 2001, "Selected Contribution: Time Course and Heterogeneity of Contractile Responses in Cultured Human Airway Smooth Muscle Cells," *J. Appl. Physiol.*, **91**(2), pp. 986–994.
- [254] Wang, N., Tolic-Norrelykke, I. M., Chen, J., Mijailovich, S. M., Butler, J. P., Fredberg, J. J., and Stamenovic, D., 2002, "Cell Prestress. I. Stiffness and Prestress Are Closely Associated in Adherent Contractile Cells," *Am. J. Physiol. Cell Physiol.*, **282**(3), pp. C606–C616.
- [255] Wang, N., and Ingber, D. E., 1995, "Probing Transmembrane Mechanical Coupling and Cytochemicals Using Magnetic Twisting Cytometry," *Biochem. Cell Biol.*, **73**(7–8), pp. 327–335.
- [256] Chen, J., Fabry, B., Schiffrin, E. L., and Wang, N., 2001, "Twisting Integrin Receptors Increases Endothelin-1 Gene Expression in Endothelial Cells," *Am. J. Physiol. Cell Physiol.*, **280**(6), pp. C1475–C1484.
- [257] Goldschmidt, M. E., McLeod, K. J., and Taylor, W. R., 2001, "Integrin-Mediated Mechanotransduction in Vascular Smooth Muscle Cells: Frequency and Force Response Characteristics," *Circ. Res.*, **88**(7), pp. 674–680.
- [258] Yoshida, M., Westlin, F., Wang, N., Ingber, D. E., Rosenzweig, A., Resnick, N., and Gimbrone, M. A., Jr., 1996, "Leukocyte Adhesion to Vascular Endothelium Induces E-Selectin Linkage to the Actin Cytoskeleton," *J. Cell Biol.*, **133**(2), pp. 445–455.
- [259] Potard, U. S., Butler, J. P., and Wang, N., 1997, "Cytoskeletal Mechanics in Confluent Epithelial Cells Probed through Integrins and E-Cadherins," *Am. J. Physiol.*, **272**, pp. C1654–C1663.
- [260] Lenormand, G., Millet, E., Fabry, B., Butler, J. P., and Fredberg, J. J., 2004, "Linearity and Time-Scale Invariance of the Creep Function in Living Cells," *J. R. Soc. Interface*, **1**(1), pp. 91–97.
- [261] Na, S., and Wang, N., 2008, "Application of Fluorescence Resonance Energy Transfer and Magnetic Twisting Cytometry to Quantify Mechanochemical Signaling Activities in a Living Cell," *Sci. Signal*, **1**(34), p. 69932.
- [262] Meyer, C. J., Alenghat, F. J., Rim, P., Fong, J. H., Fabry, B., and Ingber, D. E., 2000, "Mechanical Control of Cyclic Amp Signalling and Gene Transcription Through Integrins," *Nat. Cell Biol.*, **2**(9), pp. 666–668.
- [263] Deng, L., Fairbank, N. J., Fabry, B., Smith, P. G., and Maksym, G. N., 2004, "Localized Mechanical Stress Induces Time-Dependent Actin Cytoskeletal Remodeling and Stiffening in Cultured Airway Smooth Muscle Cells," *Am. J. Physiol. Cell Physiol.*, **287**(2), pp. C440–C448.
- [264] Hu, S., Eberhard, L., Chen, J., Love, J. C., Butler, J. P., Fredberg, J. J., Whitesides, G. M., and Wang, N., 2004, "Mechanical Anisotropy of Adherent Cells Probed by a Three-Dimensional Magnetic Twisting Device," *Am. J. Physiol. Cell Physiol.*, **287**(5), pp. C1184–C1191.
- [265] Hu, S., Chen, J., Fabry, B., Numaguchi, Y., Gouldstone, A., Ingber, D. E., Fredberg, J. J., Butler, J. P., and Wang, N., 2003, "Intracellular Stress Tomography Reveals Stress Focusing and Structural Anisotropy in Cytoskeleton of Living Cells," *Am. J. Physiol. Cell Physiol.*, **285**(5), pp. C1082–C1090.
- [266] Chen, C., Krishnan, R., Zhou, E., Ramachandran, A., Tambe, D., Rajendran, K., Adam, R. M., Deng, L., and Fredberg, J. J., 2010, "Fluidization and Resolidification of the Human Bladder Smooth Muscle Cell in Response to Transient Stretch," *PLoS One*, **5**(8), e12035.
- [267] Krishnan, R., Trepat, X., Nguyen, T. T., Lenormand, G., Oliver, M., and Fredberg, J. J., 2008, "Airway Smooth Muscle and Bronchospasm: Fluctuating, Fluidizing, Freezing," *Respir. Physiol. Neurobiol.*, **163**(1–3), pp. 17–24.
- [268] Dipaolo, B. C., Lenormand, G., Fredberg, J. J., and Margulies, S. S., 2010, "Stretch Magnitude and Frequency-Dependent Actin Cytoskeleton Remodeling in Alveolar Epithelia," *Am. J. Physiol. Cell Physiol.*, **299**(2), pp. C345–C353.
- [269] Kang, J., Steward, R. L., Kim, Y., Schwartz, R. S., Leduc, P. R., and Puskas, K. M., 2011, "Response of an Actin Filament Network Model Under Cyclic Stretching Through a Coarse Grained Monte Carlo Approach," *J. Theor. Biol.*, **274**(1), pp. 109–119.
- [270] Steward, R. L., Cheng, C. M., Ye, J. D., Bellin, R. M., and Leduc, P. R., 2011, "Mechanical Stretch and Shear Flow Induced Reorganization and Recruitment of Fibronectin in Fibroblasts," *Sci. Rep.*, **1**, pp. 147–159.
- [271] Lin, Y. W., Cheng, C. M., Leduc, P. R., and Chen, C. C., 2009, "Understanding Sensory Nerve Mechanotransduction Through Localized Elastomeric Matrix Control," *PLoS One*, **4**(1), p. e4293.
- [272] Diederichs, S., Bohm, S., Peterbauer, A., Kasper, C., Scheper, T., and Van Griensven, M., 2010, "Application of Different Strain Regimes in Two-Dimensional and Three-Dimensional Adipose Tissue-Derived Stem Cell Cultures Induces Osteogenesis: Implications for Bone Tissue Engineering," *J. Biomed. Mater. Res. A*, **94**(3), pp. 927–936.
- [273] Katsumi, A., Milanini, J., Kiosses, W. B., Del Pozo, M. A., Kaunas, R., Chien, S., Hahn, K. M., and Schwartz, M. A., 2002, "Effects of Cell Tension on the Small GTPase RAC," *J. Cell Biol.*, **158**(1), pp. 153–164.
- [274] Brown, T. D., 2000, "Techniques for Mechanical Stimulation of Cells in vitro: A Review," *J. Biomech.*, **33**(1), pp. 3–14.
- [275] Freeman, P. M., Natarajan, R. N., Kimura, J. H., and Andriacchi, T. P., 1994, "Chondrocyte Cells Respond Mechanically to Compressive Loads," *J. Orthop. Res.*, **12**(3), pp. 311–320.
- [276] Bader, D. L., Ohashi, T., Knight, M. M., Lee, D. A., and Sato, M., 2002, "Deformation Properties of Articular Chondrocytes: A Critique of Three Separate Techniques," *Biorheology*, **39**(1–2), pp. 69–78.
- [277] Cheng, C. M., Steward, R. L., Jr., and Leduc, P. R., 2009, "Probing Cell Structure by Controlling the Mechanical Environment with Cell-Substrate Interactions," *J. Biomech.*, **42**(2), pp. 187–192.
- [278] Hiramoto, Y., 1970, "Rheological Properties of Sea Urchin Eggs," *Biorheology*, **6**(3), pp. 201–234.
- [279] Cole, K. S., 1932, "Surface Forces of the Arbacia Egg," *J. Cell. Comp. Physiol.*, **1**(1), pp. 1–9.
- [280] Danielli, J. F., 1952, "Division of the Flattened Egg," *Nature*, **170**(4325), p. 496.
- [281] Hiramoto, Y., 1963, "Mechanical Properties of Sea Urchin Eggs. II. Changes in Mechanical Properties from Fertilization to Cleavage," *Exp. Cell Res.*, **32**, pp. 76–89.
- [282] Hiramoto, Y., 1963, "Mechanical Properties of Sea Urchin Eggs. I. Surface Force and Elastic Modulus of the Cell Membrane," *Exp. Cell Res.*, **32**, pp. 59–75.
- [283] Yoneda, M., 1964, "Tension at the Surface of Sea-Urchin Egg: A Critical Examination of Cole's Experiment," *J. Exp. Biol.*, **41**, pp. 893–906.
- [284] Brighton, C. T., Fisher, J. R., Jr., Levine, S. E., Corsetti, J. R., Reilly, T., Landsman, A. S., Williams, J. L., and Thibault, L. E., 1996, "The Biochemical Pathway Mediating the Proliferative Response of Bone Cells to a Mechanical Stimulus," *J. Bone Joint Surg. Am.*, **78**(9), pp. 1337–1347.
- [285] Thoumine, O., and Ott, A., 1997, "Time Scale Dependent Viscoelastic and Contractile Regimes in Fibroblasts Probed by Microplate Manipulation," *J. Cell Sci.*, **110**, pp. 2109–2116.
- [286] Peeters, E. A., Oomens, C. W., Bouten, C. V., Bader, D. L., and Baaijens, F. P., 2005, "Viscoelastic Properties of Single Attached Cells under Compression," *ASME J. Biomech. Eng.*, **127**(2), pp. 237–243.
- [287] Shieh, A. C., and Athanasiou, K. A., 2006, "Biomechanics of Single Zonal Chondrocytes," *J. Biomech.*, **39**(9), pp. 1595–1602.
- [288] Leipzig, N. D., and Athanasiou, K. A., 2005, "Unconfined Creep Compression of Chondrocytes," *J. Biomech.*, **38**(1), pp. 77–85.
- [289] Caille, N., Thoumine, O., Tardy, Y., and Meister, J. J., 2002, "Contribution of the Nucleus to the Mechanical Properties of Endothelial Cells," *J. Biomech.*, **35**(2), pp. 177–187.
- [290] Blackman, B. R., Garcia-Cardena, G., and Gimbrone, M. A., Jr., 2002, "A New in vitro Model to Evaluate Differential Responses of Endothelial Cells to Simulated Arterial Shear Stress Waveforms," *ASME J. Biomech. Eng.*, **124**(4), pp. 397–407.
- [291] Bussolari, S. R., Dewey, C. F., and Gimbrone, M. A., 1982, "Apparatus for Subjecting Living Cells to Fluid Shear-Stress," *Rev. Sci. Instrum.*, **53**(12), pp. 1851–1854.
- [292] Davies, P. F., Dewey, C. F., Jr., Bussolari, S. R., Gordon, E. J., and Gimbrone, M. A., Jr., 1984, "Influence of Hemodynamic Forces on Vascular Endothelial Function. In vitro Studies of Shear Stress and Pinocytosis in Bovine Aortic Cells," *J. Clin. Invest.*, **73**(4), pp. 1121–1129.
- [293] Dewey, C. F., Jr., Bussolari, S. R., Gimbrone, M. A., Jr., and Davies, P. F., 1981, "The Dynamic Response of Vascular Endothelial Cells to Fluid Shear Stress," *ASME J. Biomech. Eng.*, **103**(3), pp. 177–185.
- [294] Li, S., Kim, M., Hu, Y. L., Jalali, S., Schlaepfer, D. D., Hunter, T., Chien, S., and Shyy, J. Y., 1997, "Fluid Shear Stress Activation of Focal Adhesion Kinase. Linking to Mitogen-Activated Protein Kinases," *J. Biol. Chem.*, **272**(48), pp. 30455–30462.

- [295] Galbraith, C. G., Skalak, R., and Chien, S., 1998, "Shear Stress Induces Spatial Reorganization of the Endothelial Cell Cytoskeleton," *Cell Motil. Cytoskeleton*, **40**(4), pp. 317–330.
- [296] Li, S., Chen, B. P. C., Azuma, N., Hu, Y. L., Wu, S. Z., Sumpio, B. E., Shyy, J. Y. J., and Chien, S., 1999, "Distinct Roles for the Small GTPases CDC42 and Rho in Endothelial Responses to Shear Stress," *J. Clin. Invest.*, **103**(8), pp. 1141–1150.
- [297] Davies, P. F., 1995, "Flow-Mediated Endothelial Mechanotransduction," *Physiol. Rev.*, **75**(3), pp. 519–560.
- [298] Del Alamo, J. C., Norwich, G. N., Li, Y. S., Lasheras, J. C., and Chien, S., 2008, "Anisotropic Rheology and Directional Mechanotransduction in Vascular Endothelial Cells," *Proc. Natl. Acad. Sci. U.S.A.*, **105**(40), pp. 15411–15416.
- [299] Chen, K. D., Li, Y. S., Kim, M., Li, S., Yuan, S., Chien, S., and Shyy, J. Y., 1999, "Mechanotransduction in Response to Shear Stress. Roles of Receptor Tyrosine Kinases, Integrins, and SHC," *J. Biol. Chem.*, **274**(26), pp. 18393–183400.
- [300] Young, A., Wu, W., Sun, W., Larman, H. B., Wang, N. P., Li, Y. S., Shyy, J. Y., Chien, S., and Garcia-Cardena, G., 2009, "Flow Activation of Amp-Activated Protein Kinase in Vascular Endothelium Leads to Kruppel-Like Factor 2 Expression," *Arterioscler., Thromb., Vasc. Biol.*, **29**(11), pp. 1902–1908.
- [301] Lin, K., Hsu, P. P., Chen, B. P., Yuan, S., Usami, S., Shyy, J. Y., Li, Y. S., and Chien, S., 2000, "Molecular Mechanism of Endothelial Growth Arrest by Laminar Shear Stress," *Proc. Natl. Acad. Sci. U.S.A.*, **97**(17), pp. 9385–9389.
- [302] Lee, D. Y., Li, Y. S. J., Chang, S. F., Zhou, J., Ho, H. M., Chiu, J. J., and Chien, S., 2010, "Oscillatory Flow-Induced Proliferation of Osteoblast-Like Cells Is Mediated by $\alpha_v\beta_3$ and β_1 Integrins through Synergistic Interactions of Focal Adhesion Kinase and SHC with Phosphatidylinositol 3-Kinase and the Akt/Mtor/P70s6k Pathway," *J. Biol. Chem.*, **285**(1), pp. 30–42.
- [303] Sotoudeh, M., Li, Y. S., Yajima, N., Chang, C. C., Tsou, T. C., Wang, Y. B., Usami, S., Ratcliffe, A., Chien, S., and Shyy, J. Y. J., 2002, "Induction of Apoptosis in Vascular Smooth Muscle Cells by Mechanical Stretch," *Am. J. Physiol. Heart Circ. Physiol.*, **282**(5), pp. H1709–H1716.
- [304] Wu, C. C., Li, Y. S., Haga, J. H., Kaunas, R., Chiu, J. J., Su, F. C., Usami, S., and Chien, S., 2007, "Directional Shear Flow and Rho Activation Prevent the Endothelial Cell Apoptosis Induced by Micropatterned Anisotropic Geometry," *Proc. Natl. Acad. Sci. U.S.A.*, **104**(4), pp. 1254–1259.
- [305] Chen, B. P., Li, Y. S., Zhao, Y., Chen, K. D., Li, S., Lao, J., Yuan, S., Shyy, J. Y., and Chien, S., 2001, "DNA Microarray Analysis of Gene Expression in Endothelial Cells in Response to 24-H Shear Stress," *Physiol. Genomics*, **7**(1), pp. 55–63.
- [306] Wang, N. P., Miao, H., Li, Y. S., Zhang, P., Haga, J. H., Hu, Y. L., Young, A., Yuan, S. L., Nguyen, P., Wu, C. C., and Chien, S., 2006, "Shear Stress Regulation of Kruppel-Like Factor 2 Expression is Flow Pattern-Specific," *Biochem. Biophys. Res. Commun.*, **341**(4), pp. 1244–1251.
- [307] Hsu, P. P., Li, S., Li, Y. S., Usami, S., Ratcliffe, A., Wang, X., and Chien, S., 2001, "Effects of Flow Patterns on Endothelial Cell Migration into a Zone of Mechanical Denudation," *Biochem. Biophys. Res. Commun.*, **285**(3), pp. 751–759.
- [308] Li, S., Bhatia, S., Hu, Y. L., Shiu, Y. T., Li, Y. S., Usami, S., and Chien, S., 2001, "Effects of Morphological Patterning on Endothelial Cell Migration," *Biorheology*, **38**(2–3), pp. 101–108.
- [309] Li, S., Butler, P., Wang, Y., Hu, Y., Han, D. C., Usami, S., Guan, J. L., and Chien, S., 2002, "The Role of the Dynamics of Focal Adhesion Kinase in the Mechanotaxis of Endothelial Cells," *Proc. Natl. Acad. Sci. U.S.A.*, **99**(6), pp. 3546–3551.
- [310] Shiu, Y. T., Li, S., Marganski, W. A., Usami, S., Schwartz, M. A., Wang, Y. L., Dembo, M., and Chien, S., 2004, "Rho Mediates the Shear-Enhancement of Endothelial Cell Migration and Traction Force Generation," *Biophys. J.*, **86**(4), pp. 2558–2565.
- [311] Chien, S., Li, S., Shiu, Y. T., and Li, Y. S., 2005, "Molecular Basis of Mechanical Modulation of Endothelial Cell Migration," *Front Biosci.*, **10**, pp. 1985–2000.
- [312] Jalali, S., Del Pozo, M. A., Chen, K., Miao, H., Li, Y., Schwartz, M. A., Shyy, J. Y., and Chien, S., 2001, "Integrin-Mediated Mechanotransduction Requires its Dynamic Interaction With Specific Extracellular Matrix (ECM) Ligands," *Proc. Natl. Acad. Sci. U.S.A.*, **98**(3), pp. 1042–1046.
- [313] Wang, Y. X., Miao, H., Li, S., Chen, K. D., Li, Y. S., Yuan, S. L., Shyy, J. Y. J., and Chien, S., 2002, "Interplay Between Integrins and FLK-1 in Shear Stress-Induced Signaling," *Am. J. Physiol. Cell Physiol.*, **283**(5), pp. C1540–C1547.
- [314] Tong, Z., Cheung, L. S., Stebe, K. J., and Konstantopoulos, K., 2012, "Selectin-Mediated Adhesion in Shear Flow Using Micropatterned Substrates: Multiple-Bond Interactions Govern the Critical Length for Cell Binding," *Integr. Biol. (Camb)*, **4**(8), pp. 847–856.
- [315] Miao, H., Hu, Y. L., Shiu, Y. T., Yuan, S. L., Zhao, Y. H., Kaunas, R., Wang, Y. X., Jin, G., Usami, S., and Chien, S., 2005, "Effects of Flow Patterns on the Localization and Expression of Ve-Cadherin at Vascular Endothelial Cell Junctions: In Vivo and In Vitro Investigations," *J. Vasc. Res.*, **42**(1), pp. 77–89.
- [316] Gossett, D. R., Tse, H. T., Lee, S. A., Ying, Y., Lindgren, A. G., Yang, O. O., Rao, J., Clark, A. T., and Di Carlo, D., 2012, "Hydrodynamic Stretching of Single Cells for Large Population Mechanical Phenotyping," *Proc. Natl. Acad. Sci. U.S.A.*, **109**(20), pp. 7630–7635.
- [317] Shelby, J. P., White, J., Ganesan, K., Rathod, P. K., and Chiu, D. T., 2003, "A Microfluidic Model for Single-Cell Capillary Obstruction by Plasmodium Falciparum-Infected Erythrocytes," *Proc. Natl. Acad. Sci. U.S.A.*, **100**(25), pp. 14618–14622.
- [318] Rosenbluth, M. J., Lam, W. A., and Fletcher, D. A., 2008, "Analyzing Cell Mechanics in Hematologic Diseases With Microfluidic Biophysical Flow Cytometry," *Lab Chip*, **8**(7), pp. 1062–1070.
- [319] Preira, P., Leoni, T., Valignat, M. P., Lellouch, A., Robert, P., Forel, J. M., Papazian, L., Dumenil, G., Bongrand, P., and Theodoly, O., 2012, "Microfluidic Tools to Investigate Pathologies in the Blood Microcirculation," *Int. J. Nanotechnol.*, **9**(3–7), pp. 529–547.
- [320] Bow, H., Pivkin, I. V., Diez-Silva, M., Goldfless, S. J., Dao, M., Niles, J. C., Suresh, S., and Han, J., 2011, "A Microfabricated Deformability-Based Flow Cytometer with Application to Malaria," *Lab Chip*, **11**(6), pp. 1065–1073.
- [321] Abkarian, M., Faivre, M., and Stone, H. A., 2006, "High-Speed Microfluidic Differential Manometer for Cellular-Scale Hydrodynamics," *Proc. Natl. Acad. Sci. U.S.A.*, **103**(3), pp. 538–542.
- [322] Zheng, W., Jiang, B., Wang, D., Zhang, W., Wang, Z., and Jiang, X., 2012, "A Microfluidic Flow-Stretch Chip for Investigating Blood Vessel Biomechanics," *Lab Chip*, **12**(18), pp. 3441–3450.
- [323] Douville, N. J., Zamankhan, P., Tung, Y. C., Li, R., Vaughan, B. L., Tai, C. F., White, J., Christensen, P. J., Grothberg, J. B., and Takayama, S., 2011, "Combination of Fluid and Solid Mechanical Stresses Contribute to Cell Death and Detachment in a Microfluidic Alveolar Model," *Lab Chip*, **11**(4), pp. 609–619.
- [324] Wang, F., Wang, H., Wang, J., Wang, H. Y., Rummel, P. L., Garimella, S. V., and Lu, C., 2008, "Microfluidic Delivery of Small Molecules into Mammalian Cells Based on Hydrodynamic Focusing," *Biotechnol. Bioeng.*, **100**(1), pp. 150–158.
- [325] Li, J., Zhu, L., Zhang, M., and Lin, F., 2012, "Microfluidic Device for Studying Cell Migration in Single or Co-Existing Chemical Gradients and Electric Fields," *Biomicrofluidics*, **6**(2), pp. 24121–24123.
- [326] Vanapalli, S. A., Duits, M. H., and Mugele, F., 2009, "Microfluidics as a Functional Tool for Cell Mechanics," *Biomicrofluidics*, **3**(1), p. 012006.
- [327] Shi, J., Ahmed, D., Mao, X., Lin, S. C., Lawit, A., and Huang, T. J., 2009, "Acoustic Tweezers: Patterning Cells and Microparticles Using Standing Surface Acoustic Waves (SSAW)," *Lab Chip*, **9**(20), pp. 2890–2895.
- [328] Campbell, C., and Burgess, J. C., 1991, "Surface Acoustic Wave Devices and Their Signal Processing Applications," *J. Acoust. Soc. Am.*, **89**(3), pp. 1479–1480.
- [329] Ding, X., Lin, S. C., Kiraly, B., Yue, H., Li, S., Chiang, I. K., Shi, J., Benkovic, S. J., and Huang, T. J., 2012, "On-Chip Manipulation of Single Microparticles, Cells, and Organisms Using Surface Acoustic Waves," *Proc. Natl. Acad. Sci. U.S.A.*, **109**(28), pp. 11105–11109.
- [330] Kim, D. H., Haake, A., Sun, Y., Neild, A. P., Ihm, J. E., Dual, J., Hubbell, J. A., Ju, B. K., and Nelson, B. J., 2004, "High-Throughput Cell Manipulation Using Ultrasound Fields," *Conf. Proc. IEEE Eng. Med. Biol. Soc.*, **4**, pp. 2571–2574.
- [331] Saitakis, M., and Gizeli, E., 2012, "Acoustic Sensors as a Biophysical Tool for Probing Cell Attachment and Cell/Surface Interactions," *Cell Mol. Life Sci.*, **69**(3), pp. 357–371.
- [332] Tymchenko, N., Nileback, E., Voinova, M. V., Gold, J., Kasemo, B., and Svedhem, S., 2012, "Reversible Changes in Cell Morphology Due to Cytoskeletal Rearrangements Measured in Real-Time by QCM-D," *Biointerphases*, **7**(1–4), pp. 43–51.
- [333] Kobayashi, Y., Sakai, D., Iwashina, T., Iwabuchi, S., and Mochida, J., 2009, "Low-Intensity Pulsed Ultrasound Stimulates Cell Proliferation, Proteoglycan Synthesis and Expression of Growth Factor-Related Genes in Human Nucleus Pulposus Cell Line," *Eur. Cell Mater.*, **17**, pp. 15–22.
- [334] Duarte, L. R., 1983, "The Stimulation of Bone Growth by Ultrasound," *Arch. Orthop. Trauma Surg.*, **101**(3), pp. 153–159.
- [335] Iwashina, T., Mochida, J., Miyazaki, T., Watanabe, T., Iwabuchi, S., Ando, K., Hotta, T., and Sakai, D., 2006, "Low-Intensity Pulsed Ultrasound Stimulates Cell Proliferation and Proteoglycan Production in Rabbit Intervertebral Disc Cells Cultured in Alginate," *Biomaterials*, **27**(3), pp. 354–361.
- [336] Fassina, L., Saino, E., De Angelis, M. G., Magenes, G., Benazzo, F., and Visai, L., 2010, "Low-Power Ultrasounds as a Tool to Culture Human Osteoblasts inside Cancellous Hydroxyapatite," *Bioinorg. Chem. Appl.*, **456**240.
- [337] Choi, W. H., Choi, B. H., Min, B. H., and Park, S. R., 2011, "Low-Intensity Ultrasound Increased Colony Forming Unit-Fibroblasts of Mesenchymal Stem Cells During Primary Culture," *Tissue Eng. Part C, Methods*, **17**(5), pp. 517–526.
- [338] Lee, J., Lee, C., Kim, H. H., Jakob, A., Lemor, R., Teh, S. Y., Lee, A., and Shung, K. K., 2011, "Targeted Cell Immobilization by Ultrasound Microbeam," *Biotechnol. Bioeng.*, **108**(7), pp. 1643–1650.
- [339] Lee, H. J., Choi, B. H., Min, B. H., Son, Y. S., and Park, S. R., 2006, "Low-Intensity Ultrasound Stimulation Enhances Chondrogenic Differentiation in Alginate Culture of Mesenchymal Stem Cells," *Artif. Organs*, **30**(9), pp. 707–715.
- [340] Hwang, J. Y., Lee, J., Lee, C., Jakob, A., Lemor, R., Medina-Kauwe, L. K., and Shung, K. K., 2012, "Fluorescence Response of Human HER2+ Cancer and MCF-12f Normal Cells to 200 Mhz Ultrasound Microbeam Stimulation: A Preliminary Study of Membrane Permeability Variation," *Ultrasonics*, **52**(7), pp. 803–808.
- [341] Stark, D. J., Killian, T. C., and Raphael, R. M., 2011, "A Microfabricated Magnetic Force Transducer-Microaspiration System for Studying Membrane Mechanics," *Phys. Biol.*, **8**(5), p. 056008.

- [342] Macqueen, L. A., Buschmann, M. D., and Wertheimer, M. R., 2010, "Mechanical Properties of Mammalian Cells in Suspension Measured by Electro-Deformation," *J. Micromech. Microeng.*, **20**(6), p. 065007.
- [343] Chen, J., Abdelgawad, M., Yu, L. M., Shakiba, N., Chien, W. Y., Lu, Z., Geddie, W. R., Jewett, M. A. S., and Sun, Y., 2011, "Electrodeformation for Single Cell Mechanical Characterization," *J. Micromech. Microeng.*, **21**(5), p. 054012.
- [344] Voldman, J., Gray, M. L., Toner, M., and Schmidt, M. A., 2002, "A Microfabrication-Based Dynamic Array Cytometer," *Anal. Chem.*, **74**(16), pp. 3984–3990.
- [345] Guido, I., Jaeger, M. S., and Duschl, C., 2011, "Dielectrophoretic Stretching of Cells Allows for Characterization of Their Mechanical Properties," *Eur. Biophys. J. Biophys. Lett.*, **40**(3), pp. 281–288.
- [346] Pethig, R., and Markx, G. H., 1997, "Applications of Dielectrophoresis in Biotechnology," *Trends Biotechnol.*, **15**(10), pp. 426–432.
- [347] Gnerlich, M., Perry, S. F., and Tatic-Lucic, S., 2012, "A Submersible Piezoresistive Membrane Lateral Force Sensor for a Diagnostic Biomechanics Platform," *Sens. Actuators A*, **188**, pp. 111–119.
- [348] Hsu, Y. H., and Tang, W. C., 2009, "A Microfabricated Piezoelectric Transducer Platform for Mechanical Characterization of Cellular Events," *Smart Mater. Struct.*, **18**(9), p. 095014.
- [349] Doll, J. C., Harjee, N., Klejwa, N., Kwon, R., Coulthard, S. M., Petzold, B., Goodman, M. B., and Pruitt, B. L., 2009, "SU-8 Force Sensing Pillar Arrays for Biological Measurements," *Lab Chip*, **9**(10), pp. 1449–1454.
- [350] Wong, P. K., Tan, W., and Ho, C. M., 2005, "Cell Relaxation after Electrodeformation: Effect of Latrunculin A on Cytoskeletal Actin," *J. Biomech.*, **38**(3), pp. 529–535.
- [351] Hronik-Tupaj, M., and Kaplan, D. L., 2012, "A Review of the Responses of Two- and Three-Dimensional Engineered Tissues to Electric Fields," *Tissue Eng. Part B, Rev.*, **18**(3), pp. 167–180.
- [352] McCaig, C. D., Rajniecek, A. M., Song, B., and Zhao, M., 2005, "Controlling Cell Behavior Electrically: Current Views and Future Potential," *Physiol. Rev.*, **85**(3), pp. 943–978.
- [353] Tai, G., Reid, B., Cao, L., and Zhao, M., 2009, "Electrotaxis and Wound Healing: Experimental Methods to Study Electric Fields as a Directional Signal for Cell Migration," *Methods Mol. Biol.*, **571**, pp. 77–97.
- [354] Zhao, Z., Watt, C., Karystinou, A., Roelofs, A. J., McCaig, C. D., Gibson, I. R., and De Bari, C., 2011, "Directed Migration of Human Bone Marrow Mesenchymal Stem Cells in a Physiological Direct Current Electric Field," *Eur. Cell Mater.*, **22**, pp. 344–358.
- [355] Zhang, J., Calafiore, M., Zeng, Q., Zhang, X., Huang, Y., Li, R. A., Deng, W., and Zhao, M., 2011, "Electrically Guiding Migration of Human Induced Pluripotent Stem Cells," *Stem Cell Rev.*, **7**(4), pp. 987–996.
- [356] Zhao, M., Agius-Fernandez, A., Forrester, J. V., and McCaig, C. D., 1996, "Directed Migration of Corneal Epithelial Sheets in Physiological Electric Fields," *Invest. Ophthalmol. Vis. Sci.*, **37**(13), pp. 2548–2558.
- [357] Guo, A., Song, B., Reid, B., Gu, Y., Forrester, J. V., Jahoda, C. A., and Zhao, M., 2010, "Effects of Physiological Electric Fields on Migration of Human Dermal Fibroblasts," *J. Invest. Dermatol.*, **130**(9), pp. 2320–2327.
- [358] Erickson, C. A., and Nuccitelli, R., 1984, "Embryonic Fibroblast Motility and Orientation can be Influenced by Physiological Electric-Fields," *J. Cell Biol.*, **98**(1), pp. 296–307.
- [359] Brown, M. J., and Loew, L. M., 1994, "Electric Field-Directed Fibroblast Locomotion Involves Cell-Surface Molecular Reorganization and is Calcium-Independent," *J. Cell Biol.*, **127**(1), pp. 117–128.
- [360] Long, H., Yang, G., and Wang, Z., 2011, "Galvanotactic Migration of Ea.Hy926 Endothelial Cells in a Novel Designed Electric Field Bioreactor," *Cell Biochem. Biophys.*, **61**(3), pp. 481–491.
- [361] Li, X. F., and Kolega, J., 2002, "Effects of Direct Current Electric Fields on Cell Migration and Actin Filament Distribution in Bovine Vascular Endothelial Cells," *J. Vasc. Res.*, **39**(5), pp. 391–404.
- [362] Li, J., Nandagopal, S., Wu, D., Romanuk, S. F., Paul, K., Thomson, D. J., and Lin, F., 2011, "Activated T Lymphocytes Migrate toward the Cathode of DC Electric Fields in Microfluidic Devices," *Lab Chip*, **11**(7), pp. 1298–1304.
- [363] Franke, K., and Gruler, H., 1990, "Galvanotaxis of Human Granulocytes—Electric-Field Jump Studies," *Eur. Biophys. J.*, **18**(6), pp. 335–346.
- [364] Sun, Y. S., Peng, S. W., Lin, K. H., and Cheng, J. Y., 2012, "Electrotaxis of Lung Cancer Cells in Ordered Three-Dimensional Scaffolds," *Biomicrofluidics*, **6**(1), pp. 14102–14114.
- [365] Djamgoz, M. B. A., Mycielska, M., Madeja, Z., Fraser, S. P., and Korohoda, W., 2001, "Directional Movement of Rat Prostate Cancer Cells in Direct-Current Electric Field: Involvement of Voltage-Gated Na⁺ Channel Activity," *J. Cell Sci.*, **114**(14), pp. 2697–2705.
- [366] Huang, C. W., Cheng, J. Y., Yen, M. H., and Young, T. H., 2009, "Electrotaxis of Lung Cancer Cells in a Multiple-Electric-Field Chip," *Biosens. Bioelectron.*, **24**(12), pp. 3510–3516.
- [367] Curtze, S., Dembo, M., Miron, M., and Jones, D. B., 2004, "Dynamic Changes in Traction Forces with DC Electric Field in Osteoblast-Like Cells," *J. Cell Sci.*, **117**, pp. 2721–2729.
- [368] Radisic, M., Park, H., Shing, H., Consi, T., Schoen, F. J., Langer, R., Freed, L. E., and Vunjak-Novakovic, G., 2004, "Functional Assembly of Engineered Myocardium by Electrical Stimulation of Cardiac Myocytes Cultured on Scaffolds," *Proc. Natl. Acad. Sci. U.S.A.*, **101**(52), pp. 18129–18134.
- [369] Hart, F. X., 2010, "Cytoskeletal Forces Produced by Extremely Low-Frequency Electric Fields Acting on Extracellular Glycoproteins," *Bioelectromagnetics*, **31**(1), pp. 77–84.
- [370] Sathaye, A., Bursac, N., Sheehy, S., and Tung, L., 2006, "Electrical Pacing Counteracts Intrinsic Shortening of Action Potential Duration of Neonatal Rat Ventricular Cells in Culture," *J. Mol. Cell Cardiol.*, **41**(4), pp. 633–641.
- [371] Harris, A. K., Wild, P., and Stopak, D., 1980, "Silicone Rubber Substrata: A New Wrinkle in the Study of Cell Locomotion," *Science*, **208**(4440), pp. 177–179.
- [372] Burton, K., and Taylor, D. L., 1997, "Traction Forces of Cytokinesis Measured with Optically Modified Elastic Substrata," *Nature*, **385**(6615), pp. 450–454.
- [373] Harris, A. K., Stopak, D., and Wild, P., 1981, "Fibroblast Traction as a Mechanism for Collagen Morphogenesis," *Nature*, **290**(5803), pp. 249–251.
- [374] Ting, L. H., and Sniadecki, N. J., 2011, *Comprehensive Biomaterials*, Elsevier, Oxford, UK.
- [375] Nahmias, Y., and Bhatia, S., 2009, *Methods in Bioengineering: Microdevices in Biology and Medicine*, Artech House, Norwood, MA.
- [376] Doyle, A. D., and Lee, J., 2005, "Cyclic Changes in Keratocyte Speed and Traction Stress Arise from Ca²⁺-Dependent Regulation of Cell Adhesiveness," *J. Cell Sci.*, **118**, pp. 369–379.
- [377] Iwadate, Y., and Yumura, S., 2008, "Actin-Based Propulsive Forces and Myosin-II-Based Contractile Forces in Migrating Dictyostelium Cells," *J. Cell Sci.*, **121**, pp. 1314–1324.
- [378] Tolic-Norrelykke, I. M., and Wang, N., 2005, "Traction in Smooth Muscle Cells Varies With Cell Spreading," *J. Biomech.*, **38**(7), pp. 1405–1412.
- [379] Wang, Y., Botvinick, E. L., Zhao, Y., Berns, M. W., Usami, S., Tsien, R. Y., and Chien, S., 2005, "Visualizing the Mechanical Activation of SRC," *Nature*, **434**(7036), pp. 1040–1045.
- [380] Lombardi, M. L., Knecht, D. A., Dembo, M., and Lee, J., 2007, "Traction Force Microscopy in Dictyostelium Reveals Distinct Roles for Myosin II Motor and Actin-Crosslinking Activity in Polarized Cell Movement," *J. Cell Sci.*, **120**, pp. 1624–1634.
- [381] Chen, J., Li, H., Sundarraj, N., and Wang, J. H., 2007, "α-Smooth Muscle Actin Expression Enhances Cell Traction Force," *Cell Motil. Cytoskeleton*, **64**(4), pp. 248–257.
- [382] Wang, H. B., Dembo, M., and Wang, Y. L., 2000, "Substrate Flexibility Regulates Growth and Apoptosis of Normal but Not Transformed Cells," *Am. J. Physiol. Cell Physiol.*, **279**(5), pp. C1345–C1350.
- [383] Rosel, D., Brabek, J., Tolde, O., Mierke, C. T., Zitterbart, D. P., Raupach, C., Bicanova, K., Kollmannsberger, P., Pankova, D., Vesely, P., Folk, P., and Fabry, B., 2008, "Up-Regulation of Rho/Rock Signaling in Sarcoma Cells Drives Invasion and Increased Generation of Protrusive Forces," *Mol. Cancer Res.*, **6**(9), pp. 1410–1420.
- [384] Marganski, W. A., De Biase, V. M., Burgess, M. L., and Dembo, M., 2003, "Demonstration of Altered Fibroblast Contractile Activity in Hypertensive Heart Disease," *Cardiovasc. Res.*, **60**(3), pp. 547–556.
- [385] Beningo, K. A., Dembo, M., Kaverina, I., Small, J. V., and Wang, Y. L., 2001, "Nascent Focal Adhesions are Responsible for the Generation of Strong Propulsive Forces in Migrating Fibroblasts," *J. Cell Biol.*, **153**(4), pp. 881–888.
- [386] Munevar, S., Wang, Y., and Dembo, M., 2001, "Traction Force Microscopy of Migrating Normal and H-Ras Transformed 3T3 Fibroblasts," *Biophys. J.*, **80**(4), pp. 1744–1757.
- [387] Munevar, S., Wang, Y. L., and Dembo, M., 2001, "Distinct Roles of Frontal and Rear Cell-Substrate Adhesions in Fibroblast Migration," *Mol. Biol. Cell*, **12**(12), pp. 3947–3954.
- [388] Delanoé-Ayari, H., Iwaya, S., Maeda, Y. T., Inose, J., Riviere, C., Sano, M., and Rieu, J. P., 2008, "Changes in the Magnitude and Distribution of Forces at Different Dictyostelium Developmental Stages," *Cell Motil. Cytoskeleton*, **65**(4), pp. 314–331.
- [389] Li, B., Lin, M., Tang, Y., Wang, B., and Wang, J. H., 2008, "A Novel Functional Assessment of the Differentiation of Micropatterned Muscle Cells," *J. Biomech.*, **41**(16), pp. 3349–3353.
- [390] Li, F., Li, B., Wang, Q. M., and Wang, J. H., 2008, "Cell Shape Regulates Collagen Type I Expression in Human Tendon Fibroblasts," *Cell Motil. Cytoskeleton*, **65**(4), pp. 332–341.
- [391] Franck, C., Maskarinec, S. A., Tirrell, D. A., and Ravichandran, G., 2011, "Three-Dimensional Traction Force Microscopy: A New Tool for Quantifying Cell-Matrix Interactions," *PLoS One*, **6**(3), e17833.
- [392] Maskarinec, S. A., Franck, C., Tirrell, D. A., and Ravichandran, G., 2009, "Quantifying Cellular Traction Forces in Three Dimensions," *Proc. Natl. Acad. Sci. U.S.A.*, **106**(52), pp. 22108–22113.
- [393] Legant, W. R., Miller, J. S., Blakely, B. L., Cohen, D. M., Genin, G. M., and Chen, C. S., 2010, "Measurement of Mechanical Traction Forces by Cells in Three-Dimensional Matrices," *Nat. Methods*, **7**(12), pp. 969–971.
- [394] Khetan, S., Guvendiren, M., Legant, W. R., Cohen, D. M., Chen, C. S., and Burdick, J. A., 2013, "Degradation-Mediated Cellular Traction Directs Stem Cell Fate in Covalently Crosslinked Three-Dimensional Hydrogels," *Nat. Mater.*, **12**(5), pp. 458–465.
- [395] Legant, W. R., Choi, C. K., Miller, J. S., Shao, L., Gao, L., Betzig, E., and Chen, C. S., 2013, "Multidimensional Traction Force Microscopy Reveals Out-of-Plane Rotational Moments About Focal Adhesions," *Proc. Natl. Acad. Sci. U.S.A.*, **110**(3), pp. 881–886.
- [396] Walker, G. M., Sai, J., Richmond, A., Stremler, M., Chung, C. Y., and Wikswold, J. P., 2005, "Effects of Flow and Diffusion on Chemotaxis Studies in a Microfabricated Gradient Generator," *Lab Chip*, **5**(6), pp. 611–618.
- [397] Das, T., Maiti, T. K., and Chakraborty, S., 2008, "Traction Force Microscopy On-Chip: Shear Deformation of Fibroblast Cells," *Lab Chip*, **8**(8), pp. 1308–1318.
- [398] Galbraith, C. G., and Sheetz, M. P., 1997, "A Micromachined Device Provides a New Bend on Fibroblast Traction Forces," *Proc. Natl. Acad. Sci. U.S.A.*, **94**(17), pp. 9114–9118.

- [399] Galbraith, C. G., and Sheetz, M. P., 1999, "Keratocytes Pull With Similar Forces on Their Dorsal and Ventral Surfaces," *J. Cell Biol.*, **147**(6), pp. 1313–1323.
- [400] Sniadecki, N. J., and Chen, C. S., 2006, *Medical Devices and Systems*, CRC Press, Boca Raton, FL.
- [401] Yang, S. M., and Saif, T. A., 2005, "Micromachined Force Sensors for the Study of Cell Mechanics," *Rev. Sci. Instrum.*, **76**(4), 044301.
- [402] Saif, M. T. A., Sager, C. R., and Coyer, S., 2003, "Functionalized Biomicroelectromechanical Systems Sensors for Force Response Study at Local Adhesion Sites of Single Living Cells on Substrates," *Ann. Biomed. Eng.*, **31**(8), pp. 950–961.
- [403] Park, J., Kim, J., Roh, D., Park, S., Kim, B., and Chun, K., 2006, "Fabrication of Complex 3D Polymer Structures for Cell–Polymer Hybrid Systems," *J. Micromech. Microeng.*, **16**(8), pp. 1614–1619.
- [404] Park, J., Ryu, J., Choi, S. K., Seo, E., Cha, J. M., Ryu, S., Kim, J., Kim, B., and Lee, S. H., 2005, "Real-Time Measurement of the Contractile Forces of Self-Organized Cardiomyocytes on Hybrid Biopolymer Microcantilevers," *Anal. Chem.*, **77**(20), pp. 6571–6580.
- [405] Yang, S. M., and Saif, T. A., 2005, "Reversible and Repeatable Linear Local Cell Force Response under Large Stretches," *Exp. Cell Res.*, **305**(1), pp. 42–50.
- [406] Yang, S. M., and Saif, T. A., 2006, "MEMS Based Force Sensors for the Study of Indentation Response of Single Living Cells," *Sens. Actuators A*, **135**(1), pp. 16–22.
- [407] Yang, S. M., and Saif, T. A., 2007, "Force Response and Actin Remodeling (Agglomeration) in Fibroblasts Due to Lateral Indentation," *Acta Biomater.*, **3**(1), pp. 77–87.
- [408] Yang, S., Siechen, S., Sung, J., Chiba, A., and Saif, T., 2008, "MEMS Based Sensors to Explore the Role of Tension in Axons for Neuro-Transmission," *Proceedings of the 21st IEEE International Conference on Micro Electro Mechanical Systems*, January 13–17, Tucson, AZ, pp. 308–310.
- [409] Sun, Y., Wan, K. T., Roberts, K. P., Bischof, J. C., and Nelson, B. J., 2003, "Mechanical Property Characterization of Mouse Zona Pellucida," *IEEE Trans. Nanobiosci.*, **2**(4), pp. 279–286.
- [410] Gopal, A., Luo, Z., Lee, J. Y., Kumar, K., Li, B., Hoshino, K., Schmidt, C., Ho, P. S., and Zhang, X., 2008, "Nano-Opto-Mechanical Characterization of Neuron Membrane Mechanics under Cellular Growth and Differentiation," *Biomed. Microdev.*, **10**(5), pp. 611–622.
- [411] Park, K., Jang, J., Irimia, D., Sturgis, J., Lee, J., Robinson, J. P., Toner, M., and Bashir, R., 2008, "Living Cantilever Arrays for Characterization of Mass of Single Live Cells in Fluids," *Lab Chip*, **8**(7), pp. 1034–1041.
- [412] Kolodney, M. S., and Wysolmerski, R. B., 1992, "Isometric Contraction by Fibroblasts and Endothelial Cells in Tissue Culture: A Quantitative Study," *J. Cell Biol.*, **117**(1), pp. 73–82.
- [413] Zimmermann, W. H., Fink, C., Kralisch, D., Remmers, U., Weil, J., and Eschenhagen, T., 2000, "Three-Dimensional Engineered Heart Tissue from Neonatal Rat Cardiac Myocytes," *Biotechnol. Bioeng.*, **68**(1), pp. 106–114.
- [414] Shaikh, F. M., O'Brien, T. P., Callanan, A., Kavanagh, E. G., Burke, P. E., Grace, P. A., and McGloughlin, T. M., 2010, "New Pulsatile Hydrostatic Pressure Bioreactor for Vascular Tissue-Engineered Constructs," *Artif. Organs*, **34**(2), pp. 153–158.
- [415] Naing, M. W., and Williams, D. J., 2011, "Three-Dimensional Culture and Bioreactors for Cellular Therapies," *Cytotherapy*, **13**(4), pp. 391–399.
- [416] Toda, M., Yamamoto, K., Shimizu, N., Obi, S., Kumagaya, S., Igarashi, T., Kamiya, A., and Ando, J., 2008, "Differential Gene Responses in Endothelial Cells Exposed to a Combination of Shear Stress and Cyclic Stretch," *J. Biotechnol.*, **133**(2), pp. 239–244.
- [417] Wille, J. J., Elson, E. L., and Okamoto, R. J., 2006, "Cellular and Matrix Mechanics of Bioartificial Tissues During Continuous Cyclic Stretch," *Ann. Biomed. Eng.*, **34**(11), pp. 1678–1690.
- [418] Sniadecki, N. J., and Chen, C. S., 2007, *Methods in Cell Biology: Cell Mechanics*, Elsevier Inc., Amsterdam, The Netherlands.
- [419] Schoen, I., Hu, W., Klotzsch, E., and Vogel, V., 2010, "Probing Cellular Traction Forces by Micropillar Arrays: Contribution of Substrate Warping to Pillar Deflection," *Nano Lett.*, **10**(5), pp. 1823–1830.
- [420] Yang, M. T., Sniadecki, N. J., and Chen, C. S., 2007, "Geometric Considerations of Micro- to Nanoscale Elastomeric Post Arrays to Study Cellular Traction Forces," *Adv. Mater.*, **19**(20), pp. 3119–3123.
- [421] Chen, C. S., Tan, J. L., Tien, J., Pirone, D. M., Gray, D. S., and Bhadriraju, K., 2003, "Cells Lying on a Bed of Microneedles: An Approach to Isolate Mechanical Force," *Proc. Natl. Acad. Sci. U.S.A.*, **100**(4), pp. 1484–1489.
- [422] Lemmon, C. A., Sniadecki, N. J., Ruiz, S. A., Tan, J. L., Romer, L. H., and Chen, C. S., 2005, "Shear Force at the Cell–Matrix Interface: Enhanced Analysis for Microfabricated Post Array Detectors," *Mech. Chem. Biosyst.*, **2**(1), pp. 1–16.
- [423] Du Roure, O., Saez, A., Buguin, A., Austin, R. H., Chavrier, P., Silberzan, P., and Ladoux, B., 2005, "Force Mapping in Epithelial Cell Migration," *Proc. Natl. Acad. Sci. U.S.A.*, **102**(7), pp. 2390–2395.
- [424] Sochol, R. D., Higa, A. T., Janairo, R. R. R., Li, S., and Lin, L., 2011, "Effects of Micropost Spacing and Stiffness on Cell Motility," *Micro Nano Lett.*, **6**(5), pp. 323–326.
- [425] Ricart, B. G., Yang, M. T., Hunter, C. A., Chen, C. S., and Hammer, D. A., 2011, "Measuring Traction Forces of Motile Dendritic Cells on Micropost Arrays," *Biophys. J.*, **101**(11), pp. 2620–2628.
- [426] Rabodzey, A., Alcaide, P., Luscinskas, F. W., and Ladoux, B., 2008, "Mechanical Forces Induced by the Transendothelial Migration of Human Neutrophils," *Biophys. J.*, **95**(3), pp. 1428–1438.
- [427] Liu, Z., Sniadecki, N. J., and Chen, C. S., 2010, "Mechanical Forces in Endothelial Cells During Firm Adhesion and Early Transmigration of Human Monocytes," *Cell Mol. Bioeng.*, **3**(1), pp. 50–59.
- [428] Rodriguez, A. G., Han, S. J., Regnier, M., and Sniadecki, N. J., 2011, "Substrate Stiffness Increases Twitch Power of Neonatal Cardiomyocytes in Correlation With Changes in Myofibril Structure and Intracellular Calcium," *Biophys. J.*, **101**(10), pp. 2455–2464.
- [429] Uemura, A., Nguyen, T. N., Steele, A. N., and Yamada, S., 2011, "The Lim Domain of Zyxin is Sufficient for Force-Induced Accumulation of Zyxin During Cell Migration," *Biophys. J.*, **101**(5), pp. 1069–1075.
- [430] Pirone, D. M., Liu, W. F., Ruiz, S. A., Gao, L., Raghavan, S., Lemmon, C. A., Romer, L. H., and Chen, C. S., 2006, "An Inhibitory Role for Fak in Regulating Proliferation: A Link Between Limited Adhesion and RhoA-Rock Signaling," *J. Cell Biol.*, **174**(2), pp. 277–288.
- [431] Ganz, A., Lambert, M., Saez, A., Silberzan, P., Buguin, A., Mege, R. M., and Ladoux, B., 2006, "Traction Forces Exerted through N-Cadherin Contacts," *Biol. Cell*, **98**(12), pp. 721–730.
- [432] Liu, Z., Tan, J. L., Cohen, D. M., Yang, M. T., Sniadecki, N. J., Ruiz, S. A., Nelson, C. M., and Chen, C. S., 2010, "Mechanical Tugging Force Regulates the Size of Cell–Cell Junctions," *Proc. Natl. Acad. Sci. U.S.A.*, **107**(22), pp. 9944–9949.
- [433] Lemmon, C. A., Chen, C. S., and Romer, L. H., 2009, "Cell Traction Forces Direct Fibronectin Matrix Assembly," *Biophys. J.*, **96**(2), pp. 729–738.
- [434] Ladoux, B., Saez, A., Du Roure, O., Buguin, A., Chavrier, P., and Silberzan, P., 2004, "Force Mapping in Epithelial Cell Migration," *Mol. Biol. Cell*, **15**, pp. 161a–162a.
- [435] Saez, A., Anon, E., Ghibaudo, M., Du Roure, O., Di Meglio, J. M., Hersen, P., Silberzan, P., Buguin, A., and Ladoux, B., 2010, "Traction Forces Exerted by Epithelial Cell Sheets," *J. Phys. Condens. Matter*, **22**(19), 194119.
- [436] Liang, X. M., Han, S. J., Reems, J. A., Gao, D., and Sniadecki, N. J., 2010, "Platelet Retraction Force Measurements Using Flexible Post Force Sensors," *Lab Chip*, **10**(8), pp. 991–998.
- [437] Legant, W. R., Pathak, A., Yang, M. T., Deshpande, V. S., McMeeking, R. M., and Chen, C. S., 2009, "Microfabricated Tissue Gauges to Measure and Manipulate Forces from 3D Microtissues," *Proc. Natl. Acad. Sci. U.S.A.*, **106**(25), pp. 10097–10102.
- [438] Sakar, M. S., Neal, D., Boudou, T., Borochin, M. A., Li, Y., Weiss, R., Kamm, R. D., Chen, C. S., and Asada, H. H., 2012, "Formation and Optogenetic Control of Engineered 3D Skeletal Muscle Bioactuators," *Lab Chip*, **12**(23), pp. 4976–4985.
- [439] Boudou, T., Legant, W. R., Mu, A., Borochin, M. A., Thavandiran, N., Radisic, M., Zandstra, P. W., Epstein, J. A., Margulies, K. B., and Chen, C. S., 2011, "A Microfabricated Platform to Measure and Manipulate the Mechanics of Engineered Cardiac Microtissues," *Tissue Eng., Part A*, pp. 910–919.
- [440] West, A. R., Zaman, N., Cole, D. J., Walker, M. J., Legant, W. R., Boudou, T., Chen, C. S., Favreau, J. T., Gaudette, G. R., Cowley, E. A., and Maksym, G. N., 2013, "Development and Characterization of a 3D Multicell Microtissue Model of Airway Smooth Muscle," *Am. J. Physiol. Lung Cell Mol. Physiol.*, **304**(1), pp. L4–L6.
- [441] Legant, W. R., Chen, C. S., and Vogel, V., 2012, "Force-Induced Fibronectin Assembly and Matrix Remodeling in a 3D Microtissue Model of Tissue Morphogenesis," *Integr. Biol. (Camb)*, **4**(10), pp. 1164–1174.
- [442] Zhao, R., Boudou, T., Wang, W. G., Chen, C. S., and Reich, D. H., 2013, "Decoupling Cell and Matrix Mechanics in Engineered Microtissues Using Magnetically Actuated Microcantilevers," *Adv. Mater.*, **25**(12), pp. 1699–1705.
- [443] Saez, A., Buguin, A., Silberzan, P., and Ladoux, B., 2005, "Is the Mechanical Activity of Epithelial Cells Controlled by Deformations or Forces?," *Biophys. J.*, **89**(6), pp. L52–L54.
- [444] Ghibaudo, M., Saez, A., Trichet, L., Xayaphoummine, A., Browaeys, J., Silberzan, P., Buguin, A., and Ladoux, B., 2008, "Traction Forces and Rigidity Sensing Regulate Cell Functions," *Soft Matter*, **4**(9), pp. 1836–1843.
- [445] Han, S. J., Bielawski, K. S., Ting, L. H., Rodriguez, M. L., and Sniadecki, N. J., 2012, "Decoupling Substrate Stiffness, Spread Area, and Micropost Density: A Close Spatial Relationship Between Traction Forces and Focal Adhesions," *Biophys. J.*, **103**(4), pp. 640–648.
- [446] Fu, J., Wang, Y. K., Yang, M. T., Desai, R. A., Yu, X., Liu, Z., and Chen, C. S., 2010, "Mechanical Regulation of Cell Function With Geometrically Modulated Elastomeric Substrates," *Nat. Methods*, **7**(9), pp. 733–736.
- [447] Sun, Y., Villa-Diaz, L. G., Lam, R. H., Chen, W., Krebsbach, P. H., and Fu, J., 2012, "Mechanics Regulates Fate Decisions of Human Embryonic Stem Cells," *PLoS One*, **7**(5), e37178.
- [448] Saez, A., Ghibaudo, M., Buguin, A., Silberzan, P., and Ladoux, B., 2007, "Rigidity-Driven Growth and Migration of Epithelial Cells on Microstructured Anisotropic Substrates," *Proc. Natl. Acad. Sci. U.S.A.*, **104**(20), pp. 8281–8286.
- [449] Sochol, R. D., Higa, A. T., Janairo, R. R. R., Li, S., and Lin, L. W., 2011, "Unidirectional Mechanical Cellular Stimuli Via Micropost Array Gradients," *Soft Matter*, **7**(10), pp. 4606–4609.
- [450] Sniadecki, N. J., Anguelouch, A., Yang, M. T., Lamb, C. M., Liu, Z., Kirschner, S. B., Liu, Y., Reich, D. H., and Chen, C. S., 2007, "Magnetic Microposts as an Approach to Apply Forces to Living Cells," *Proc. Natl. Acad. Sci. U.S.A.*, **104**(37), pp. 14553–14558.
- [451] Sniadecki, N. J., Lamb, C. M., Liu, Y., Chen, C. S., and Reich, D. H., 2008, "Magnetic Microposts for Mechanical Stimulation of Biological Cells: Fabrication, Characterization, and Analysis," *Rev. Sci. Instrum.*, **79**(4), p. 044302.

- [452] Ting, L. H., Jahn, J. R., Jung, J. I., Shuman, B. R., Feghhi, S., Han, S. J., Rodriguez, M. L., and Sniadecki, N. J., 2012, "Flow Mechanotransduction Regulates Traction Forces, Intercellular Forces, and Adherens Junctions," *Am. J. Physiol. Heart Circ. Physiol.*, **302**(11), pp. H2220–H2229.
- [453] Lam, R. H. W., Sun, Y. B., Chen, W. Q., and Fu, J. P., 2012, "Elastomeric Microposts Integrated into Microfluidics for Flow-Mediated Endothelial Mechanotransduction Analysis," *Lab Chip*, **12**(10), pp. 1865–1873.
- [454] Mann, J. M., Lam, R. H., Weng, S., Sun, Y., and Fu, J., 2012, "A Silicone-Based Stretchable Micropost Array Membrane for Monitoring Live-Cell Subcellular Cytoskeletal Response," *Lab Chip*, **12**(4), pp. 731–740.
- [455] McGarry, J. P., Fu, J., Yang, M. T., Chen, C. S., McMeeking, R. M., Evans, A. G., and Deshpande, V. S., 2009, "Simulation of the Contractile Response of Cells on an Array of Micro-Posts," *Philos. Trans. R. Soc. London, Ser. A*, **367**(1902), pp. 3477–3497.
- [456] Fu, J. P., Wang, Y. K., Yang, M. T., Desai, R. A., Yu, X. A., Liu, Z. J., and Chen, C. S., 2010, "Mechanical Regulation of Cell Function With Geometrically Modulated Elastomeric Substrates," *Nat. Methods*, **7**, pp. 733–736.
- [457] Saez, A., Ladoux, B., Du Roure, O., Silberzan, P., Buguin, A., Chavrier, P., and Austin, R. H., 2005, "An Array of Micro Fabricated Pillars to Map Forces During Epithelial Cell Migration," *Biophys. J.*, **88**(1), pp. 518a–518a.
- [458] Lim, C. T., Zhou, E. H., and Quek, S. T., 2006, "Mechanical Models for Living Cells—A Review," *J. Biomech.*, **39**(2), pp. 195–216.
- [459] Yeung, A., and Evans, E., 1989, "Cortical Shell-Liquid Core Model for Passive Flow of Liquid-Like Spherical Cells into Micropipets," *Biophys. J.*, **56**(1), pp. 139–149.
- [460] Tran-Son-Tay, R., Needham, D., Yeung, A., and Hochmuth, R. M., 1991, "Time-Dependent Recovery of Passive Neutrophils after Large Deformation," *Biophys. J.*, **60**(4), pp. 856–866.
- [461] Needham, D., and Hochmuth, R. M., 1990, "Rapid Flow of Passive Neutrophils into a 4 Microns Pipet and Measurement of Cytoplasmic Viscosity," *ASME J. Biomech. Eng.*, **112**(3), pp. 269–276.
- [462] Hochmuth, R. M., Ting-Beall, H. P., Beaty, B. B., Needham, D., and Tran-Son-Tay, R., 1993, "Viscosity of Passive Human Neutrophils Undergoing Small Deformations," *Biophys. J.*, **64**(5), pp. 1596–1601.
- [463] Kan, H. C., Udaykumar, H. S., Shyy, W., and Tran-Son-Tay, R., 1998, "Hydrodynamics of a Compound Drop With Application to Leukocyte Modeling," *Phys. Fluids*, **10**(4), pp. 760–774.
- [464] Kan, H. C., Shyy, W., Udaykumar, H. S., Vigneron, P., and Tran-Son-Tay, R., 1999, "Effects of Nucleus on Leukocyte Recovery," *Ann. Biomed. Eng.*, **27**(5), pp. 648–655.
- [465] Tran-Son-Tay, R., Kan, H. C., Udaykumar, H. S., Damay, E., and Shyy, W., 1998, "Rheological Modelling of Leukocytes," *Med. Biol. Eng. Comput.*, **36**(2), pp. 246–250.
- [466] Tsai, M. A., Frank, R. S., and Waugh, R. E., 1993, "Passive Mechanical Behavior of Human Neutrophils: Power-Law Fluid," *Biophys. J.*, **65**(5), pp. 2078–2088.
- [467] Drury, J. L., and Dembo, M., 2001, "Aspiration of Human Neutrophils: Effects of Shear Thinning and Cortical Dissipation," *Biophys. J.*, **81**(6), pp. 3166–3177.
- [468] Fabry, B., Maksym, G. N., Butler, J. P., Glogauer, M., Navajas, D., Taback, N. A., Millet, E. J., and Fredberg, J. J., 2003, "Time Scale and Other Invariants of Integrative Mechanical Behavior in Living Cells," *Phys. Rev. E*, **68**, p. 041914.
- [469] Dong, C., Skalak, R., Sung, K. L., Schmid-Schonbein, G. W., and Chien, S., 1988, "Passive Deformation Analysis of Human Leukocytes," *ASME J. Biomech. Eng.*, **110**(1), pp. 27–36.
- [470] Dong, C., and Skalak, R., 1992, "Leukocyte Deformability: Finite Element Modeling of Large Viscoelastic Deformation," *J. Theor. Biol.*, **158**(2), pp. 173–193.
- [471] Dong, C., Skalak, R., and Sung, K. L., 1991, "Cytoplasmic Rheology of Passive Neutrophils," *Biorheology*, **28**(6), pp. 557–567.
- [472] Guilak, F., Erickson, G. R., and Ting-Beall, H. P., 2002, "The Effects of Osmotic Stress on the Viscoelastic and Physical Properties of Articular Chondrocytes," *Biophys. J.*, **82**(2), pp. 720–727.
- [473] Theret, D. P., Levesque, M. J., Sato, M., Nerem, R. M., and Wheeler, L. T., 1988, "The Application of a Homogeneous Half-Space Model in the Analysis of Endothelial-Cell Micropipette Measurements," *ASME J. Biomech. Eng.*, **110**(3), pp. 190–199.
- [474] Schmid-Schonbein, G. W., Sung, K. L., Tozeren, H., Skalak, R., and Chien, S., 1981, "Passive Mechanical Properties of Human Leukocytes," *Biophys. J.*, **36**(1), pp. 243–256.
- [475] Dimilla, P. A., Barbee, K., and Lauffenburger, D. A., 1991, "Mathematical Model for the Effects of Adhesion and Mechanics on Cell Migration Speed," *Biophys. J.*, **60**(1), pp. 15–37.
- [476] Milner, J. S., Grol, M. W., Beaucage, K. L., Dixon, S. J., and Holdsworth, D. W., 2012, "Finite-Element Modeling of Viscoelastic Cells During High-Frequency Cyclic Strain," *J. Funct. Biomater.*, **3**(1), pp. 209–224.
- [477] Haider, M. A., and Guilak, F., 2000, "An Axisymmetric Boundary Integral Model for Incompressible Linear Viscoelasticity: Application to the Micropipette Aspiration Contact Problem," *ASME J. Biomech. Eng.*, **122**(3), pp. 236–244.
- [478] Verbruggen, S. W., Vaughan, T. J., and McNamara, L. M., 2012, "Strain Amplification in Bone Mechanobiology: A Computational Investigation of the in vivo Mechanics of Osteocytes," *J. R. Soc. Interface*, **9**(75), pp. 2735–2744.
- [479] McGarry, J. P., 2009, "Characterization of Cell Mechanical Properties by Computational Modeling of Parallel Plate Compression," *Ann. Biomed. Eng.*, **37**(11), pp. 2317–2325.
- [480] McGarry, J. P., and McHugh, P. E., 2008, "Modelling of In Vitro Chondrocyte Detachment," *J. Mech. Phys. Solids*, **56**(4), pp. 1554–1565.
- [481] Fabry, B., Maksym, G. N., Butler, J. P., Glogauer, M., Navajas, D., and Fredberg, J. J., 2001, "Scaling the Microrheology of Living Cells," *Phys. Rev. Lett.*, **87**(14), p. 148102.
- [482] Hoffman, B. D., and Crocker, J. C., 2009, "Cell Mechanics: Dissecting the Physical Responses of Cells to Force," *Ann. Rev. Biomed. Eng.*, **11**, pp. 259–288.
- [483] Vaziri, A., Xue, Z., Kamm, R. D., and Mofrad, M. R. K., 2007, "A Computational Study on Power-Law Rheology of Soft Glassy Materials With Application to Cell Mechanics," *Comput. Methods Appl. Mech. Eng.*, **196**(31–32), pp. 2965–2971.
- [484] Puig-De-Morales, M., Grabulosa, M., Alcaraz, J., Mollo, J., Maksym, G. N., Fredberg, J. J., and Navajas, D., 2001, "Measurement of Cell Microrheology by Magnetic Twisting Cytometry With Frequency Domain Demodulation," *J. Appl. Physiol.*, **91**(3), pp. 1152–1159.
- [485] Stamenovic, D., Suki, B., Fabry, B., Wang, N., and Fredberg, J. J., 2004, "Rheology of Airway Smooth Muscle Cells is Associated With Cytoskeletal Contractile Stress," *J. Appl. Physiol.*, **96**(5), pp. 1600–1605.
- [486] Alcaraz, J., Buscemi, L., Grabulosa, M., Trepast, X., Fabry, B., Farre, R., and Navajas, D., 2003, "Microrheology of Human Lung Epithelial Cells Measured by Atomic Force Microscopy," *Biophys. J.*, **84**(3), pp. 2071–2079.
- [487] Alexopoulos, L. G., Williams, G. M., Upton, M. L., Setton, L. A., and Guilak, F., 2005, "Osteoarthritic Changes in the Biphasic Mechanical Properties of the Chondrocyte Pericellular Matrix in Articular Cartilage," *J. Biomech.*, **38**(3), pp. 509–517.
- [488] Chahine, N. O., Hung, C. T., and Ateshian, G. A., 2007, "In-Situ Measurements of Chondrocyte Deformation under Transient Loading," *Eur. Cell Mater.*, **13**, pp. 100–111.
- [489] Korhonen, R. K., Julkunen, P., Rieppo, J., Lappalainen, R., Kontinen, Y. T., and Jurvelin, J. S., 2006, "Collagen Network of Articular Cartilage Modulates Fluid Flow and Mechanical Stresses in Chondrocyte," *Biomech. Model. Mechanobiol.*, **5**(2–3), pp. 150–159.
- [490] Korhonen, R. K., Julkunen, P., Wilson, W., and Herzog, W., 2008, "Importance of Collagen Orientation and Depth-Dependent Fixed Charge Densities of Cartilage on Mechanical Behavior of Chondrocytes," *ASME J. Biomech. Eng.*, **130**(2), p. 021003.
- [491] Kim, E., Guilak, F., and Haider, M. A., 2008, "The Dynamic Mechanical Environment of the Chondrocyte: A Biphasic Finite Element Model of Cell–Matrix Interactions Under Cyclic Compressive Loading," *ASME J. Biomech. Eng.*, **130**(6), p. 061009.
- [492] Guilak, F., and Mow, V. C., 2000, "The Mechanical Environment of the Chondrocyte: A Biphasic Finite Element Model of Cell–Matrix Interactions in Articular Cartilage," *J. Biomech.*, **33**(12), pp. 1663–1673.
- [493] Haider, M. A., 2004, "A Radial Biphasic Model for Local Cell–Matrix Mechanics in Articular Cartilage," *SIAM J. Appl. Math.*, **64**(5), pp. 1588–1608.
- [494] Kim, E., Guilak, F., and Haider, M. A., 2010, "An Axisymmetric Boundary Element Model for Determination of Articular Cartilage Pericellular Matrix Properties In Situ via Inverse Analysis of Chondron Deformation," *ASME J. Biomech. Eng.*, **132**(3), p. 031011.
- [495] Cao, L., Guilak, F., and Setton, L. A., 2009, "Pericellular Matrix Mechanics in the Anulus Fibrosus Predicted by a Three-Dimensional Finite Element Model and In Situ Morphology," *Cell. Mol. Bioeng.*, **2**(3), pp. 306–319.
- [496] Julkunen, P., Wilson, W., Jurvelin, J. S., and Korhonen, R. K., 2009, "Composition of the Pericellular Matrix Modulates the Deformation Behaviour of Chondrocytes in Articular Cartilage under Static Loading," *Med. Biol. Eng. Comput.*, **47**(12), pp. 1281–1290.
- [497] Huang, C. Y., Soltz, M. A., Kopacz, M., Mow, V. C., and Ateshian, G. A., 2003, "Experimental Verification of the Roles of Intrinsic Matrix Viscoelasticity and Tension-Compression Nonlinearity in the Biphasic Response of Cartilage," *ASME J. Biomech. Eng.*, **125**(1), pp. 84–93.
- [498] Ingber, D. E., 1993, "Cellular Tensegrity—Defining New Rules of Biological Design that Govern the Cytoskeleton," *J. Cell Sci.*, **104**, pp. 613–627.
- [499] Ingber, D. E., 2003, "Tensegrity I. Cell Structure and Hierarchical Systems Biology," *J. Cell Sci.*, **116**(7), pp. 1157–1173.
- [500] Wang, N., Naruse, K., Stamenovic, D., Fredberg, J. J., Mijailovich, S. M., Tolic-Norreykkye, I. M., Polte, T., Mannix, R., and Ingber, D. E., 2001, "Mechanical Behavior in Living Cells Consistent With the Tensegrity Model," *Proc. Natl. Acad. Sci. U.S.A.*, **98**(14), pp. 7765–7770.
- [501] Kumar, S., Maxwell, I. Z., Heisterkamp, A., Polte, T. R., Lele, T. P., Salanga, M., Mazur, E., and Ingber, D. E., 2006, "Viscoelastic Retraction of Single Living Stress Fibers and Its Impact on Cell Shape, Cytoskeletal Organization, and Extracellular Matrix Mechanics," *Biophys. J.*, **90**(10), pp. 3762–3773.
- [502] Stamenovic, D., Fredberg, J. J., Wang, N., Butler, J. P., and Ingber, D. E., 1996, "A Microstructural Approach to Cytoskeletal Mechanics Based on Tensegrity," *J. Theor. Biol.*, **181**(2), pp. 125–136.
- [503] Satcher, R. L., Jr., and Dewey, C. F., Jr., 1996, "Theoretical Estimates of Mechanical Properties of the Endothelial Cell Cytoskeleton," *Biophys. J.*, **71**(1), pp. 109–118.
- [504] Satcher, R., Dewey, C. F., Jr., and Hartwig, J. H., 1997, "Mechanical Remodeling of the Endothelial Surface and Actin Cytoskeleton Induced by Fluid Flow," *Microcirculation*, **4**(4), pp. 439–453.
- [505] Stamenovic, D., 2005, "Effects of Cytoskeletal Prestress on Cell Rheological Behavior," *Acta Biomater.*, **1**(3), pp. 255–262.

- [506] Stamenovic, D., Mijailovich, S. M., Tolic-Norrelykke, I. M., and Wang, N., 2003, "Experimental Tests of the Cellular Tensegrity Hypothesis," *Biorheology*, **40**(1–3), pp. 221–225.
- [507] Sultan, C., Stamenovic, D., and Ingber, D. E., 2004, "A Computational Tensegrity Model Predicts Dynamic Rheological Behaviors in Living Cells," *Ann. Biomed. Eng.*, **32**(4), pp. 520–530.
- [508] Stamenovic, D., 2008, "Rheological Behavior of Mammalian Cells," *Cell Mol. Life Sci.*, **65**(22), pp. 3592–3605.
- [509] Fereol, S., Fodil, R., Pelle, G., Louis, B., and Isabey, D., 2008, "Cell Mechanics of Alveolar Epithelial Cells (AECs) and Macrophages (AMS)," *Respir. Physiol. Neurobiol.*, **163**(1–3), pp. 3–16.
- [510] Canadas, P., Wendling-Mansuy, S., and Isabey, D., 2006, "Frequency Response of a Viscoelastic Tensegrity Model: Structural Rearrangement Contribution to Cell Dynamics," *ASME J. Biomech. Eng.*, **128**(4), pp. 487–495.
- [511] Ingber, D. E., 1997, "Tensegrity: The Architectural Basis of Cellular Mechanotransduction," *Ann. Rev. Physiol.*, **59**, pp. 575–599.
- [512] McGarry, J. G., and Prendergast, P. J., 2004, "A Three-Dimensional Finite Element Model of an Adherent Eukaryotic Cell," *Eur. Cell Mater.*, **7**, pp. 27–33.
- [513] De Santis, G., Lennon, A. B., Boschetti, F., Verheghe, B., Verdonck, P., and Prendergast, P. J., 2011, "How Can Cells Sense the Elasticity of a Substrate? An Analysis Using a Cell Tensegrity Model," *Eur. Cell Mater.*, **22**, pp. 202–213.
- [514] Baudriller, H., Maurin, B., Canadas, P., Montcourrier, P., Parmeggiani, A., and Bettache, N., 2006, "Form-Finding of Complex Tensegrity Structures: Application to Cell Cytoskeleton Modelling," *C. R. Mec.*, **334**(11), pp. 662–668.
- [515] Kardas, D., Nackenhorst, U., and Balzani, D., 2012, "Computational Model for the Cell–Mechanical Response of the Osteocyte Cytoskeleton Based on Self-Stabilizing Tensegrity Structures," *Biomech. Model. Mechanobiol.*, pp. 167–183.
- [516] McGarry, J. G., Klein-Nulend, J., Mullender, M. G., and Prendergast, P. J., 2005, "A Comparison of Strain and Fluid Shear Stress in Stimulating Bone Cell Responses—A Computational and Experimental Study," *FASEB J.*, **19**(3), pp. 482–484.
- [517] Bursa, J., Lebis, R., and Holata, J., 2012, "Tensegrity Finite Element Models of Mechanical Tests of Individual Cells," *Technol. Health Care*, **20**(2), pp. 135–150.
- [518] Wang, S., and Wolynes, P. G., 2012, "Tensegrity and Motor-Driven Effective Interactions in a Model Cytoskeleton," *J. Chem. Phys.*, **136**(14), p. 145102.
- [519] Mehrbod, M., and Mofrad, M. R. K., 2011, "On the Significance of Microtubule Flexural Behavior in Cytoskeletal Mechanics," *PLoS One*, **6**(10), e25627.
- [520] Chen, T. J., Wu, C. C., Tang, M. J., Huang, J. S., and Su, F. C., 2010, "Complexity of the Tensegrity Structure for Dynamic Energy and Force Distribution of Cytoskeleton During Cell Spreading," *PLoS One*, **5**(12), e14392.
- [521] Mackintosh, F. C., Kas, J., and Janmey, P. A., 1995, "Elasticity of Semiflexible Biopolymer Networks," *Phys. Rev. Lett.*, **75**(24), pp. 4425–4428.
- [522] Zemel, A., Bischofs, I. B., and Safran, S. A., 2006, "Active Elasticity of Gels with Contractile Cells," *Phys. Rev. Lett.*, **97**(12), p. 128103.
- [523] Zemel, A., Rehfeldt, F., Brown, A. E., Discher, D. E., and Safran, S. A., 2010, "Optimal Matrix Rigidity for Stress Fiber Polarization in Stem Cells," *Nat. Phys.*, **6**(6), pp. 468–473.
- [524] Zemel, A., Rehfeldt, F., Brown, A. E. X., Discher, D. E., and Safran, S. A., 2010, "Cell Shape, Spreading Symmetry, and the Polarization of Stress-Fibers in Cells," *J. Phys.: Condens. Matter*, **22**(19), p. 194110.
- [525] Zemel, A., and Safran, S. A., 2007, "Active Self-Polarization of Contractile Cells in Asymmetrically Shaped Domains," *Phys. Rev. E*, **76**, p. 021905.
- [526] Peskin, C. S., Odell, G. M., and Oster, G. F., 1993, "Cellular Motions and Thermal Fluctuations: The Brownian Ratchet," *Biophys. J.*, **65**, pp. 316–324.
- [527] Mogilner, A., and Oster, G., 1996, "Cell Motility Driven by Actin Polymerization," *Biophys. J.*, **71**(6), pp. 3030–3045.
- [528] Marcy, Y., Prost, J., Carlier, M. F., and Sykes, C., 2004, "Forces Generated During Actin-Based Propulsion: A Direct Measurement by Micro-manipulation," *Proc. Natl. Acad. Sci. U.S.A.*, **101**(16), pp. 5992–5997.
- [529] Lin, Y., 2009, "Mechanics Model for Actin-Based Motility," *Phys. Rev. E*, **79**, p. 021916.
- [530] Mogilner, A., and Edelstein-Keshet, L., 2002, "Regulation of Actin Dynamics in Rapidly Moving Cells: A Quantitative Analysis," *Biophys. J.*, **83**(3), pp. 1237–1258.
- [531] Mogilner, A., and Rubinstein, B., 2005, "The Physics of Filopodial Protrusion," *Biophys. J.*, **89**(2), pp. 782–795.
- [532] Atilgan, E., Wirtz, D., and Sun, S. X., 2006, "Mechanics and Dynamics of Actin-Driven Thin Membrane Protrusions," *Biophys. J.*, **90**(1), pp. 65–76.
- [533] Lan, Y., and Paojian, G. A., 2008, "The Stochastic Dynamics of Filopodial Growth," *Biophys. J.*, **94**(10), pp. 3839–3852.
- [534] Inoue, Y., and Adachi, T., 2011, "Coarse-Grained Brownian Ratchet Model of Membrane Protrusion on Cellular Scale," *Biomech. Model. Mechanobiol.*, **10**(4), pp. 495–503.
- [535] Kaunas, R., and Hsu, H. J., 2009, "A Kinematic Model of Stretch-Induced Stress Fiber Turnover and Reorientation," *J. Theor. Biol.*, **257**(2), pp. 320–330.
- [536] Kaunas, R., Usami, S., and Chien, S., 2006, "Regulation of Stretch-Induced JNK Activation by Stress Fiber Orientation," *Cell. Signal.*, **18**(11), pp. 1924–1931.
- [537] Kaunas, R., and Deguchi, S., 2011, "Multiple Roles for Myosin II in Tensional Homeostasis Under Mechanical Loading," *Cell. Mol. Bioeng.*, **4**(2), pp. 182–191.
- [538] Safran, S. A., and De, R., 2009, "Nonlinear Dynamics of Cell Orientation," *Phys. Rev. E*, **80**, p. 060901.
- [539] Vernerey, F. J., and Farsad, M., 2011, "A Constrained Mixture Approach to Mechano-Sensing and Force Generation in Contractile Cells," *J. Mech. Behav. Biomed. Mater.*, **4**(8), pp. 1683–1699.
- [540] Foucard, L., and Vernerey, F. J., 2012, "A Thermodynamical Model for Stress-Fiber Organization in Contractile Cells," *Appl. Phys. Lett.*, **100**(1), p. 013702.
- [541] Roberts, S. R., Knight, M. M., Lee, D. A., and Bader, D. L., 2001, "Mechanical Compression Influences Intracellular Ca²⁺ Signaling in Chondrocytes Seeded in Agarose Constructs," *J. Appl. Physiol.*, **90**(4), pp. 1385–1391.
- [542] Mitrossili, D., Foucard, J., Guiry, A., Desprat, N., Rodriguez, N., Fabry, B., and Asnacios, A., 2009, "Single-Cell Response to Stiffness Exhibits Muscle-Like Behavior," *Proc. Natl. Acad. Sci. U.S.A.*, **106**(43), pp. 18243–18248.
- [543] Deshpande, V. S., McMeeking, R. M., and Evans, A. G., 2007, "A Model for the Contractility of the Cytoskeleton Including the Effects of Stress-Fiber Formation and Dissociation," *Proc. R. Soc. London, Ser. A*, **463**(2079), pp. 787–815.
- [544] Dowling, E. P., Ronan, W., Ofek, G., Deshpande, V. S., McMeeking, R. M., Athanasiou, K. A., and McGarry, J. P., 2012, "The Effect of Remodelling and Contractility of the Actin Cytoskeleton on the Shear Resistance of Single Cells: A Computational and Experimental Investigation," *J. R. Soc. Interface*, pp. 3469–3479.
- [545] Vaziri, A., and Gopinath, A., 2008, "Cell and Biomolecular Mechanics in Silico," *Nat. Mater.*, **7**(1), pp. 15–23.
- [546] Wei, Z., Deshpande, V. S., McMeeking, R. M., and Evans, A. G., 2008, "Analysis and Interpretation of Stress Fiber Organization in Cells Subject to Cyclic Stretch," *ASME J. Biomech. Eng.*, **130**(3), p. 031009.
- [547] Kaunas, R., Nguyen, P., Usami, S., and Chien, S., 2005, "Cooperative Effects of Rho and Mechanical Stretch on Stress Fiber Organization," *Proc. Natl. Acad. Sci. U.S.A.*, **102**(44), pp. 15895–15900.
- [548] Wang, H., Ip, W., Boissy, R., and Grood, E. S., 1995, "Cell Orientation Response to Cyclically Deformed Substrates: Experimental Validation of a Cell Model," *J. Biomech.*, **28**(12), pp. 1543–1552.
- [549] Wang, J. H., Goldschmidt-Clermont, P., Wille, J., and Yin, F. C., 2001, "Specificity of Endothelial Cell Reorientation in Response to Cyclic Mechanical Stretching," *J. Biomech.*, **34**(12), pp. 1563–1572.
- [550] Wang, J. H., Goldschmidt-Clermont, P., and Yin, F. C., 2000, "Contractility Affects Stress Fiber Remodeling and Reorientation of Endothelial Cells Subjected to Cyclic Mechanical Stretching," *Ann. Biomed. Eng.*, **28**(10), pp. 1165–1171.
- [551] Han, S. J., and Sniadecki, N. J., 2011, "Simulations of the Contractile Cycle in Cell Migration Using a Bio-Chemical-Mechanical Model," *Comput. Methods Biomech. Biomed. Eng.*, **14**(5), pp. 459–468.
- [552] Deshpande, V. S., Mrksich, M., McMeeking, R. M., and Evans, A. G., 2008, "A Bio-Mechanical Model for Coupling Cell Contractility With Focal Adhesion Formation," *J. Mech. Phys. Solids*, **56**, pp. 1484–1510.
- [553] Pathak, A., Deshpande, V. S., McMeeking, R. M., and Evans, A. G., 2008, "The Simulation of Stress Fibre and Focal Adhesion Development in Cells on Patterned Substrates," *J. R. Soc. Interface*, **5**(22), pp. 507–524.
- [554] Thery, M., Pepin, A., Dressaire, E., Chen, Y., and Bornens, M., 2006, "Cell Distribution of Stress Fibres in Response to the Geometry of the Adhesive Environment," *Cell Motil. Cytoskeleton*, **63**(6), pp. 341–355.
- [555] Pathak, A., McMeeking, R. M., Evans, A. G., and Deshpande, V. S., 2011, "An Analysis of the Cooperative Mechano-Sensitive Feedback Between Intracellular Signalling, Focal Adhesion Development, and Stress Fiber Contractility," *J. Appl. Mech.*, **78**(4), p. 041001.
- [556] Adams, W. J., Pong, T., Geisse, N. A., Sheehy, S. P., Diop-Frimpong, B., and Parker, K. K., 2007, "Engineering Design of a Cardiac Myocyte," *J. Comput. Aided Mater. Des.*, **14**(1), pp. 19–29.
- [557] Jungbauer, S., Gao, H. J., Spatz, J. P., and Kemkemer, R., 2008, "Two Characteristic Regimes in Frequency-Dependent Dynamic Reorientation of Fibroblasts on Cyclically Stretched Substrates," *Biophys. J.*, **95**(7), pp. 3470–3478.
- [558] Ronan, W., Deshpande, V. S., McMeeking, R. M., and McGarry, J. P., 2012, "Numerical Investigation of the Active Role of the Actin Cytoskeleton in the Compression Resistance of Cells," *J. Mech. Behav. Biomed. Mater.*, (in press).
- [559] Byfield, F. J., Reen, R. K., Shentu, T. P., Levitan, I., and Gooch, K. J., 2009, "Endothelial Actin and Cell Stiffness is Modulated by Substrate Stiffness in 2D and 3D," *J. Biomech.*, **42**(8), pp. 1114–1119.
- [560] Weafer, P. P., Ronan, W., Jarvis, S. P., and McGarry, J. P., 2013, "Experimental and Computational Investigation of the Role of Stress Fiber Contractility in the Resistance of Osteoblasts to Compression," *Bull. Math. Biol.*, **75**(8), pp. 1284–1303.
- [561] Ronan, W., Deshpande, V. S., McMeeking, R. M., and McGarry, J. P., 2013, "Cellular Contractility and Substrate Elasticity: A Numerical Investigation of the Actin Cytoskeleton and Cell Adhesion," *Biomech. Model. Mechanobiol.*, (in press).
- [562] Dowling, E. P., Ronan, W., and McGarry, J. P., 2013, "Computational Investigation of In Situ Chondrocyte Deformation and Actin Cytoskeleton

- Remodelling Under Physiological Loading," *Acta Biomater.*, **9**(4), pp. 5943–5955.
- [563] Knight, M. M., Toyoda, T., Lee, D. A., and Bader, D. L., 2006, "Mechanical Compression and Hydrostatic Pressure Induce Reversible Changes in Actin Cytoskeletal Organisation in Chondrocytes in Agarose," *J. Biomech.*, **39**(8), pp. 1547–1551.
- [564] Campbell, J. J., Blain, E. J., Chowdhury, T. T., and Knight, M. M., 2007, "Loading Alters Actin Dynamics and Up-Regulates Cofilin Gene Expression in Chondrocytes," *Biochem. Biophys. Res. Commun.*, **361**(2), pp. 329–334.
- [565] Lennon, A. B., 2011, *Cellular and Biomolecular Mechanics and Mechanobiology*, Springer, Heidelberg, Germany, pp. 297–329.